Chromatic Monitoring Of Transformer Oil Condition Using CCD Camera Technology

Thesis submitted in accordance with the requirements of
the University of Liverpool for the degree of Doctor in Philosophy

by

Ezzaldeen Elzagzoug

June 26, 2013

Abstract

Power transformers are essential components within the power distribution system. Transformer failures having a high economic impact on the distribution operators and the industrial and domestic customers.

Dielectric mineral oil is used in transformers for electrical insulation between live parts, cooling and protection of the insulation papers in the transformer. Oil contamination and changes in the chemical structure of the oil result in the decay of insulation paper and reduced insulation and cooling which can lead to a transformer failure.

The general approach to oil monitoring has been for an operator to examine the colour index (ASTM) of the oil, electrical strength, acidity, water contents and dissolved gas analysis results and form an opinion as to the extent of oil degradation.

Chromatic techniques enable data from different sources to be combined to give an overall evaluation about the condition of a system being monitored. One of the main goals for this work was to use chromatic techniques for integrating the oil data from the different sources and sensors. In addition the chromatic approach enables liquids to be monitored optically so a second aim was to apply chromatic optical oil monitoring using portable system by transmitting polychromatic light through the oil sample, which is contained in a transparent cuvette

and imaged using a mobile phone camera.

A number of oil samples were optically analysed with portable chromatic system and the optical data was compared with the colour index and chromatically companied with the dissolved gas and other oil data to give overall evaluation of oil degradation.

The chromatic optical result compared favourably with the colour index. It was also possible to classify the oil samples chromatically into categories of low, medium and high degradation. This enabled the chromatic data combination approach to be implemented as a prototype system in Matlab software that an operator could use to get a classification of an oil sample. Essential experiment was introduced to monitor different oil particles by obtaining the result of different filtered samples through the filter paper.

Beside the ability to analyse data and distinguish between fresh and contaminated oil samples the chromatic technique has the ability to track the history of different degraded oil samples which can give an indication about failure faults and it could give a prediction of any future faults.

Therefore a commercially viable reliable system can be developed to extend the service life and extend the maintenance schedules. These monitoring systems could lead to extending the service life of the transformers, making the electricity supply more reliable and giving the consumer a better quality of life.

Contents

List of Figures

List of Tables

Acknowledgement

First and above all, *I praise God, the almighty for providing me this opportunity and granting me the capability to proceed successfully during my education life.* This thesis appears in its current form due to the assistance and guidance of several people.

I have been indebted in the preparation of this project to **Prof Joseph Spencer** who gave me the opportunity and the encouragement to do this project. In particular I would like to thank **Prof. Gordon Jones**, for the patient guidance, encouragement and advice he has provided throughout my project time. I have been extremely lucky to have supervisors who cared so much about my work, and who responded to my questions and queries so promptly.

I would like to thank all the members of staff at **CIMS** laboratory team at Liverpool University (**Anthony Deakin, Ducan Smith and Jim Humphries**) who helped me during my project period and who they approved reading my project thesis.

One person who has always been ready to help was our secretary **Jacqueline Cowan**. She took care of all non-scientific works. Thank you **Jacq** for all your support!

I have had the great pleasure of working on my project with **Electrical North West (ENW)** who they sponsored my project and supplied me with all needed

information.

Special thanks to **Peter Watt** from the NHS physical department at the Royal Liverpool Hospital who has a workshop full of treasures, which he kindly made it available for my needs.

Special thanks to **Malcolm Brown** and **Ultramedic team** who they gave me the opportunity to put in practice what I have had learned during the last ten years and they gave me the opportunity to be introduced to different technology.

In addition I would like to thanks my friends for their support and help(**Omer Khan, Nael and Hamza Al-Zubi and Waqar Aslam**). Special thanks to **Fadi Kharoufeh** for his time spend reading my thesis.

Last but not the least I would like thanks my parents and my paternal grandfather **Hassan Al-sharkawi and Saad Al-Zain** for all their love and encouragement. For my parents who raised me with a love of science and supported me in all my pursuits. In particular I would like to thanks my mother who I cant describe her in any word. She is the person who dedicated her life supporting me and my brothers to achieve the highest educations and who was there to encourage and support at all time. Special thanks to my uncle **Dr M Al-Sharkawi** who played a very important role in my life.

Finally a very special thanks to **Dr S. Hamad** for his advises and supports during my master and PhD study.

Chapter 1

Introduction

1.1 Introduction to Oil Transformer

As the world population increases so does the demand for electricity, which has already increased significantly over the last decade. This increase in demand along with market forces will open the door for the power industry to introduce small companies to the market and commercial competition. The liberalisation of power by the 1990s in Europe gave an opportunity for users to choose between different companies with different deals in competitive domestic markets. To achieve this market competition, different distribution companies need to be able to produce and distribute electricity independently. Competition will be present between the different utility companies with the door always being open for new competitors. The main aim of this competition is for a robust and efficient supply of electricity with a reduction in maintenance and improved cost management. These important factors will not be possible without a more robust supply, which needs ongoing investments in maintenance to create fault free operation systems. Such demands are likely to result in system failures due to overload, ageing, arcing, thermal heating etc. Therefore smart systems that can manage such demands are needed.

The introduction of transformers with different power ratings and sizes make the distribution of electricity to the end users at long distances from the generation point more scalable. The advantage of these transformers is their ability to step the system voltage from hundreds to thousands of volts so reducing the current flow and decreasing the cable dimensions.

In recent years questions have been raised about the failure of transformers and their servicerlife since most of these transformers were installed in the 1950s and 1960s Chiesa (2010).

Investigations into defective transformers have concluded that the rapid growth in the population and the need for electricity in the new era of the digital world have become more critical. These facts result in transformers being subject to overloading and age acceleration so shortening the end life of the transformer. Replacement transformers have a huge impact on the economy of market competition, resulting in high penalty fees and compensation for loss of supply.

The transformer is part of a vital power system. When transformer health monitoring equipment is installed, this should reduce the consequences and resultant costs in both power and customer inconvenience during replacement of the transformer. This research has primarily been focused on the study of the different internal components of the transformer, such as insulation paper materials, acid formation, and electrical strength of different dielectric materials such as mineral oil, tap changing and partial discharges. Additionally, a critical evaluation of the research undertaken by different researches has been evaluated, with this previous work being focused on each of the components limitations. One of the most important and reliable type of transformer are mineral oil transformers, where the mineral oil is considered to be a good dielectric material and environmentally friendly when compared to polychlorinated biphenyl (PCB). In 1979, the Environmental Protection Agency (EPA) banned the use of PCB as a dielectric material Adedipe (2010). Before the ban was introduced, PCBs were considered to have far greater dielectric strength and better cooling properties than mineral oil but it was later discovered by the Environmental Protection Agency (EPA) that these PCBs are toxic and harmful to the environment. In 1979, the EPA banned the use of PCB as dielectric materials. Turcotte (2011).

A commonly asked question by the utility companies is whether it is possible to increase the service life of the transformer using condition assessment methods. Researching into this question has raised a number of issues, but the main problem facing the power industry is increasing the service life of the transformers whilst simultaneously reducing the number of faults and increasing the efficiency of the electricity supply. Degradation of oil transformers can result in the degradation of the insulation paper between the live parts within the transformer resulting in the reduction of the transformers operating quality and eventually destruction of the transformer. Today there are many different techniques and method employed to monitor the oil decay optically or by measuring its water and dissolved gases (DG). These methods can be good indicators of transformer faults but they need to be revised and improved as they are not reliable enough to give the correct condition of the aged oil to provide sufficiently accurate information about the

transformers condition regularly.

1.1.1 Scope of Work

Important models using Chromatic techniques have been translated based upon optical techniques in combination with dissolved gas and various liquid properties. The objective of the research was to study the monitoring of transformers with regard to mineral oil transformer degradation. This degradation may involve the effect of different faults such as corona, arc, electrical stress, water and change in thermal strength. One of the main challenges was in deriving data analysis and acquisition methods for assessing the transformer oil condition. It is useful for such techniques to be implemented on a portable system with potential for site use. The analyses developed are for optical, liquid and dissolved gas data, which give different views of the degraded oil. The results of the analyses can be combined to give a total assessment of the oil degradation and transformer health to various degrees of detail. The following aspects have been addressed during the development of the theoretical models:

- Development of accurate and reliable analysis.
- The analytical results should be displayed clearly and conveniently understood.
- The system should be portable.
- The software for achieving this method should be described and implemented.

1.1.2 Research Context

The work presented in this project was sponsored and supported by Electricity North West LTD (ENW). The insulation and mineral oil degradation is known to be one of the most important factors affecting the transformer performance and failure.

1.1.3 Thesis Outline

This thesis is structured as follow:-

Chapter 1 Outlines the motivations and context of this work.

Chapter 2 Provides a literature review, detailing the background history and work undertaken by different researchers including a review of the equipment used by the utility chemical laboratories to monitor the degradation of mineral oil. It also describes different methods used to monitor degradation of mineral oil. The market prediction and view about the cost and time spent on transformer failures and the resulting impact on the economy is also covered in this chapter.

Chapter 3 Gives details about the chromatic methodology used to accomplish this work and details about the fundamental chromatic formulae. It also explains the different properties of light. The concept of colour and the different colour models available are discussed with regards to the human colour perception system. The nature of polychromatic light and its rich information content is considered. Different chromatic models such as Polar, Cartesian, Lightness and XY diagrams are introduced. Finally the concept of CMOS and CCD camera operation used in the present study is explained briefly.

Chapter 4 Presents the different experimental optical setups. This chapter contains information about the portable system produced in the university laboratory. The experimental setups utilised a camera to capture different images and a laptop screen for producing light to transmit through a cuvette containing oil samples. In addition a filter paper system used to filter solid particles from different oil samples is considered.

Chapter 5 This chapter contains two sections, the first covering experimental results measured in the laborotary and the second containing the test data results provided by industry. The main results from both sections presented in this chapter are the raw unprocessed data. The raw data is then used to create different analytical models being based on the introduction of secondary processors such as optical, dissolved gases, liquid and filtered oil samples.

Chapter 6 Discusses both the experimental, preprocessed and post processed results. This chapter is divided into sections, with the first discussing

the results obtained from the processed data models (optical, dissolved gas, liquid and filtered papers particles and filtered oil). The second section covers the post processed data, which is the reprocessing of the processed data, giving more details on the oil sample condition.

Chapter 7 Contains the main conclusion of this work and suggests topics for further research.

Appendices present the raw experimental optical results for different RGB spectra and images. In addition the raw data for test results (dissolved gas and liquid) is also presented. The developed chromatic software by CIMS laboratory (Droptri) Deakin C. (2010) was used to obtain the raw RGB data. These raw RGB data analysed by using the designed and developed automated oil monitoring software using Matlab toolbox.

Chapter 2

LITERATURE REVIEW

2.1 Introduction

Electric power is one of the most important infrastructures of supporting modern digital life. Electricity is considered to be the main lifeblood of quality utilities companies and economic growth. Failure of the electric power system could result in a catastrophic loss, which would have a deleterious impact on modern society.

Transformers are important devices used for the supply of electricity. They enable electricity to be transmitted effectively from a substation to consumers. Modern growth in population makes increasing demands on power supplies and on the load on the transformers. Consequently improved maintenance and care of transformers is considered to be essential.

Historically, transformers have evolved through different stages of research and development. A number of different types of transformers have been produced such as mineral oil transformer, vacuum transformers etc. One of the most reliable type of transformers is the mineral oil transformer. It is small and can provide medium and high voltage.

Mineral oil is a dielectric fluid that has the ability to also cool transformers and provide dielectric insulation between live parts of transformers. Oil filed transformers operate to maximise the efficiency of supplying reliable power. However as time has passed the number of failures have increased causing critical problems within transformers such as arc, thermal, corona etc. faults. These faults are economically disruptive and costly.

Most transformers operating at present are approaching or have already approached their life limit and so require special care and investigation. As a result

much research has been conducted into transformer faults. This research has indicated that a key failure is due to the degradation of the electrical insulation of the transformer, due to the decay of the mineral oil. Different methods and techniques have been developed such as Dissolve Gas Analysis (DGA), IEC (International Electrotechnical Commission) ratio etc. which they are based on the calculation of the ratio of gas concentrations.

Thus monitoring of oil degradation becomes an important issue, as it can be an early indication of transformer failures. This indication can help in solving the faults, with advantages of producing a longer reliable operation of the transformers and a robust supply of power.

This chapter covers the historical background of oil transformers and describes the chemical structure of mineral oil and gases dissolved in it. Different techniques for oil monitoring such as optical, dissolved gases and liquid degradation are described. Some equipment used by utilities such as voltage breakdown, colour measurement and dissolved gas analysis with the Duval triangle, Roger ratio etc. are introduced and explained in this chapter.

Statistics and predictions based on the occurrence of earlier faults and the cost are presented. Surveys made by different organizations are introduced as supporting evidence of the cost and the number of defective transformers, which have occurred over many years.

2.2 High Voltage Transformer Oil

2.2.1 History of transformer oil

The principles upon which electrical transformers were based are established in the late 1800. These were developed by Faraday, Maxwell and Tesla and introduced to the power industry by Edison and Westinghouse. Although the transformer principles have remained unchanged for over 100 years, their design has continued to be improved, which lead to different types of transformers being developed figure (2.1) Boser (2003).

In 1890 the first oil-cooled, two-phase transformer was developed by Brown. It opened the way for developing high voltage transformers which operated at 2000 MVA capacity. Petroleum oil as a low viscosity component started to be used before 1887. It proved the ability of providing electrical insulation and thermal cooling for heated equipment and reducing electric losses when it infused into paper or other dielectric materials. The oxidation of oil causes the chemical bond of the dielectric insulation to be broken which reduces the efficiency of heat transfer and dielectric insulation Shankar.Vishal and Prashant (2011).

At the beginning of the 1920s detachable radiators were introduced into transformers. By the 1930s radiators with cooling fans were introduced to high voltage transformers (three-phase transformers) to cool the dielectric insulation (oil). Forced oil pumps were introduced in the 1950s, which helped cooling the oil with the help of side air fans Lucas (2000).

Transformers these days contain mineral oil as a dielectric compound, which is considered as being reliable and able to operate under extreme conditions.

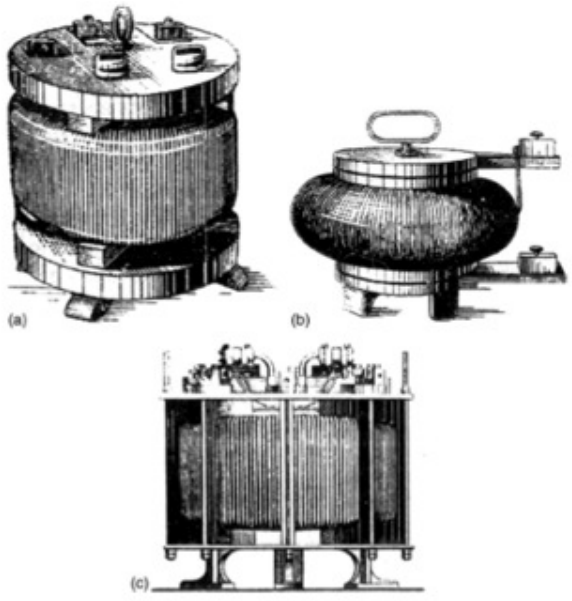

Figure 2.1: Earlier transformer types
Andreev and Chubraeva (2007).

2.2.2 Purpose of transformer oil

A transformer is a vital device used by power utilities to provide reliable power supply and transfer power efficiently and continually from internal electrical sources to external loads Texas Instruments Incorporated (2001).

It maintains reliable voltages and currents transmitted 24 hours a day by transforming voltage from one level to another usually from higher voltage to lower voltage (step down) or vice versa (step up) figure (2.2). This operation is completed using the principle of magnetic induction between coils Gary W Castleberry (2008).

This magnetic induction between coils converts current or voltage by a step up or step down process. At commercial or industrial sites, transformers operating at temperature of 40 to 50 $^{\circ}C$ are acceptable and the internal temperature can reach 100 $^{\circ}C$. A cooling component such as dielectric materials (OIL) can control the heat, which maintains uniform heat across the transformer windings. A dielectric fluid is a material used to prevent transformers from overheating by cooling and electrically insulating live parts from each other.

The oil is normally inserted into a transformer through an inlet at the bottom of a tank. The oil at the bottom of the tank is at a low temperature. The oil is

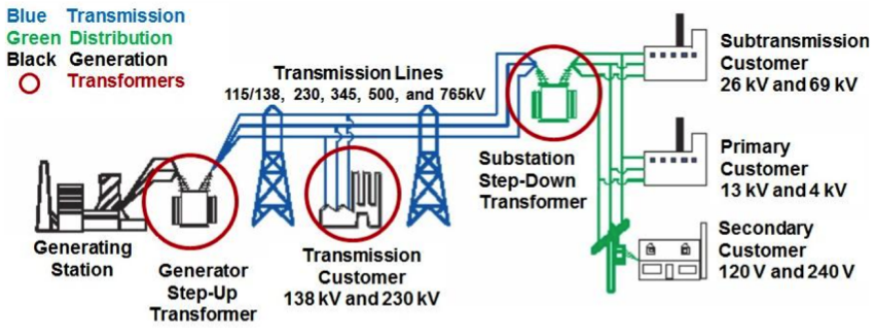

Figure 2.2: Electrical power grid
Friedman K. (2012).

then circulated vertically within ducts in the transformer and it absorbs the heat from the live windings figure (2.3). Once the oil reaches the top of the tank with a high temperature, it enters cooling fins or radiators, and then flow down the radiators to the bottom of the tank (main tank) Hart (2012).

Some transformers are called self cooled transformers since they are governed by a series of cooling fans directing air against the cooling radiator. This process increases the rate of heat transfer within the oil and increases the rate of cooling in the transformer windings. Some large oil transformers contain a pump which forces oil to circulate. This helps to provide a uniform temperature within the windings and helps the oil to have a low temperature at the top of the tank Terrell Croft (2008)TOSHIBA (2012).

2.2.3 Structure of an oil transformer and its operation

A transformer consists basically of two windings or coils. These windings are inductors, which transform AC voltages. When an alternating current is connected to the primary coil or winding, a magnetic field is created (magnetic flux) which links to the secondary winding and induces a voltage across it. The secondary winding is placed close to the primary winding and they are separated by isolation paper. The magnitude of the voltage or current is proportional to the number of turns on each of the windings according to the following formula Choi et al. (1996):

$$\frac{Voltage of secondary}{Voltage of primary} = \frac{Numbers of turns of secondary}{Number of turns of primary}$$

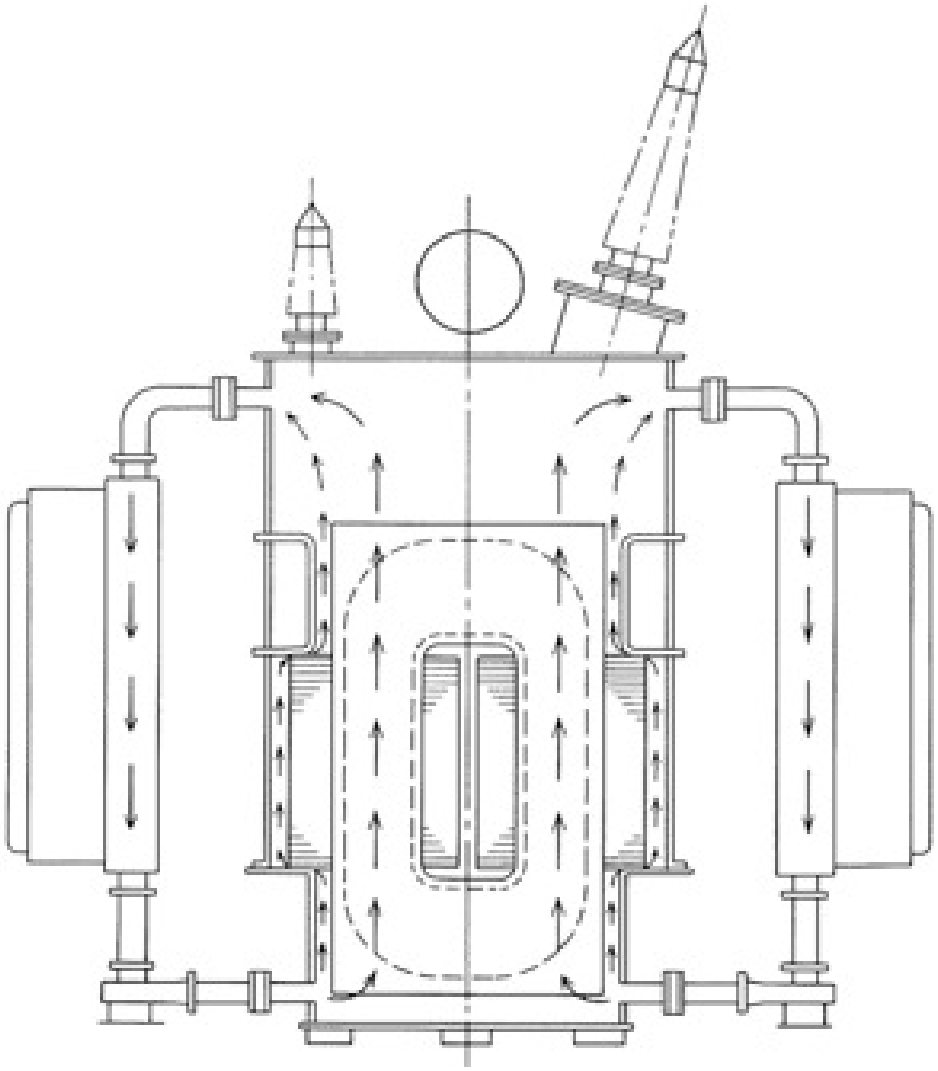

Figure 2.3: Oil circulation within transformer
U.S. Department of Energy (2005).

An iron core is introduced between the primary and secondary coils figure (2.4) to maximize the magnetic flux linkage to the secondary coilHarlow (2004).

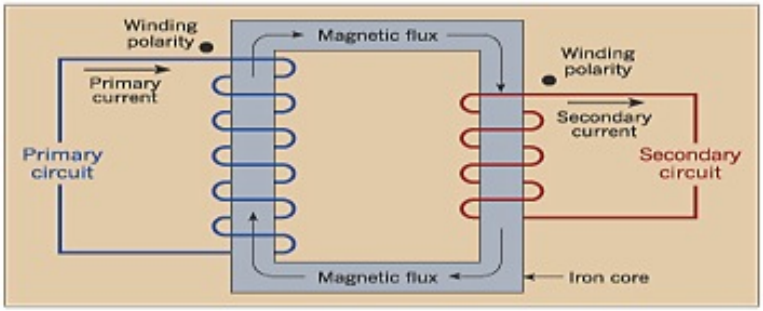

Figure 2.4: Transformer coils and iron core
Electrical Construction Maintenance (2003).

If the number of turns on the primary coil is greater than the number of turns on the secondary coil of a transformer it will cause the high voltage transmitted through overhead lines to be converted to a medium or low voltage which can be transmitted through appropriate cables. This is known as a step down transformer. Alternatively if the number of turns on the secondary coils is greater than the number of turns on the primary the transformer is a step up transformer, which converts medium or low voltages into a high voltage figure (2.5) U.S. Department of the Interior (2005).

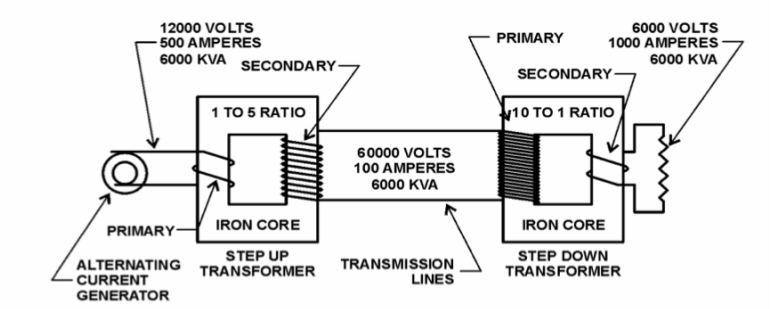

Figure 2.5: Structural diagram for step up and step down transformers
U.S. Department of the Interior (2005).

The polarity of the winding determine the direction of the coil winding and it determines if the flux is additive or subtractive with respect to the flux produced by the second coil Lim et al. (2005)

Transformer oil is involved in vital parts of a transformer as illustrated in figure 2.6. These parts are as follow:

- Primary coil/ windings.
- Secondary coil/ windings.
- Iron core.
- Insulation papers such as wood, sands, silicon etc.
- Oil tanks and pipes for oil circulation.
- Ducts and radiators to cool heated oil, (some transformers will have an oil pump and an air fan as an extra cooling device).

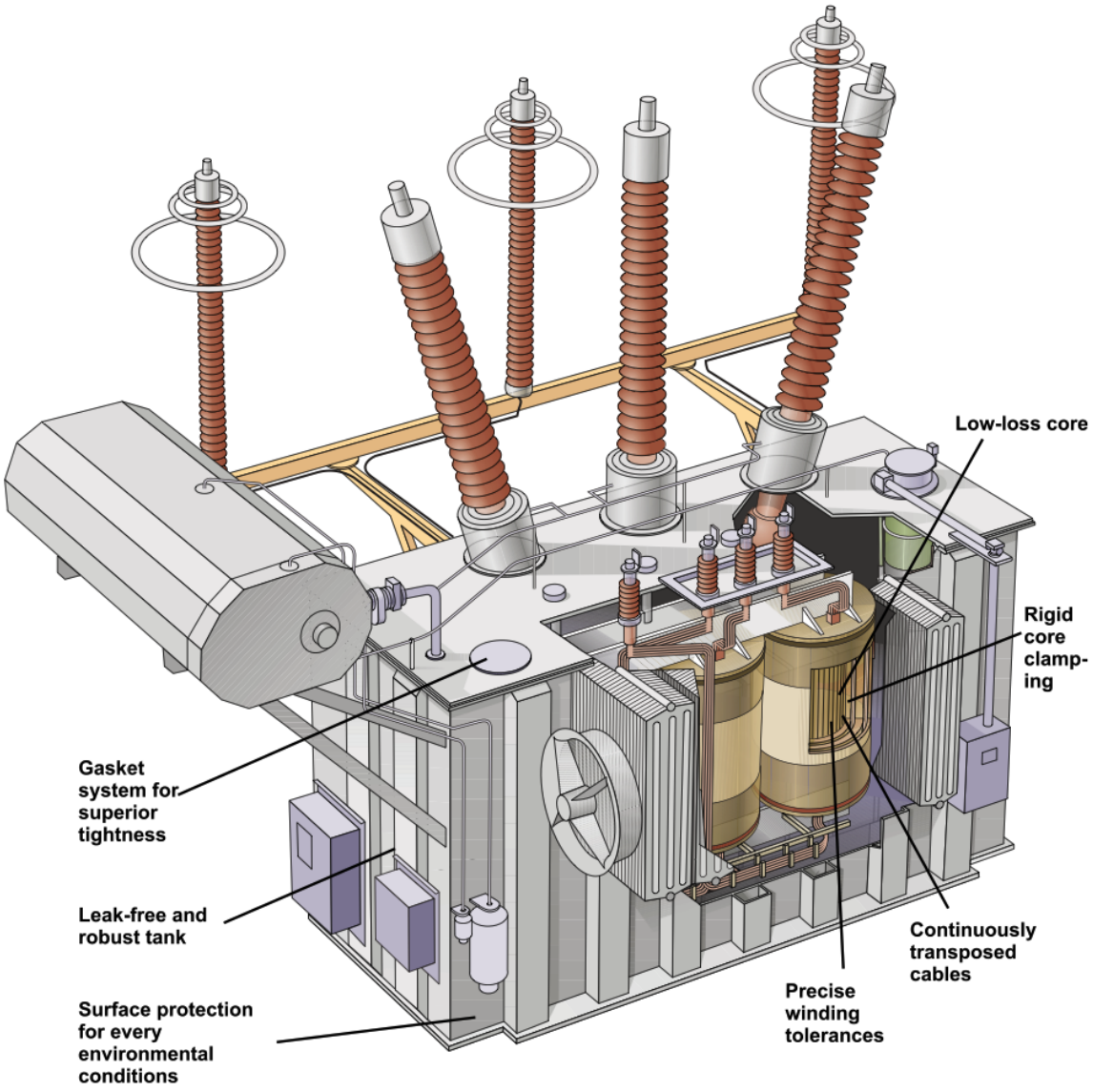

Figure 2.6: Internal transformer parts U.S. Department of the Interior (2005)

.

2.3 Review Of Mineral Oil Used In Transformers

2.3.1 Degradation of oil

The molecular structure of pure transformer oil is shown on figure (2.7). Mechanical stress and electrical failure could result in affecting the oil and insulation materials, which lead to the mineral oil being contaminated due to chemical interaction with the windings and insulation papers caused by high temperature operation. As a result the oil chemical chain figure (2.7) will tend to break down, resulting in the oil being degraded over many years, and with the consequence of the oil losing its desirable properties. In addition, the oil may be subjected to corona, arcing, sparking etc. which will lead to the oil being contaminated by different types of gases Electronical (2012).

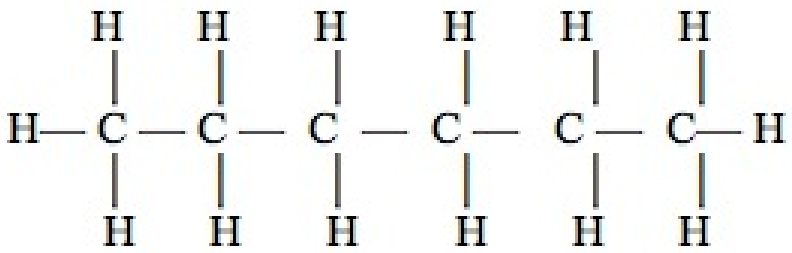

Figure 2.7: Mineral oil molecular structure
DiGiorgio (2005).

Therefore testing the oil is seriously considered in most utility companies worldwide. These tests are used to give information about the type of any faults without the need of putting transformers out of service Wang (2003).

2.3.1.1 Optical degradation

ASTM (American Society for Testing and Materials) colour scale (D1500) is a method used to visually monitor the degradation of mineral oil by comparing different samples to a colour scale figure (2.8) Golden et al. (1995). With regards to oil samples colour could be used as an indicator on the degree of oil degradation or contamination. However colour is not always a reliable guide to indicate the quality of the condition Dervos et al. (2005b),Dervos et al. (2005a) .

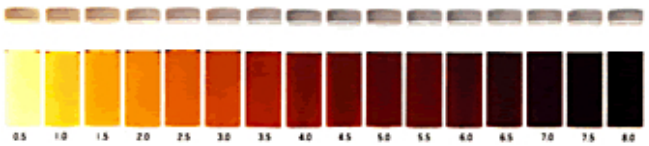

Figure 2.8: ASTM D1500 colour scale
Corp (2012).

2.3.1.2 Liquid degradation

Water content, acidity and electrical strength are vital factors in oil degradation. The presence of water within the oil is an indication of insulation paper ageing, which is known as a cellulose fault. Water is usually introduced from the degraded insulation paper. As water and oxygen levels in mineral oil increase, the more the insulating paper is degraded as the oil starts to lose its dielectric properties, which is a sign of mineral oil becoming deteriorated. The degradation of oil and insulation paper could lead to a catastrophic failure of transformers Shoureshi et al. (2004). A high temperature of a transformer and oil is an indication of water formation and a cellulose fault Kirtley Jr et al. (1996). Acidity is defined as the production of oxidation, which forms acids. As acids are created within transformer oil, a sludge is created due to a chemical reaction between the metal in the transformer oil tank and the acids. This will reduce the cooling and dielectric properties of the oil. Investigation of sludge within mineral oil indicated that, sludge is formed in the oil when the acid level reached or exceeded 0.4 mgKOH/gram Hamrick (2009b).

Electrical stress occurs when the oil insulation/dielectric properties is lost and live parts come in contact with each other. This in turn will result in the current passing through the oil between windings. This will lead to partial discharges and electric heating. Other types of stress, which are caused by the loss of the oil's dielectric property are thermal, ambient and mechanical stress. Most of these stresses are also related to environmental factors such as humidity, ultraviolet radiation, corrosive chemical etc. The molecular structure and chemical composition of insulation materials can be affected by all these types of stress, which will result in the decomposition of the insulation structure Yuliastuti (2010).

2.3.1.3 Dissolved gas degradation

Dissolved gases are a compound consisting of different gases introduced in the form of a solution in a solvent. For mineral oil filled transformers, there are key

gases ratios, which identify different kinds of faults based on a type of gas, mixed gases and quantity of gases table (2.1) Hamrick (2009a).

Table 2.1: Dissolved Gases Analysed for Oil Degradation Investigations DiGiorgio (2005) Hamrick (2009a).

Gas Description **Sever Potential Fault Type**	**Gas Symbol**	**Normal Limits**	**Action Limits**
Carbon Monoxide Sever Overheating	(CO)	500	1000
Carbon Dioxide Sever Overheating	(CO_2)	10000	15000
Ethylene Sever Overheating	(C_2H_4)	20	150
Ethane Local Overheating	(C_2H_6)	10	35
Acetylene Arcing	(C_2H_2)	15	70
Hydrogen Corona	(H_2)	150	1000
Methane Sparking	(CH_4)	25	80

These gases are soluble in oil since they can break the structural bonding of the hydrocarbon molecules of the mineral oil and create different types of chemical gases from the produced energy Meng (2009). These gases listed on table (2.1) above are as follow:

- Hydrogen(H_2)
- Methane (CH_4)
- Ethane (C_2H_6)
- Ethylene (C_2H_4)
- Acetylene (C_2H_2)
- Carbon Dioxide (CO_2)
- Carbon Monoxide (CO)

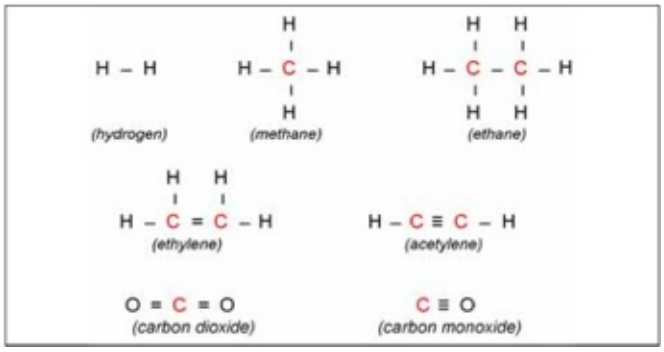

Figure 2.9: Chemical structure of the key gases Meng (2009).

and their chemical structure is illustrated on figure 2.9.

The decay of mineral oil due to temperature increases (from 150 to 500 $°C$) will result in the introduction of lower molecular weight gases such as H_2, CH_4 and some higher molecular weight gases such as C_2H_4, C_2H_6. With the increase of temperature caused by a fault in mineral oil, the H_2 concentrations exceeds CH_4 concentrations and significant amount of high molecular weight gases such as C_2H_2 are produced. The presence of C_2H_2 at a high temperature within the mineral oil gives an indication of a high temperature fault and an arc could occur within the transformer oil. In addition, the presence of CH_4 could be a result of a low energy thermal fault. So an early stage of oil degradation results in H_2 being formed with reduced amount of C_2H_2. On the other hand, as the degradation and temperature increase the C_2H_2 and C_2H_4 concentrations rise. An arcing fault will be produced when the quantity of C_2H_2 becomes detectable within the oil. Table (2.2) shows the relationship between faults and temperature in creating different gaseous compounds David and Rajaram (2012).

Table 2.2: Gases generated by different faults

Hamrick (2009a).

Material	**Condition**	**Gases generated**
Cellulose	Overheated >150 $°C$	Carbon Monoxide (CO), Carbon Dioxide (CO_2), +water (H_2O)
Oil	Overheated >110 $°C$	Methane (CH_4), Ethane (C_2H_6), Ethylene (C_2H_4), +Organic acids
Oil	Electrical stress (Partial discharge and arcing to 1000 $°C$)	Hydrogen (H_2), Acetylene (C_2H_2), +Waxes and water

2.4 Common Techniques Used To Monitor Transformer Oil Degradation

Historically a ratio method has been used as a tool in diagnosing the dissolved gas concentration. Five ratios have been used R1 (CH_4 /H_2), R2 (C_2H_2 / C_2H_4), R3 (C_2H_2 / CH_4), R4 (C_2H_6 / C_2H_2) and R5 (C_2H_4 / C_2H_6). The first attempt in diagnosing dissolved gas in degraded oil was in the late 1960s at the Central Electricity Generating Board (CEGB). By the 1970s Dornenburg was able to distinguish between thermal and electrical faults using six chemical gas compounds (H_2, CH_4, CO, C_2H_2, C_2H_4 and C_2H_6) and four different ratios table (2.3). In 1973 the Rogers ratio method was introduced and modified in 1975 and 1977 into the IEC standards. Doble first introduced the method of key gases in 1974 and a comparison between the key gases method and the Roger method was presented by Doble in 1978. It suggested that the key gases method was easier to use on oil transformers. Dissolved gas is a useful technique in monitoring the behavior of transformers and has led to further methods being develop such as the Duval technique Wang (2000).

Table 2.3: Ratio method used by Dornenburg

Wang (2000).

Fault	**R1**	**R2**	**R3**	**R4**
Thermal Decomposition	>1.0	<0.75	<0.3	>0.4
Corona (Low Intensity PD)	<0.1	Not Significant	<0.3	>0.4
Arcing (High Intensity PD)	>0.1 and <1.0	>0.75	>0.3	<0.4

2.4.1 Key gas method

The key gas method is a technique used by chemical laboratories, which is based on removing the gases from the oil samples and analysing them table (2.4) Laborelec (2012).

Table 2.4: Dissolved gas concentration limit ppm

Bureau of Reclamation (2003).

Status	H_2	C_{H2}	C_2H_2	C_2H_4	C_2H_6	CO	CO_2	$TDCG$
	Hydrogen	Methane	Acetylene	Ethylene	Ethane	Carbon Monoxide	Carbon Dioxide	Total Dissloved Com-bustible Gas
Condition 1	100	121	35	50	65	350	2500	720
Condition 2	101-700	121-400	36-50	51-100	66-100	351-570	2501-4000	721-1920
Condition 3	701-1800	401-1000	51-80	101-200	101-150	571-1400	4001-10000	1921-4630
Condition 4	> 1800	>1000	>80	>200	>150	>1400	>10000	>4630

Condition 1 − TDCG below 720 ppm indicates the transformer is operating satisfactorily.

Condition 2 − TDCG within the range of 721-1920 ppm indicates greater than normal combustible levels should prompt additional investigation. (any gas exceeding specified levels).

Condition 3 − TDCG within the range of 1921-4630 ppm indicates high level of decomposition (additional investigation required).

Condition 4 − TDCG >4630 indicates excessive decomposition could result in failure of the transformer.

2.4.2 Rogers ratios

Rogerss method is considered to be one of the most accurate analyses for detecting failures within electrical transformers. The Rogers technique depends on four chemical ratios. These ratios are represented on table (2.5) and Rogers faults table (2.6) are arranged depending on the value of the chemical ratio H.R.Jariwala (2012).

Table 2.5: Roger four chemical ratio H.R.Jariwala (2012)

Gas ratio	Ranges	Codes
CH4/H2	<0.1	5
	0.1-1	0
	01-Mar	1
	>3	2
C2H6/CH4	<1	0
.	>1	1
C2H4/C2H6	<1	0
	01-Mar	1
	>3	2
C2H2/C2H4	<0.5	0
	0.5-3	1
	>3	2

2.4.3 Doernenburg ratios

One of the early methods to diagnose faults within high voltage electric transformers using DGA results is the Doernenburg ratio method. This method is able to detect three different faults (thermal decomposition, corona and arcing) Cunningham (1999)

There are steps needed to be followed in order for the Doernenburg method to be successful. Firstly oil samples need to be collected from the top of the oil level in the transformer. Secondly, one of the gases (H_2, CH_4, C_2H_2 and C_2H_4) must be twice the value limit represented on table (2.7). Thirdly, ratio of R1, R2, R3 and R4 table (2.8) are assumed valid. Finally if all ratios are satisfied the fault can be indicated as shown on table (2.9) DSI Ventures (2008).

Table 2.6: Rogers different fault types H.R.Jariwala (2012)

.

No	CH4/H2	C2H6/CH4	C2H4/C2H6	C2H2/C2H4	Fault Type
1	0	0	0	0	No fault
2	1-2	0	0	0	(<150 $°C$) thermal fault
3	1-2	1	0	0	(150-200 $°C$) thermal fault
4	0	1	0	0	(200-300 $°C$) thermal fault
5	0	0	1	0	General conductor overheating
6	1	0	1	0	Winding circulating currents
7	1	0	2	0	Core and tank circulating currents, overheated joints
8	5	0	0	0	Partial discharges
9	5	0	0	1-2	Partial discharges with tracking
10	0	0	0	1	Flashover without power follow through
11	0	0	1-2	1-2	Arc with power follow through
12	0	0	2	2	Continues sparking to floating potential.

Table 2.7: Gas limitation table DSI Ventures (2008).

Dissolved Gas	Gas Value limit in ppm
Hydrogen	100
Methane	120
Carbon Monoxide	350
Acetylene	35
Ethylene	50
Ethane	65

Table 2.8: Ratio used in Doernenburg fault method DSI Ventures (2008).

Ratios Used	
R1	CH_4 /H_2
R2	C_2H_2 /C_2H_4
R3	C_2H_2 /CH_4
R4	C_2H_6 /C_2H_2

Table 2.9: Doernenburg fault indication table with gas ratio DSI Ventures (2008).

Indicated Fault Diagnosis	Ratio 1	Ratio 2	Ratio 3	Ratio 4
Thermal Decomposition	0.1- 1.0	0.75 2013 1.0	0.1 2013 0.3	0.2 2013 0.4
Corona	0.01 2013 0.1	Not significant	0.1 2013 0.3	0.2 2013 0.4
Arcing	0.1 2013 1.0	0.75 2013 1.0	0.1 2013 0.3	0.2

2.4.4 IEC Duval triangle

Duval Triangle method figure (2.10) is considered to be one of the most accurate techniques. It only depends on three main combustible gases CH_4, C_2H_4 and C_2H_2. Each one of the three main gases will be divided by the total of the main three gases and multiplied by 100% to express the percentage of each of theses gases Akbari et al. (2008); Singh and Bandyopadhyay (2010).

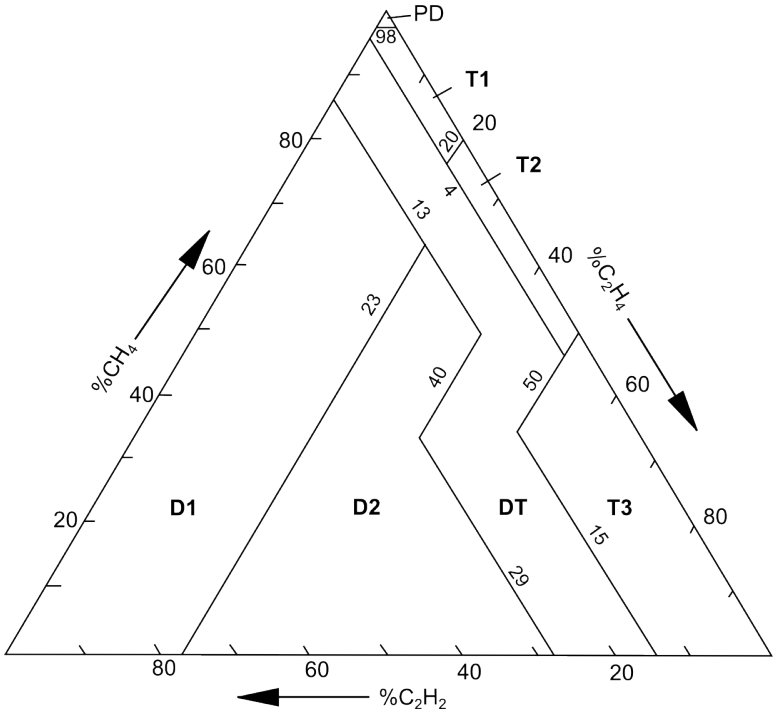

Figure 2.10: Duval Triangle Muhamad et al. (2007).

Once the percentage of each of the three gases is obtained coordinates can be drawn to identify the condition of the oil ARNO (2006).

These conditions are determined as follows:

PD Partial discharge.
T1 Low range thermal fault (below 300 °).
T2 Medium range thermal fault (300- 700 °).
T3 High range thermal fault (above 700 °).
D1 Low energy electrical discharge.
D2 High energy electrical discharge.
DT Indeterminate thermal fault or electrical discharge.

2.5 Typical Industrial Requirements For An Oil Monitoring Instrument

Past attitudes considered that if a transformer survived the first six months of its operation, it would last for the next 30 years. Today most transformers are over 60 years old. So having information and data about these aged transformers is vital. The manner for obtaining the information and understanding the condition of transformers is by monitoring them Cargol (2005).

Experience shows that most internal problems can be detected and understood by monitoring the oil. The complexity of compounds such as mineral oil is a challenging area since it requires advancesd technology to monitor the decay of oil Smith (2001).

The monitor should lead to an early detection of faults within oil transformers. Ghoneim and Ward (2012).

2.5.1 Requirement for an ideal sensor

A monitor is a sensing device that assists in a device required for monitoring online transformers while could also be used to monitor offline transformers. These sensors could operate in providing information about unexpected failures. This kind of monitor is ideal for providing continuous assessment of the transformer condition with regard to any faults developed within it, such as oil or insulation paper degradation Brian D. Sparling (2012).

2.5.2 Typical commercially available system

There are different types of online and offline transformer monitoring devices. Examples of such system are considered in this section.

2.5.2.1 Automated colorimeter and ASTM colour

Figure 2.11: Automated colour meter using ASTM D1500 koehlerinstrument (2008).

An example of an optical device used by utility companies to monitor transformer oil colour is the ASTM D1500 instrument figure (2.11). It uses light which is passed through the oil sample and analysed with respect to different optical disc colours. The spectrum of the oil is measured from 400nm to 700nm and the disc scale segment is between 0.5 to 8.0 with colour increments by 0.5 Micro Spectral Analysis (2012).

2.5.2.2 Gas guard 8 sensor

GAS-GUARD 8 figure (2.12) is a device used to measure eight critical gases. A sensor continuously samples the oil every two hours. It also measures moisture and temperature within the oil. The software package that analyses the data collected from GAS-GUARD 8 is created from the Duval triangle and Roger methods, which consist in tracing oil degradation and faults Siemens AG (2010).

2.5.2.3 Infraca filtometer

Dielectric breakdown voltage is defined as the voltage across an oil sample which causes the dielectric mineral oil to electrically conduct. On the other hand when conduction take place in air or a gas and breackdown occurs, this is known as an arc Lee et al. (2012).

Dielectric breakdown is measured by applying a voltage across the oil sample. The sample and test rig figure (2.13) has to follow the IEC 156 standards. The standards specify the test gauge size and oil collection procedures Circutor (2012).

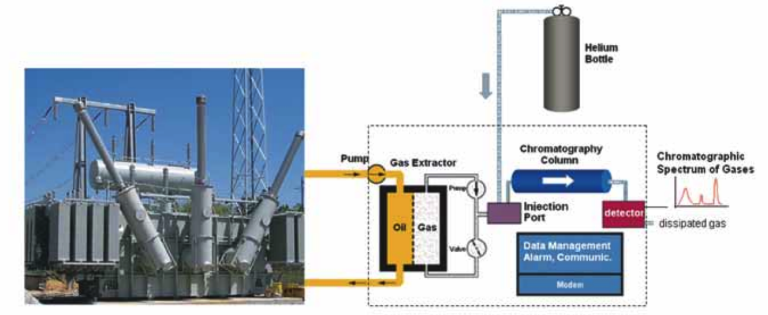

Figure 2.12: Gas guard 8 schematic diagrams connected to a transformer AG (2010).

Once the oil samples fall with in the IEC 156 specification, it is introduced into a test vessel and a uniform voltage applied starting from zero at a rate of $2kV/s \pm 0.2kV/s$ until breakdown occurs. As breakdown in insulation oil accrues there will be gases on the surface due to high voltage applied within the vessel between the two electrodes figure (2.14). Six breakdown measurements are taken for the oil sample or until the bubble gases disappear from the surface of the oil sample. The final result, which evaluate the condition of the samples, is calculated from the six measurements by taking the mean value. The ASTM D3300 introduces an additional requirement, which is that the range of the mean value must not exceed 10% in order to obtain an accurate estimate Lee et al. (2012).

2.5.2.4 Photo-Acoustic Spectroscopy for DGA

Infra red photo acoustic spectroscopy is a method used to analyse gases and to detect faults Yun et al. (2008). Broadband radiation covering the IR range is transmitted to a parabolic mirror and reflected to a measurement cell figure (2.15). A mechanical chopper to give intermittent illumination controls the light source before reaching the measurement cell. The radiation is transmitted through one of the optical filters, on the choppers, which is designed to excite a particular gas compound within the oil sample. Once the sample is excited, the acoustic signal or frequency is recorded by a microphone. These contained frequencies are further analysed to give information about the gases within the oil sample Bates (2006).

Figure 2.13: Breakdown test rig
Lee et al. (2012).

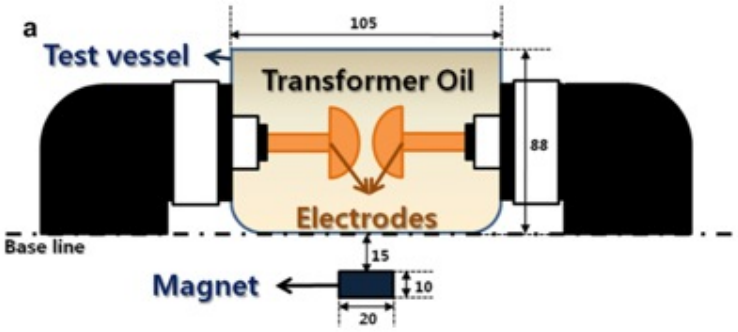

Figure 2.14: Schematic diagram of test vessel and its electrodes
Lee et al. (2012).

2.6 Possible Limitations And Cost

These days a major challenge facing the utility industry is the continuous demands being made on power transformers due to the increase in population. As the demand for power increases the transformers age with time, which makes them vulnerable to major faults. The major degradation occurs in large oil coolant transformers figure (2.16) rated at 24 MVA or above. The IMIA group was established in 1995 to investigate transformer failure and to provide an explanation about the reasons behind transformer losses. From 1997 to 2001 a major request for information about losses of transformers, their age, and cause of failure

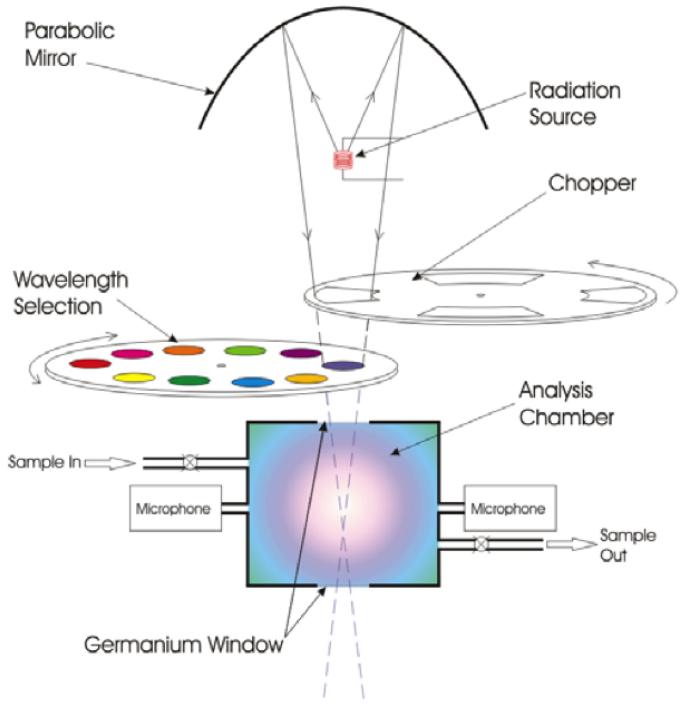

Figure 2.15: Photo acoustic spectrometer concept
Bates (2006).

etc. was published. There was a substantial limitation in providing information about the cause of failure, age of transformers etc., which led to much confusion within the power industry. In 1998 a number of transformers reached their peak loads within the USA. In the year 2000 the largest transformer losses took place causing business interruption (especially in the industrial plant sector) costing more than $86 million dollars. This amount of money loss leads to a thorough investigation into the reasons behind transformers failures. The main reason of failure is insulation table (2.10) Bartley (2003).

These failures showed a limitation in understanding these faults and the reason for them being developed where the needs of internal observation of transformers started to be vital. These investigations led to a survey showing the main reasons for failures is due to moisture, damage to winding and damage to transformer bushings. Most of these failures are due to the internal strength of the dielectric insulation being lost.

Another survey introduced by the CIGRE group regarding failures within electrical transformers indicated that about 41% were due to the tap changer

Table 2.10: Reason of failure and it cost Bartley (2003)

.

Cause of Failure	Number	Total Paid
Insulation Failure	24	$149967277
Design /Material/Workmanship	22	$64696051
Unknown	15	$29776245
Oil Contamination	4	$11836367
Overloading	5	$8568768
Fire /Explosion	3	$8045771
Line Surge	4	$4959691
Improper Maint /Operation	5	$3518783
Flood	2	$2240198
Loose Connection	6	$2186725
Lightning	3	$657935
Moisture	1	$175,000

Figure 2.16: Damage to transformer due to oil and insulation degradation Bartley (2003).

and 19% were due to the windings. In addition, other small percentages of failure such as core terminal etc. were introduced on figure (2.17) Murthy (1996).

More evidence of transformer failure data in South Africa was introduced in a report. The investigation focused on 188 high power transformers, which have been operating for 15 to 25 years figure (2.18) Wang et al. (2002).

Limitations in monitoring equipment encouraged the power industry to invest a large amount of money in research to develop techniques and methods to

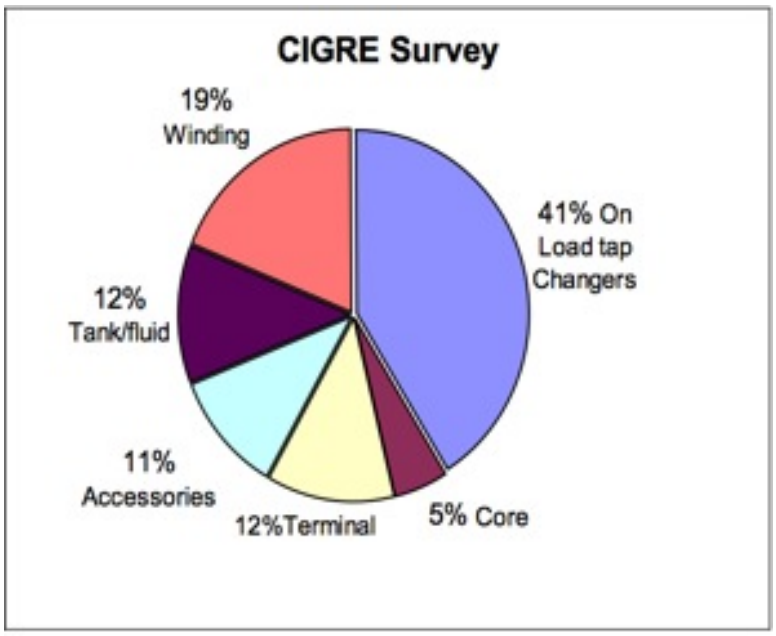

Figure 2.17: CIGRE statistic of different type of failure within transformers (load tap change) Verma (2005).

.

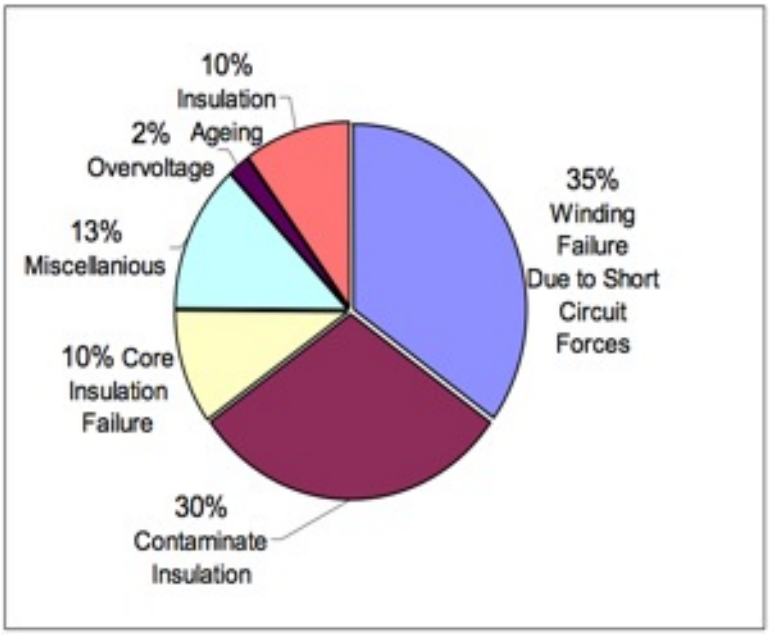

Figure 2.18: Failure statistic for high power transformers with working operation between 15 to 25 years Verma (2005).

monitor the behaviour of different parts and compounds within transformers as well as the surrounding environment. The research has built up reasons behind

insulation degradation. The main reason for the decay of insulation paper within a transformer is the contamination of the dielectric materials (oil) by different gas compounds. This degradation within the oil causes its colour to be changed due to different chemical gases being produced and which cause its properties to be lost. The most accurate method in analysing Dissolved Gases developed in aged oil is the Duval Triangle followed by the Key gas, Nomograph, IEC ratio, Roger ratio and Doernenburg method. Table (2.11) illustrates the number of prediction of each fault corresponding to different methods and the number of successful predictions. Also it shows how consistent each method is in monitoring different faults Muhamad et al. (2007).

The cost and time spent in replacing and maintain high voltage transformers are high. The time spent in replacing or repairing is between 12 to 15 months. This time could be reduced if a spare transformer was available Verma (2005).

A prediction of future failure of transformers figure (2.19) was made based upon the analysis collected every year regarding failed transformers. This prediction is alarming as it shows high numbers of transformers from 1960 and 1970 expected to have an end life and failures due to its long period of operation and to the poor maintenance provided to them by utilities. So there is a need for reliable systems to predict the life left for each transformers as well as a major change in the way they are maintained and cared for by utility companies Bartley (2002).

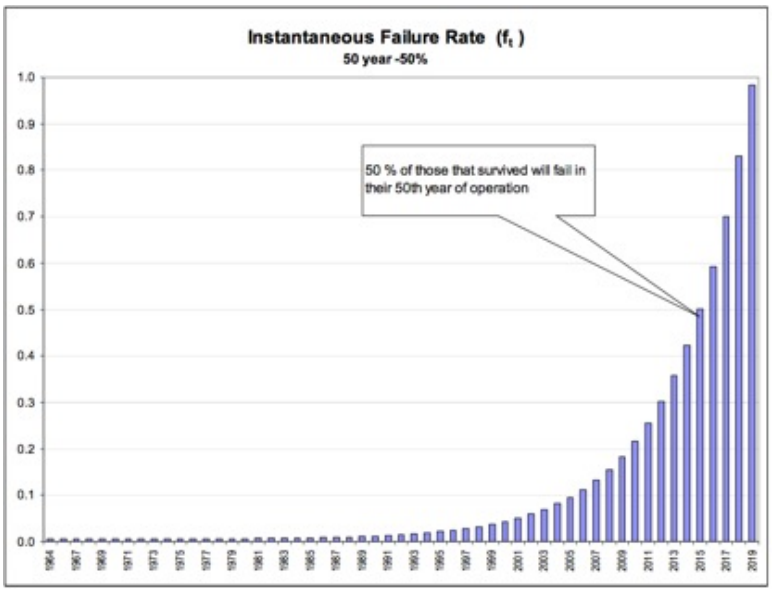

Figure 2.19: Predicted future failure transformers Bartley (2002).

Table 2.11: Result analysis for each fault with respect of the method used Muhamad et al. (2007).

Method Analysis Table			
Method	Fault	Sucssesful Prediction	Consistency
Roger	Thermal fault at low temperature	50.00%	45.00%
	Overheating and sparking	39.00%	
	Arcing	55.00%	
	Partial Discharge and Corona	57.00%	
	Normal	23.00%	
IEC	Thermal fault at low temperature	50.00%	60.00%
	Overheating and sparking	79.00%	
	Arcing	82.00%	
	Partial Discharge and Corona	64.00%	
	Normal	23.00%	
Nomograph	Thermal fault at low temperature	20.00%	74.00%
	Overheating and sparking	70.00%	
	Arcing	82.00%	
	Partial Discharge and Corona	100.00%	
	Normal	100.00%	
Doernenburg	Thermal fault at low temperature	20.00%	40.00%
	Overheating and sparking	45.00%	
	Arcing	36.00%	
	Partial Discharge and Corona	43.00%	
	Normal	54.00%	
Duval	Thermal fault at low temperature	100.00%	88.00%
	Overheating and sparking	91.00%	
	Arcing	100.00%	
	Partial Discharge and Corona	50.00%	
	Normal	100.00%	
Key gas	Thermal fault at low temperature	100.00%	78.00%
	Overheating and sparking	100.00%	
	Arcing	45.00%	
	Partial Discharge and Corona	50.00%	
	Normal	92.00%	

2.7 Summary

In this chapter a historical background for oil transformer was introduced along with a description of the transformers development steps. Investigations into transformer failure and the development of techniques and methods such as optical, liquid and dissolved gases have been introduced. DGA is a technique and method (Duval triangle, Rogeres ratio etc.), which depends on the key gas ratio, and which developed from early research analysis in monitoring oil transformers. These gases are considered to be associated with transformer failure since they are produced during degradation of dielectric insulation. Also optical and electrical strength techniques for monitoring oil degradation due to changes in the chemical composition of the mineral oil were explained.

Chapter 3

CHROMATIC METHODOLOGY

3.1 Introduction

An approach for monitoring complex conditions is needed in order to address the nature of problems within oil transformers. In other words there is a need to consider multiple dimensions including chemical, material and design components, which all add complexity to the system. This kind of complexity is rapidly increased as systems or component are developed. There is a major lag in paying attention to details in the design and fault diagnosis that could appear on the system Jianjun et al. (2007). As an example, high voltage transformers (chapter 2, section 2.1) are considered to be a major system in our daily life, which need to be monitored. One method for monitoring is with the chromatic technique Jones et al. (2009). This technique focuses on observing the general condition of the system or components, which involves monitoring different signals with three non-orthogonal processors called Red, Green, Blue Ragaa M.(2010).

These processors convert a complex signal into a simple form based upon R,G,B parameters. These parameters can be further transformed to give another three parameters where can be used to construct simple graphs in the form of polar or Cartesian graphs.

This chapter will introduce the fundamental chromatic techniques used to monitor complex conditions and how they are adopted from the human perception system. In addition, this chapter covers chromatic transformation models and chromatic maps. First, an overview of the properties of light is given since light is one physical phenomenon used in chromatically monitoring complex conditions.

3.2 Properties of Light

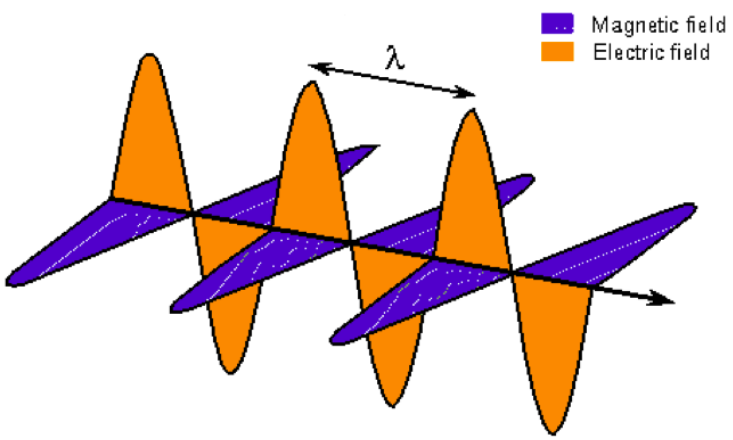

Figure 3.1: Magnetic and electrical fields perpendicular to each other Strobel (2011).

Light can give visual information about the surrounding environment which can be sensed by eye or an optical instrument. In addition it can be used in critical applications such as monitoring or transmitting information. Light is an electromagnetic wave or photon figure (3.1) Strobel (2011) of which Xray, Ultraviolet, Infrared and radio waves are examples. These different waves are distinguished by their wavelength (λ) figure (3.2), travel at velocity of 3.e6 km/sec (1.86 e5 mi/sec)Malm (1999).

Visible light exists in the wavelength range $4.0 - 7.0e{-}7$ m and is usually quoted in nanometers (400−700 nm). The energy of visible light received from an object depends upon the frequency of the wave light incident on the object, and the extent to which it is reflected, scattered or transmitted. So if light interacts with atoms in a material that has an atomic energy level lower than the light energy, the light will be absorbed. This absorption will cause a transition of electrons from the valance energy level to excited energy levels figure (3.3). The detected colour is actually the colour of the light, which has been affected by the energy absorbed by the atoms. Once colour has been detected from the light transmitted through an object, it may be considered as being the colour of the light rather than the colour of the object Faust (1997).

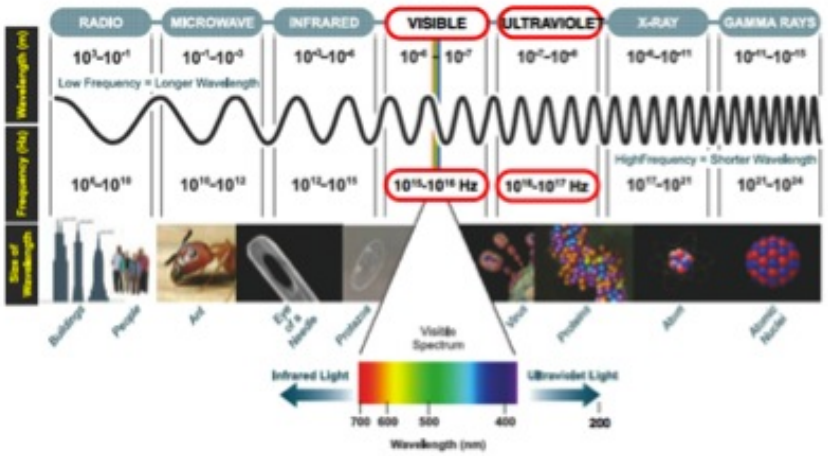

Figure 3.2: Electromagnetic spectrum and illustration of wavelength and frequency.

Ferri (2012)

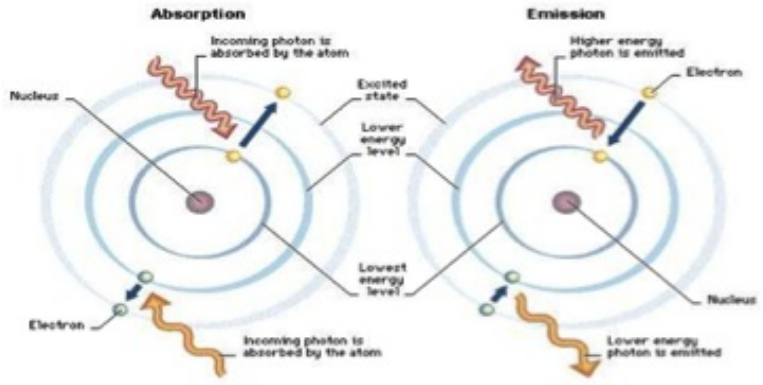

Figure 3.3: Orbital energy level of atom.
Strobel (2011)

3.2.1 Behaviour of light

Light behaves in different ways depending upon the medium through which it travels. The behaviour of light may be described in term of the following attributes:

1. Reflection
2. Refraction
3. Transmission
4. Absorption
5. Diffusion (scattering)

Reflection and refraction can be regarded as forms of coherent scattering, while diffusion is a form of incoherent scattering.

3.2.2 Reflection of light

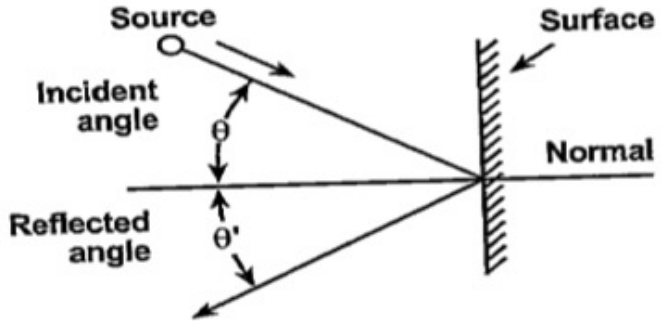

Figure 3.4: specular reflection of light
Khan (2010).

Light from a light source incident upon a reflection surface at an angle θ is reflected at the same angle as θ to the normal to the surface figure (3.4) Snyder (1996).

3.2.3 Refraction of light

A change in the phase velocity of a beam of light can be caused by a change in the density of the medium through which it travels, causing the light to be refracted. This effect will result in the wavelength being changed whilst the frequency remains constant Meister and Sheedy (2000).

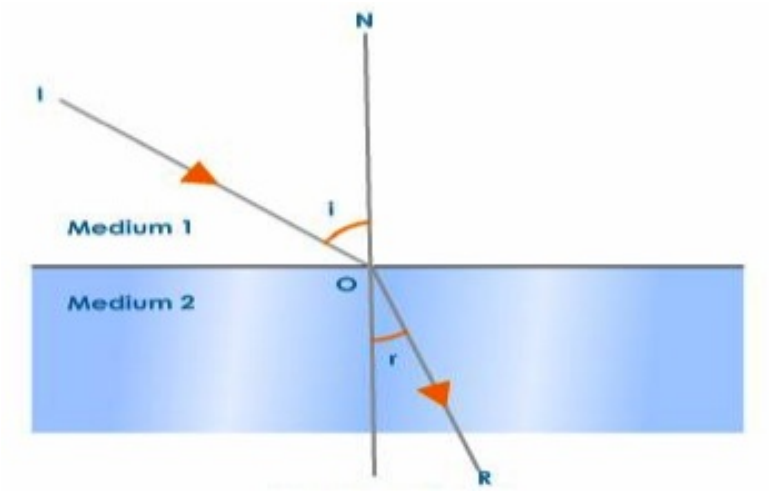

Figure 3.5: Specular refraction
Tutorvista (2012).

Snells law defines the refraction of light as it travels from one material to another, the light path is deflected and its velocity changed. This causes the light to refract, the extent depending on the incident angle (θ) figure (3.5) and the refractive index of the materials Taylor (2000).

The refractive index is defined by the measure of light refraction when passing from one medium into another. It usually changes when a medium is changed from liquid to gas to solid. So any increase in electron density within the materials also increases the reflective index Gunter and Light (1992).

The refractive index of a material (N) is the ratio of the speed of light in vacuum to the speed of light in the material:

$$N = \frac{(speed\ of\ light\ in\ vacuum)}{(speed\ of\ light\ in\ materials)} = \frac{c}{v} \tag{3.1}$$

The refraction loss is the amount of light reflected by the surface of the material and is given by Stockman (2007)

$$RefractionLoss = \frac{(Medium2 - Medium1)^2}{(Medium2 + Medium1)^2} = \frac{(M2 - M1)^2}{(M2 + M1)^2} \tag{3.2}$$

$$M_1 \sin\theta_1 = M_2 \sin\theta_2 \tag{3.3}$$

where medium is the refractive index and θ_1 is the angle between the light wavelength beam and surface normal of medium 1 (M1) and θ_2 is the angle between the refracted light and the normal to the surface of medium 2 (M2) Blackstock (2000).

3.2.4 Transmission and absorption of light

An electromagnetic wave incident upon an object will affect the atoms of the object. In the case of transmission (τ) figure (3.6) the vibrating atoms will resonate for a short period of time with small amplitude before reemitting a light wave. If the object is optically clear then the light will pass through the object with only very small amplitude changes. On the other hand, if the object is not opticaly clear and contains particles, then some of the light energy is absorbed by the atoms of the materials and converted into thermal energy. This may be manifested as a change of wavelength, which can be observed with a spectrum analyser Foot and Kilsby (1989).

Uniformity of the transmitted light is considered as an advantage.

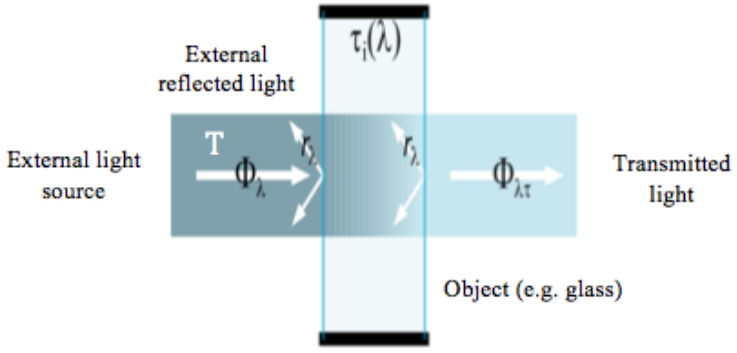

Figure 3.6: External and internal transmission through an object Ryer (1997).

The amount of absorption can vary from one material to another. The variation will depend on the shift in the wavelength and the thickness of the materials. The logarithmic relationship between internal transmission at a given wavelength and thickness is stated by Bougers law Ryer (1997):

$$\frac{\log_{10}(\tau_1)}{d_1} = \frac{\log_{10}(\tau_2)}{d_2} \tag{3.4}$$

where τ_i and d are the internal transmission of the wavelength and the thickness of the materials respectively.

$$\tau_i = \frac{T}{P_d} \tag{3.5}$$

T is the external transmission of the wavelength and P_d is the reflection factor of the material.

3.2.5 Diffusion (Incoherent Scattering)

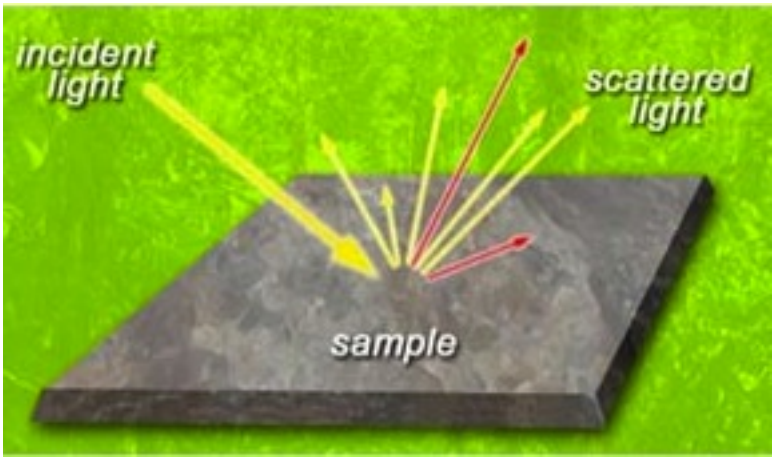

Figure 3.7: Scattered light on the surface of a material Chen (2009).

Diffused (incoherent scattered) light can be defined as follows : Whenever light is incident on a rough surface or material its interaction with atoms that form the medium causes the light to be scattered in many directions i.e. light is deviated from its original incident beam figure (3.7). As a result most objects observed in daily light is due to scattered light Bergström et al. (2005).

Furthermore, the wavelength and the interaction of the scattered light are controlled by the light atoms distribution on the surface of an object. For instance, when the atomic particles are small, such as in clear crystal (less than 250nm diameter), the scattering of the light is uniform over all wavelengths and only the propagation speed of the incident wave is changed Williams (2009).

On the other hand, if the particles are larger than 250nm (e.g gas and liquid), the fluctuations of the atoms can cause extraordinary scattering depending on the interaction of wavelength with these atoms Puentes et al. (2007). Based on this interaction, light can be scattered elastically or inelastically Souza and Miller (2012).

Elastic and inelastic light scattering is a technique used to measure shape, size and index of micro particles Bresch et al. (2008).

Usually most of the scattered light is elastic W_s=W_1 (W_S is the frequency of the scattered radiation and W_1 is the frequencies of monochromatic electromagnetic waves) but also it has a small amount of inelastically scattered light (Raman Scattering) W_S=$\mathrm{W}_1\pm$ W_M (W_M is the magnitude of the transition frequency i.e. change in radiation between different frequency). So the frequency of the incident light is equal to the frequency of the scattered light in the case of the elastic scattering due to the molecules not changing their energy state, but in the case of the inelastic scattering the frequency of the incident light is different from the frequency of the scattered light i.e. due to the molecules changing their energy states Horn (2009).

3.3 Fundamentals Of Chromatic Monitoring

Complex colour problems are an area that is vital to researchers as colour may be used for many different applications such as monitoring Jones et al. (2009).These complexities in colour may be over come by improving contrast or separation, which will lead to the introduction of a mathematical algorithm, which will act as a process for colour classification. This process will extract useful information concerning the spectral properties of the condition and discovering the best match from a set of known conditions to implement the recognition task Arivazhagan et al. (2010).Chromaticity is a monitoring technique concerned with addressing different signals detected by different detector processors with at least three overlapping filters. These chromatic filters can distinguish between complex spectral data. The complex spectral data are simplified to at least three parameters, (R,G,B) which will have a high level of traceability and contain sufficient

information Jones et al. (2009).

3.3.1 Colour

Colour is considered to be one of the fundamental characteristics of a visible image. It plays an important role in identifying an image or object for visual perception. Colour is also known to be one of the most active topics in intelligent monitoring systems since it is used to analyze complex compounds such as liquids for example by extracting pixels out of images and compering the intensity of these pixels with the intensity of pixels from other images. The pixels can be used to determine the quality of a liquid compound by extracting the three components RGB Sahin (1997). The physical properties of a liquid are commonly determined by the perception of colour, temperature, turbidity, odor and particles. Colour is an important aspect since it can determine the physical condition of the liquid without any invasive test Manahan (2000).

Colour identification can be defined as the measure of the intensity of light (electromagnetic radiation) in the spectrum in the visible region (380 to 770 nanometer), where the spectrum is considered to be the analysis of the mixture of light and colour which describe an object or component that can be addressed by a detector. The human eye or camera are examples of such detectors Willson and Shafer (1991).

Colour vision by the human eye is associated with the reflection of light from a coloured object. The spectral reflection depends on the intrinsic condition of the reflecting surface and the illumination level Woodham (2008).

In 1704 Newton stated that, the difference in colour is related to the difference in the light wavelength. The human eye has developed to be sensitive to visible light blue, green and red colours. Diffrent spectral combinations identify an object in term of its colour ZEMPLÉN (2002).

Colour may be regarded as being represented by three properties hue, lightness and saturation. These properties are psychological aspects of the optical spectrum. Hue is referred to as the effective dominate wavelength of light that is detected by the human eye (retina) causing the sensation of colour as red, green or blue etc. Saturation indicates how widely hue is spread. The lower the saturation the closer the colour is to grey whilst high saturation is close to the pure colour. The range between the high and low saturation represents the hue concentration. Lightness is the strength (energy) of the colour (brightness) ranging from zero (black, no light) to one (white, maximum red, green and blue) Konica Minolta.

(2007).

3.3.2 Human perception system

Humans have five main highly complex sensing systems that monitor the surroundings. Each one of these systems is important, but each one has its own function, which distinguishes it from the other senses AIST (2005).

Light enables a human to visually monitor surrounding objects. Similar to a camera that can capture images, the eye has its own image processor, which consists of millions of processor units. The light contains different wavelengths, which can be affected by factors such as absorption, reflection, refraction, scattering or diffraction in transmission to the human eye pupil through a lens Alshabben (2012).

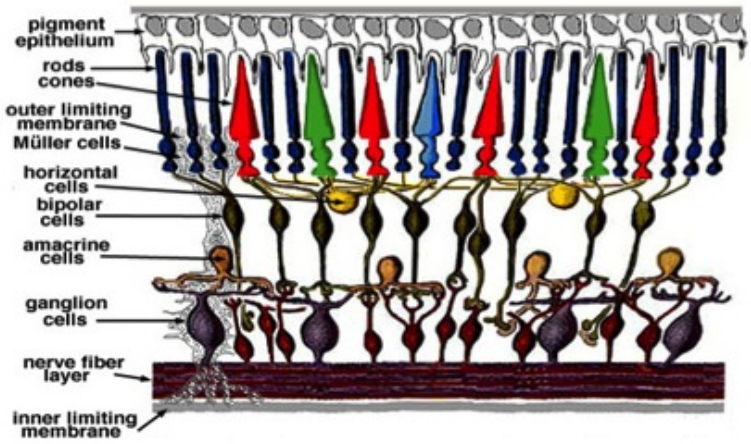

Figure 3.8: Arrangement of retina cells is shown in a cross section Kolb et al. (2005).

A schematic of retina cells and rods is shown in figure (3.8). The cells that constitute the retina are the primary sensory neurones rod and cone photoreceptors. Rods and cones are two different processors. Rods are able to sense black and white and different grey shades i.e. rods do not provide colour sensation and usually operate when it is dark. Cones are the opposite of rods as they sense colours. Cones are separated into three different types; Red, Green and Blue cones. They operate together to analyze colour as sensed by the eye King (2005).

Experiments since 1965 have confirmed that there are three types of cones figure (3.9) Williamson and Cummins (1983) ; one has a high sensitivity at long

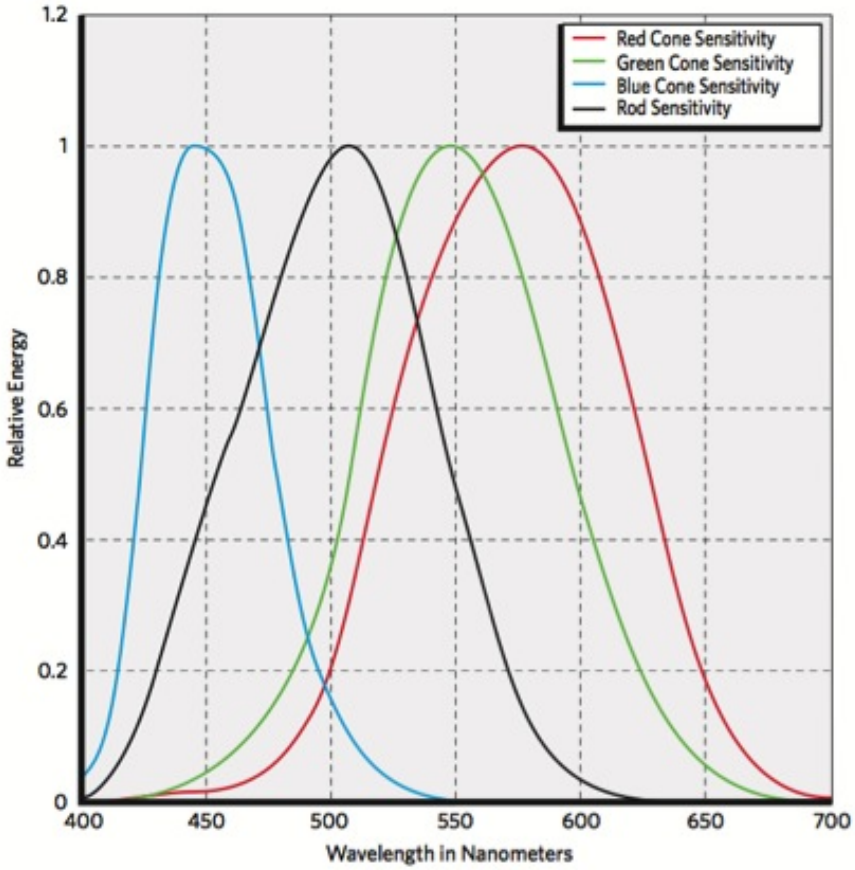

Figure 3.9: Spectral sensitivity of human rod and cone Kodak (2012).

wavelengths of visible light called red, another has a high sensitivity at middle wavelength of visible light called green and the third has a high sensitivity at short wavelength of visible light called blue cone Kodak (2012).

3.3.3 Colour model (RGB Vs. XYZ)

For decades there has been research into developing a uniform colour space Chong et al. (2008). Hermann Graβmann in1853 Parraman and Rizzi (2011) conducted an experiment using a pure primary colour source Red (R), Green (G) and Blue (B), which were weighted between 0 and 100. Hermann was able to measure the sensation of colour C based on the output from the weight of the three primary colours Scarso (2010).

$$C_1 = r_1 R + g_1 G + b_1 B \tag{3.6}$$

$$C_2 = r_2 R + g_2 G + b_2 B \tag{3.7}$$

So

$$C_3 = C_1 + C_2 \tag{3.8}$$

Where

$$C_3 = (r_1 + r_2)R + (g_1 + g_2)G + (b_1 + b_2)B \tag{3.9}$$

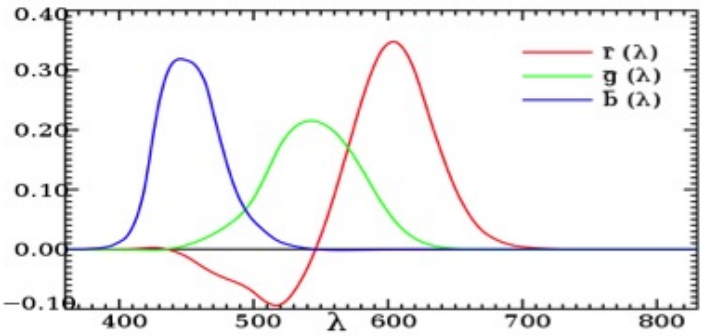

Figure 3.10: colour matching function representing the amount of primary colour needed to match monochromatic test Krzywinski (2012)

.

If C has a spectrum $P(\lambda)$ it is possible to calculate RGB according to the following equations

$$r(\lambda) = \int_0^\infty P(\lambda)\bar{r}(\lambda)d(\lambda) \tag{3.10}$$

$$g(\lambda) = \int_0^\infty P(\lambda)\bar{g}(\lambda)d(\lambda) \tag{3.11}$$

$$b(\lambda) = \int_0^\infty P(\lambda)\bar{b}(\lambda)d(\lambda) \tag{3.12}$$

where $\bar{r}$ $\bar{g}$ $\bar{b}$ are colour matching functions with respect to it's primary colour which are positive real functions varying with wavelength as shown on figure

(3.10) Krzywinski (2012).The calculation of RGB introduced negative colour values when two weighted colours are added without the third colour. This negative value is due to an adjustment made in RGB colour to match the target colour C. i.e.

$$C_X + r_X R = g_X G + b_X B \tag{3.13}$$

$$C_X = -r_X R + g_X G + b_X B \tag{3.14}$$

3.4 Chromatic Transformation

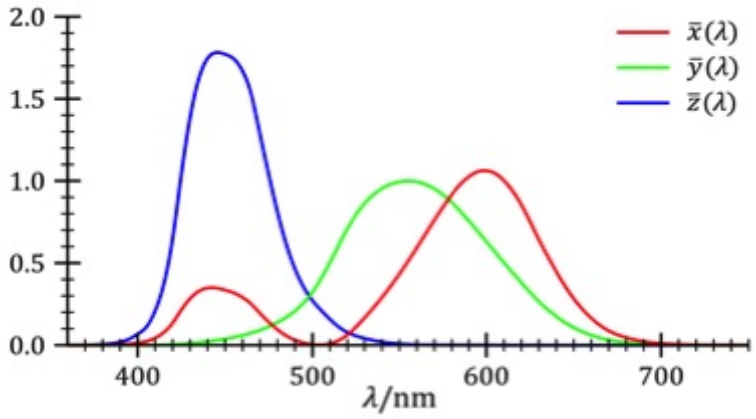

Figure 3.11: Colour matching function with respect to brightness Krzywinski (2012).

In the early 1920s colour was one of the most important phenomena that needed to be defined mathematically. The International Commission on Illumination (CIE) was experimenting with different methods to develop a mathematical model that could define different colours. By 1931 the CIE introduced a new diagram to form a two-dimensional colour coordinate diagram whereby the location of each colour could be determined with respect to its primary colours figure (3.13) Gierlinger (2005). This two−dimensional diagram is a nonorthogonal transformation method that can overcome the negative values. This method converts RGB space values into XYZ space values called CIE XYZ figure (3.12) where all the values are positive. It can also calculate XYZ with given a C and spectrum P(λ)*Fairmanet al.* (1997).

$$X = \int_0^\infty P(\lambda)\bar{x}(\lambda)d(\lambda) \tag{3.15}$$

$$Y = \int_0^\infty P(\lambda)\bar{y}(\lambda)d(\lambda) \tag{3.16}$$

$$Z = \int_0^\infty P(\lambda)\bar{z}(\lambda)d(\lambda) \tag{3.17}$$

where $\bar{x}$ $\bar{y}$ $\bar{z}$ are colour matching functions with respect to the brightness of figure 3.11 Krzywinski (2012)

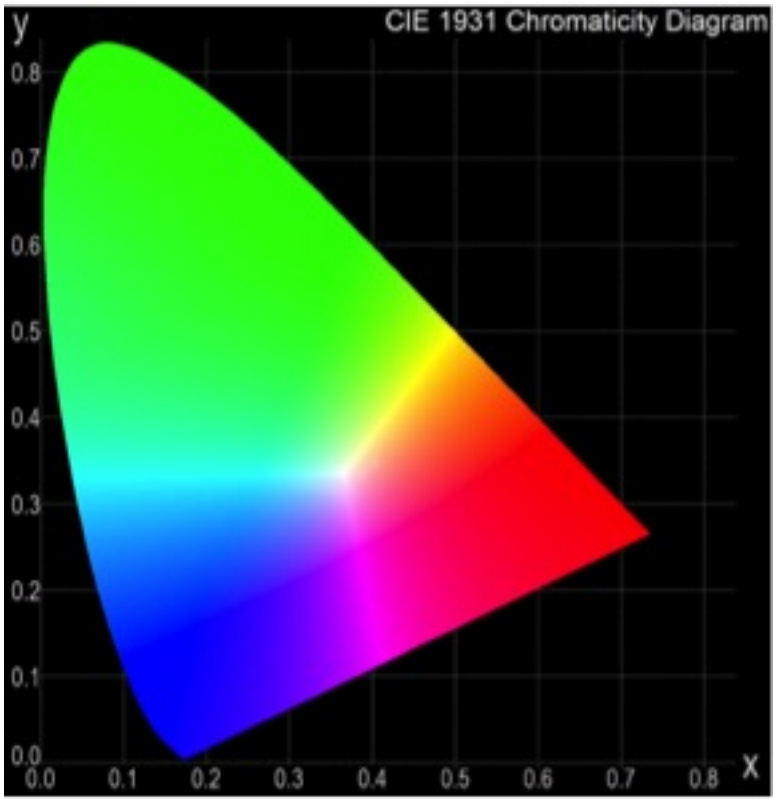

Figure 3.12: Primary colour triangular specifying the colour passed on the X and Y coordinate Nunes et al. (2007)

.

The CIE diagram is useful for plotting the relative extents of parameters since Ford and Roberts (1998)

$$X + Y + Z = 1 \tag{3.18}$$

3.4.1 Linear colour space (RGB)

There are different types of RGB colour spaces depending on the application. The RGB colour space is defined in term of the main three primary colours Red, Green and Blue. A coloured display system (CRT or similar) contains a light source, which uses RGB colour space to display coloured images using RGB pixels Koirala (2007) Linear chromatic RGB can be represented and visualized on a RGB colour cube figure (3.13) with the three axes representing the primary colours Red, Green and Blue. An image is considered black when the red, green and blue are all equal to zero. On the other hand, an image is considered white when the red, green and blue all equal to 1 figure (3.14) Ford and Roberts (1998).

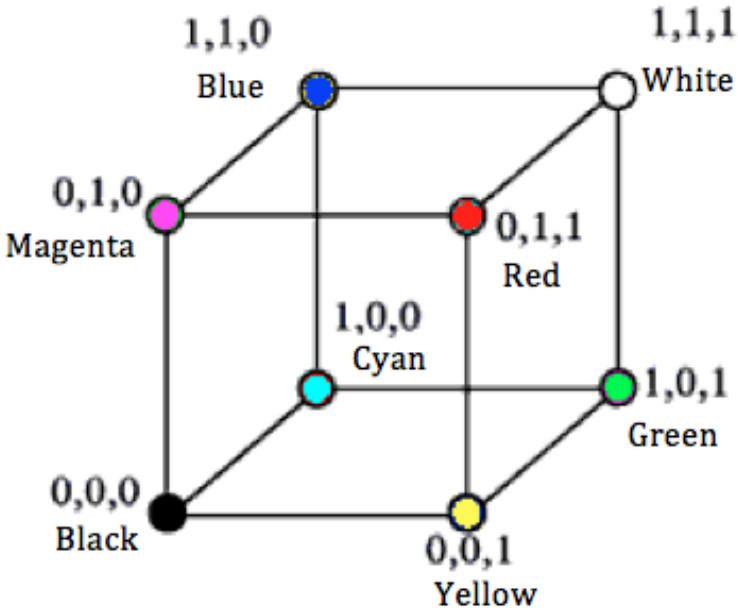

Figure 3.13: Color space tristimulus cube (RGB)
Otto (2000).

White is represented at one corner of the colour cube with coordinates of 111 whilst RGB at the opposite corner black is represented with coordinate of 000 for RGB. The diagonal between the white and black points represents the grey scale Mihai and STRĂJESCU (2007).

This Tristimulus cube is created from three primary colours (red, green and blue), which are matched with a set of reference colours such as monochromatic

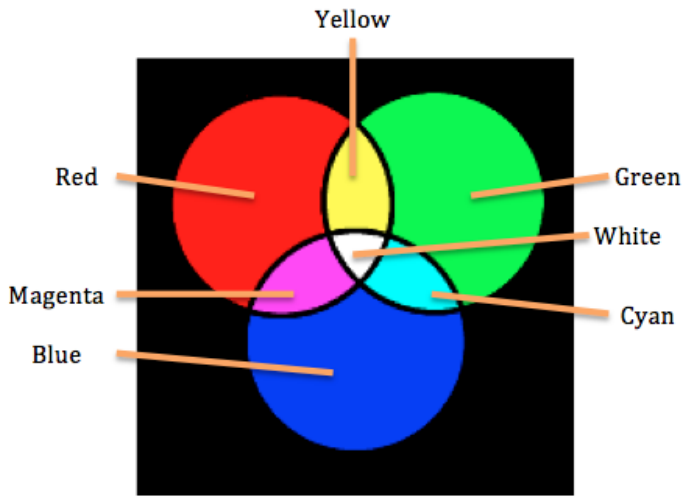

Figure 3.14: Represents white based on RGB being equal to 1 (or black when 0) Rojas (2012).

colours Stone (2003).A linear interpretation of the human colour vision system that respects the addition of colour follows the principle of superposition as illustrated on figure(3.14), which was introduced by Grassmans Jacobs (2007).

Grassmans law states that if the spectral power distributions of two colours were combined, then the value found by an observer from these combined spectral power distribution will be the sum of each primary colour of the two spectra Poynton (1995).This means that the blended colour will contain the primary colours of 1 and 2. So the primary colours will be added as follows:

$$R = R1 + R2; G = G1 + G2; B = B1 + B2 \tag{3.19}$$

3.4.2 Non linear colour system (HLS)

Transformation of the RGB colour space to a cylindrical coordinate HLS system can be achieved in terms of the parameters (Hue, lightness and saturation) Hanbury (2008).

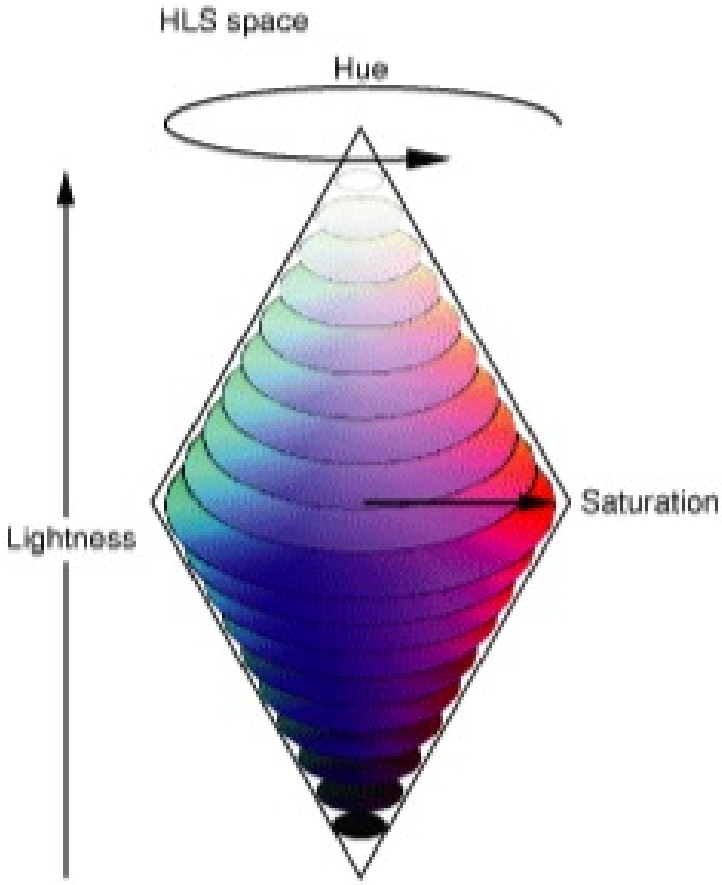

Figure 3.15: Double cylindrical coordinate HLS
Developer (2005).

In the HLS coordinate system figure (3.15) the vertical axis represents brightness. Hue correspond to the chromatic angular coordinate and saturation corresponds to the distance from chromatic axis Hanbury (2002).The transformation from RGB colour space to an HLS space is non linear and can be described by the following algorithms Jones et al. (2009).

$$\begin{aligned} H &= 240 - 120.g/(g+b) && r = 0 \\ &= 360 - 120.b/(b+r) && g = 0 \\ &= 120 - 120.r/(r+g) && b = 0 \end{aligned} \tag{3.20}$$

$$L = (R + G + B)/3 \tag{3.21}$$

$$S = [max(R, G, B) - min(R, G, B)]/[max(R, G, B] + [min(R, G, B)] \tag{3.22}$$

Where

$$r = R - min(R, G, B) \tag{3.23}$$

$$g = G - min(R, G, B) \tag{3.24}$$

$$b = B - min(R, G, B) \tag{3.25}$$

3.5 Chromatic Modelling Map

Chromatic maps are used to display data extracted from a complex condition by transforming the extracted data from nonorthogonal processors such as RGB (figure (3.16) Gaussian processor). This enables different information to be conveniently distinguished on 2−D polar diagrams, Cartesian XYZ diagram etc Jones et al. (2009).

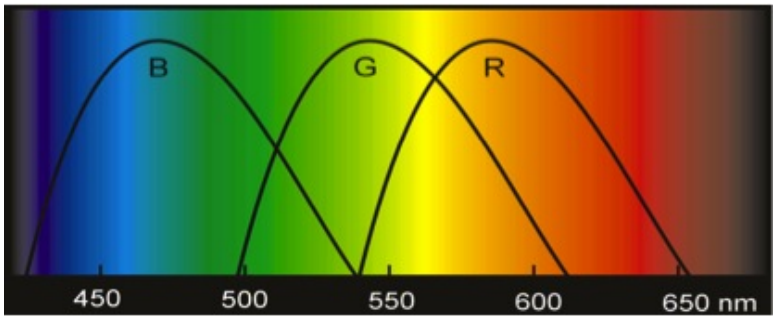

Figure 3.16: Gaussian signal processing filters.

3.5.1 2−D Polar diagram

Hue, lightness and saturation are chromatic parameters obtained from the transformation of the signal under the RGB filters. Hue (H), Lightness (L) and Saturation (S) may be represented on 2−D polar diagrams of hue-lightness (H−L) or hue-saturation (H−S) Jones et al. (2009).The values of HLS may be regard as representing a complex signal as an equivalent Gaussian signal.

A polar plot figure (3.17) can represent hue as the azimuthal angle from 0 to 360 degrees. Hue can be represented in three areas, the first area 0 to 120, is the red dominant area, the second from 120 to 240, represents the green dominant area and the last area from 240 to 360 represents blue. Lightness is the radial parameter from the origin (0,0) to the circumference (L=1.0). Alternatively H−S can be represented on a polar diagram where (1−S) figure (3.19) is the spread of the signal figure (3.18).

3.5.2 Cartesian XYZ diagram

A Cartesian XYZ diagram is shown on figure (3.20). It provides more detailed information about the relative contribution of R, G or B than Hue.

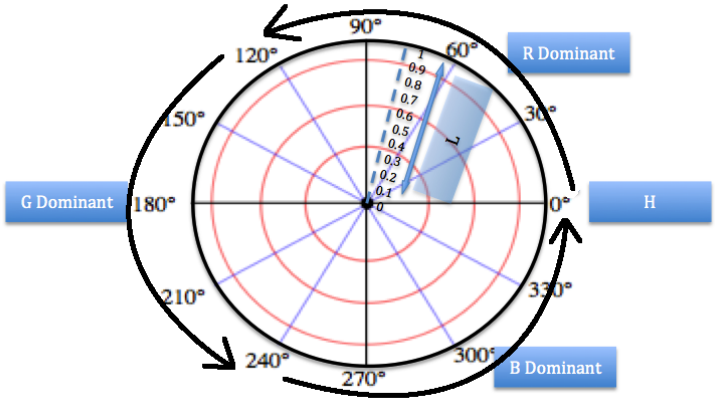

Figure 3.17: Polar diagram of H vs. L.

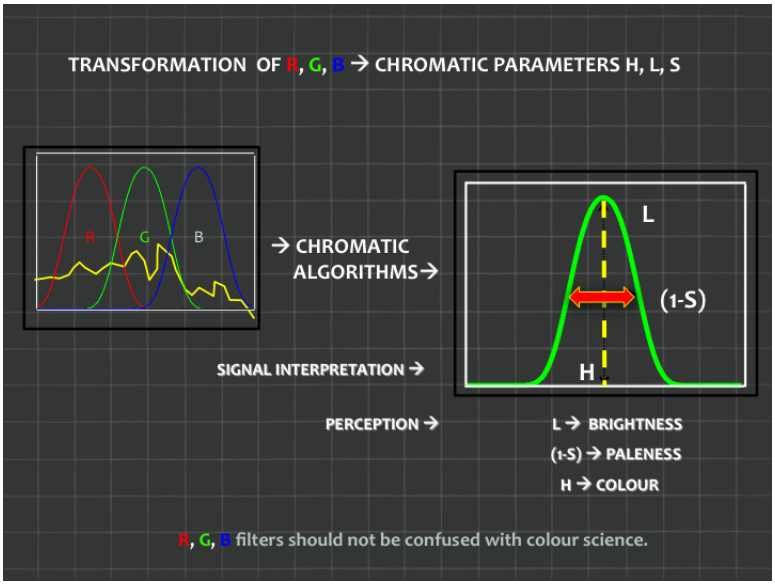

Figure 3.18: Transformation of RGB to chromatic parameter HLS.

$$X = R/(R+G+B) \tag{3.26}$$

$$Y = G/(R+G+B) \tag{3.27}$$

$$Z = B/(R+G+B) \tag{3.28}$$

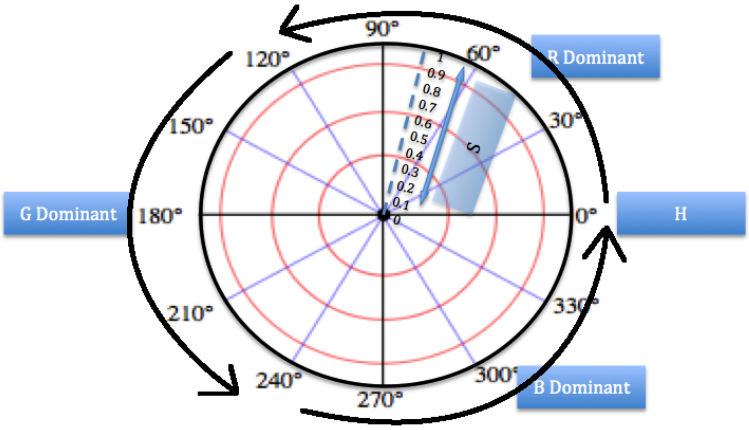

Figure 3.19: Polar diagram of H vs. S.

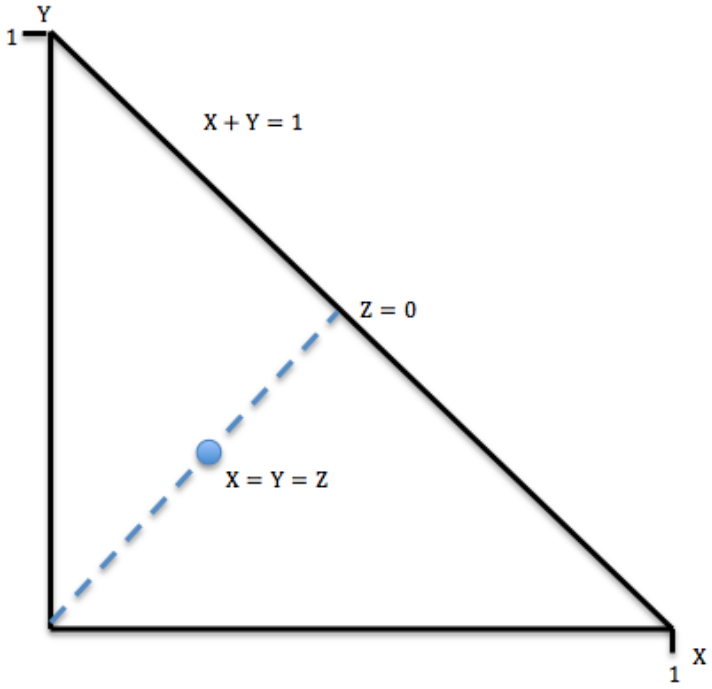

Figure 3.20: XYZ Cartesian diagram.

X, Y, Z is a representation of the relative contribution of R, G and B (section 3.3.3) with the following properties:

1. XYZ are independent of effective light intensity $(X + Y + Z)$ equations 3.26,3.27 and 3.28.
2. $X + Y + Z = 1$.
3. Locus $X + Y = 1$ correspond to $Z = 0$.
4. $X = Y = 0$ corresponds to $Z = 1$.
5. $X = Y = Z = 0.33$ represents the point at which R,G,B are equal.
6. $X/Y = R/G$ is a distmulus dominant wavelength.

$X + Y + Z = 1$ means that if two terms are known the third term can be obtained. In this way, three dimensions can be represented on a two dimension graph.

3.6 Imaging Systems

3.6.1 CCD and CMOS camera

CCD and CMOS image sensors are two different technologies. Both technologies convert photons into electrons. The difference between CCD and CMOS is that the CCD figure (3.21) is a charge coupled device where each electron produced is processed through a limited number of output nodes Litwiller (2001).Once the electrons are transferred they produce a voltage, which appears as an analogue signal for a processor Axis (2010).

CMOS figure (3.22) is a fabricated semiconductor device. It is a more advanced technology since each pixel has three transistors, which allow the pixel to have its own charge to voltage converter Wimmer (2009).

Also a CMOS circuit chip contains a digitizer, amplifier and noise elimination correction, which can give highly accurate images Helmers and Schellenberg (2003).

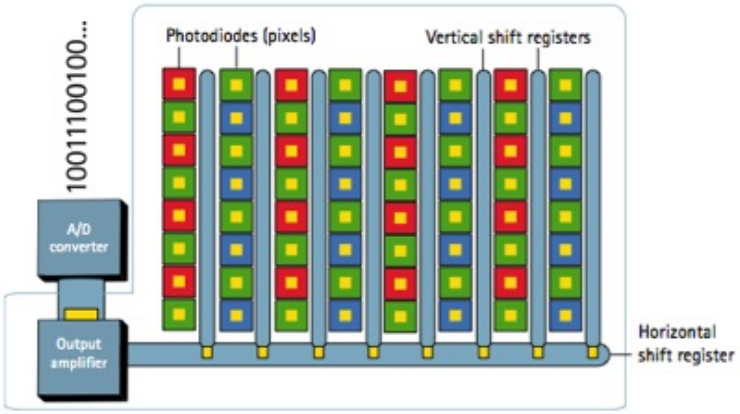

Figure 3.21: Diagram of a CCD camera pixel array Axis (2010).

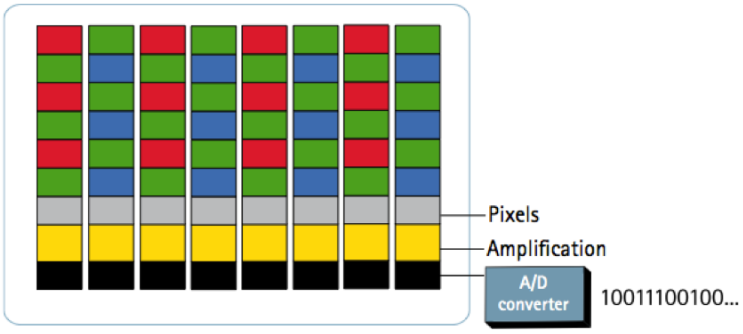

Figure 3.22: Diagram of a CMOS camera pixel array Axis (2010).

In addition, the number of CMOS sensors are less than the number of CCD sensors (figure 3.23) since they are easier to design and fabricate Zurich (2001).

The main different between CMOS and CCD cameras are: CMOS processor contain analog to digital signal converter, amplifiers and additional processing for high resolution picture. CCD processor analyzing image signal outside the processor. In addition, CMOS has a lower power consumption compared to CCD. CMOS processor can be affected by any structured noise. One of the major different between CMOS and CCD is the ability of CMOS to perform malty view streaming and it has one charge to voltage converter in each pixel, were CCD has one per sensors. Finally there is a difference in light sensitivity between CMOS

and CCD cameras Litwiller (2001).

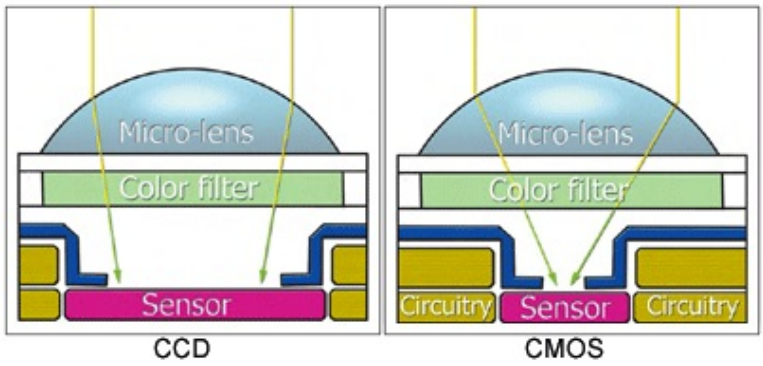

Figure 3.23: Cross section of a CCD and CMOS fabricated semiconductor sensor Digital SLR photography (2012).

3.7 Summary

This chapter has summarized the relevant properties of monochromatic light, particularly those associated with light interacting with liquids and particles. The significance of polychromatic light and the concept of colour discrimination with the human vision system have been described. The manner in which quantification methods of colour science can be extrapolated for the more general case of chromaticity has been explained. The manner in which the generic nature of chromaticity enables information contained in polychromatic light signals to be extracted has been considered and its significance for the present research indicated.

Chapter 4

OPTICAL INSTRUMENTATION DEVELOPMENT AND EXPERIMENTAL ARRANGMENTS

4.1 Introduction

This chapter describes optical instrumentation developed for chromatic oil analysis. The optical systems developed included the following:

- An optical system for addressing a cuvette containing the oil sample based upon a VDU screen as a controllable uniform light source and a webcam or a mobile phone camera for capturing images.
- An optical system used for addressing the cuvette oil and particles captured on a filtere paper using a conveniently collimated LED light system design.
- An optical spectrum system used for monitoring the optical transmission through the oil using a VDU illumination source.

4.2 Equipment For Oil Sample Monitoring

A cuvette and a filter paper are the primary elements used for all the experiments performed. The cuvette was used to contain an oil sample, transparency being an essential feature of the cuvette to allow light to be transmitted through the oil samples.

4.2.1 Cuvette structure

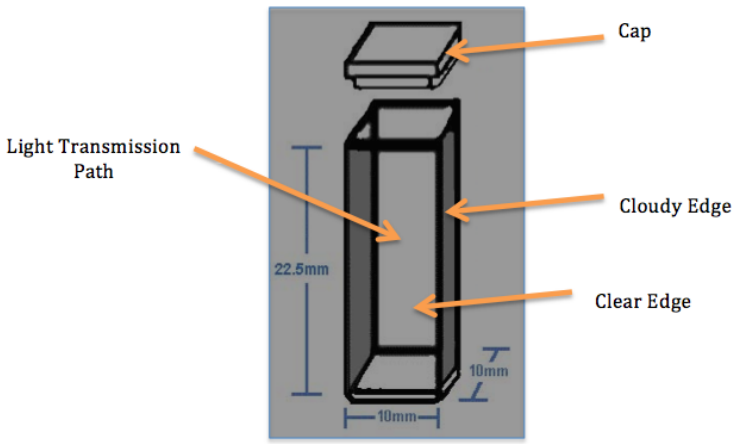

Figure 4.1: Schematic of the cuvette structure Scientific (2012).

Figure (4.1) shows a schematic diagram of the plastic transparent cuvette. It consisted of a small tube of square cross section closed at one end and open at the other. These cuvettes were made to hold samples for spectroscopic experiments Scientific (2012).

Two opposite surfaces of the cuvette are clear for light to be transmitted through them and the other two side faces are cloudy. A cap is used to keep samples away from surrounding environment such as air etc.

4.2.2 Paper filter

A filter paper is a semi permeable paper, which is normally placed perpendicular to either a liquid or airflow. During the course of this investigation the filter paper is used to separate solid particles from transformer oil Whatman (2009).

There are two types of liquid filter papers depth and surface filtration figure (4.2). Taking the case of depth filtration first, the particles are passed through a bed of granular material, which retains the solid particles making it less susceptible to clogging due to the larger filter surface area. The second type of commonly used filter is surface filtration where the solid particles are effectively sieved out of the oil, the size of the filtered solid particles are typically greater than 2 micron Jakob et al. (2005).

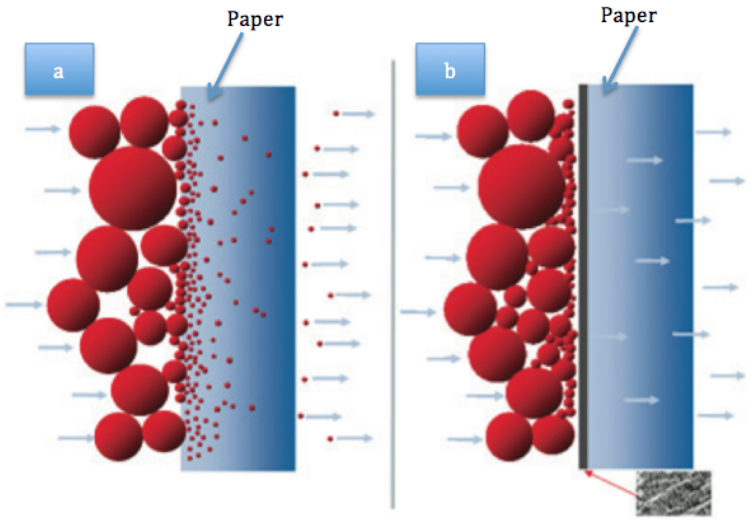

Figure 4.2: Schematic of filter paper cross section *a*)Depth filtration *b*)Surface filtration

Jakob et al. (2005).

4.3 System For Maintaining Back Illumination Of Oil Samples

Polychromatic light transmitted through an oil sample can provide useful information about the oil condition via preferential absorption or scattering within various wavelength bands.

The polychromatic signatures of various oils may be obtained using chromatic analysis techniques (chapter 3) applied to signals acquired with two method a) spectra obtained with a conventional spectrometer (Stellar Net EPP2000), b) the R, G, B outputs from a CCD camera (MAD compact *III*). In both cases,

uniform, two-dimensional illumination was obtained using the screen of a VDU as a light source described by Jones et al. (2009).

This provided the possibility of tuning the spectrum of the illumination via software installed on a laptop computer connected to the VDU which also receives an image of the screen illuminated oil sample via a CCD camera to which it was also connected.

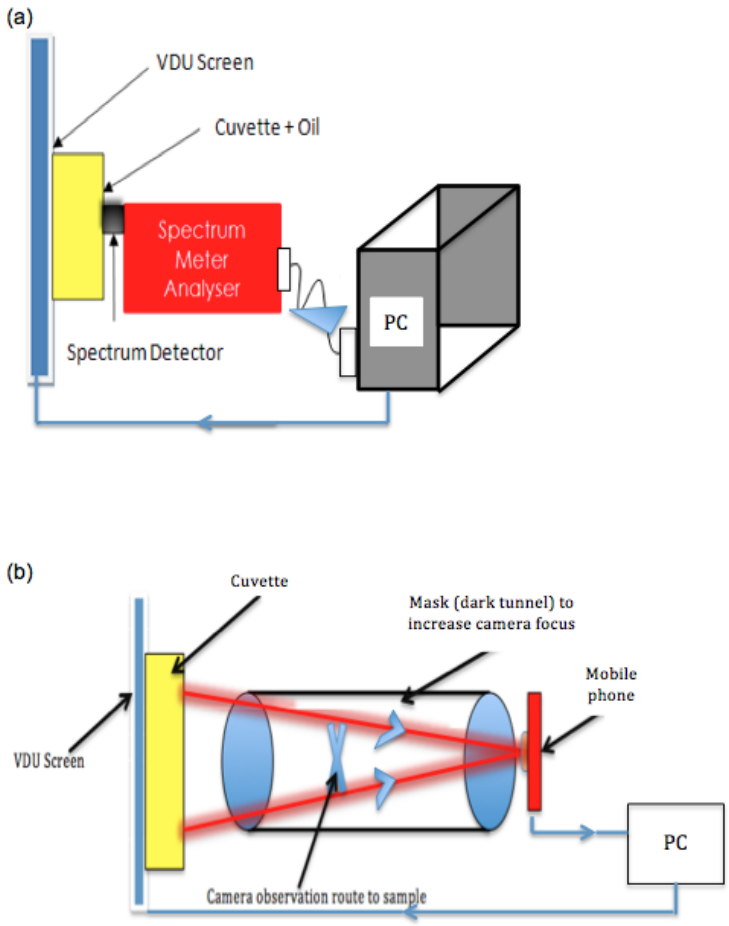

Figure 4.3: Schematics of monitoring systems *a*)Spectrum analyser *b*)Mobile phone monitoring using a VDU screen as a uniform light source Donaldson (2012)

.

The layouts of the spectrum based optical system and CMOS optical system are shown on figures (4.3) (a) and (b) respectively. Figure (4.3) (a) shows a VDU screen, which provides the back light illumination, cuvette which represents the container of the oil sample (section 4.2) in front of the VDU screen, spectrometer (StellarNet Inc. EPP2000) and a laptop for data capture and processing. The system in figure (4.3) (a) is similar to figure (4.3) (b) except for the introduction of a tunnel mask and a CMOS camera (MDA compact III) which replaced the spectrometer.

4.4 Description Of Laboratory Experiment

The connected computer controlled the colour and brightness of the light from the VDU screen. Consequently the VDU screen controlling software formed a tool for providing a uniform light source. Light produced by the screen, which passed through the sample in the cuvette, was captured for analysis using the camera and droptry software (appendix F1).The processed data was formatted in a text file as R, G and B (Red, Green and Blue) and H, L and S (Hue, Lightness and Saturation) (appendix F1, figure F2).

4.4.1 Spectrometer wizard and telechromatic monitoring (CMOS camera)

Spectrometer analyzer wizard software was used to translate data from the spectrum of figure (4.4) (a) detected by the CCD (Charge Coupled Device) or PDA (Photo Diode Array) into a spectral distribution. Such complex spectra may then be analyzed using chromatic filters (R,G,B), the output of which can be transformed to yield signal defining parameters such as H,L and S or X,Y and Z (chapter 3, section 3.3).

An HTC MDA compact mobile phone (weight 127 gm) was used to provide wireless transmission of a captured cuvette and sample data. This mobile phone was capable of capturing an image and sending it to a central command by MMS/internet or to a computer via a USB cable or Bluetooth. The handset shown on figure (4.4) (b) had a Microsoft Windows operating system with an integrated 2-mega pixel camera.

4.4.1.1 Settings applied to a telechromatic mobile phone camera

There are various camera settings, which can be employed on the mobile phone camera.

Figure (4.5) (a) shows a screen display with a sample image centrally and the various options available peripherally. These include:-

1. The mode setting function used to control the R, G and B gains of the camera by controling the exposure.

2. The Brightness function was used to accomdate light levels of the object.

3. The zoom function was used to control the reslution of the image i.e. the number of pixels covered on the image.

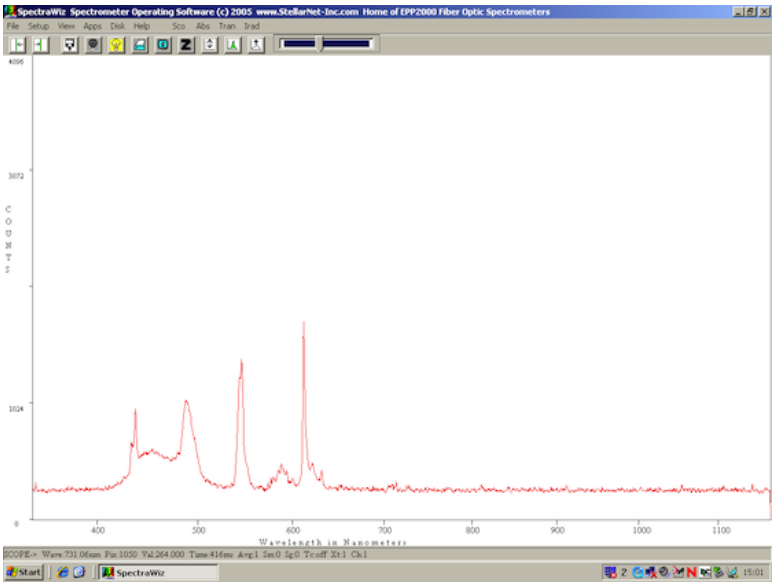

(a)

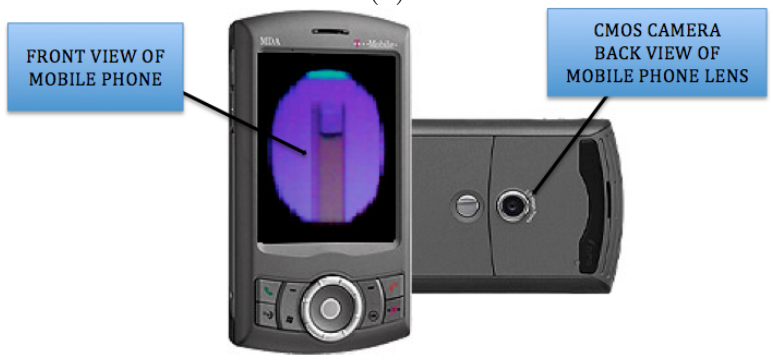

(b)

Figure 4.4: *a*)Spectrometer software analyser prompt display *b*)HTC MDA mobile phone.

4. The three snap shot function was used to obtain three sequential images so that a choice of images was available.

5. The output image size control function was used to optimise the image size for analysis.

These various functions were setup manually to the values indicated on figure (4.5) (b). They could be varied to accommodate the behaviour of the camera and adapted in a compatible way with the background screen.

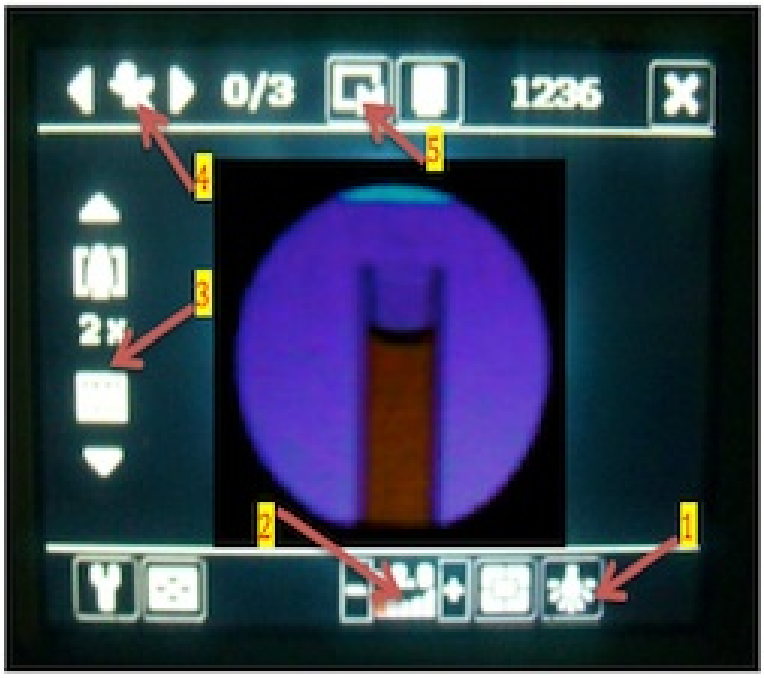

(a)

1		Mode setting for the camera (e.g. fluoresent setting).
2		Image brightness control (e.g. -2.0).
3		Zoom function used to increase resolution (e.g. a 2X).
4		3 Snap shots to be taken sequently.
5		Output image size (e.g. medium).

(b)

Figure 4.5: *a*) View of screen with sample in field of view. *b*) Camera setting options.

4.4.2 Portable chromatic oil monitoring system (PCOMS)

The portable Chromatic Oil Monitoring System is a system, which has been designed for the purpose of laboratory tests. This system was operated in a dark room and used the VDU screen for transmitting light through an oil sample to a receiver (CMOS Camera), which captured an image of the sample as explained

in figure (4.6).

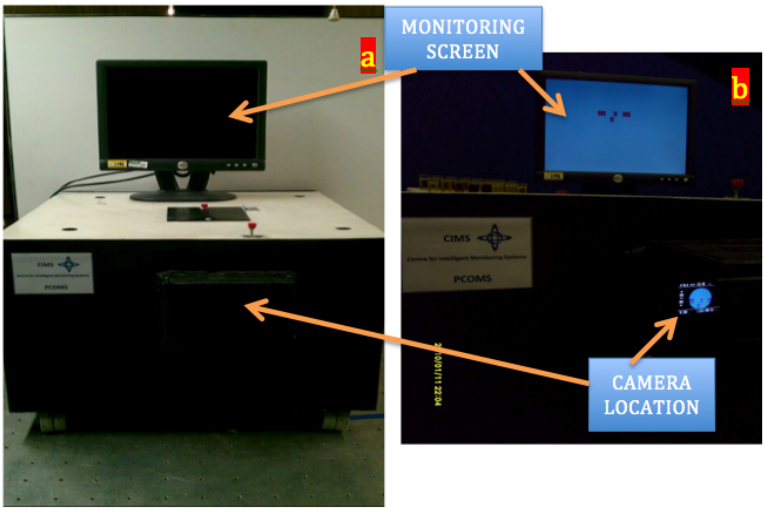

Figure 4.6: *a*) Portable Chromatic Oil Monitoring System *b*) PCOMS camera and monitoring screen location.

Figure (4.6) (a) shows the actual PCOMS. Figure(4.6) (b) shows the location of the camera (CMOS Camera) at the front of the system and a monitoring screen that displayed the camera's captured image inside the portable dark system.

Light is introduced from an LCD screen and transmitted through the sample. Transmitted light will be received by the CMOS camera.

Examples of Images of various oil samples images taken from PCOMS with VDU background screen are shown on figure(4.7).

These images of different oil samples taken by a CMOS camera and representing the following conditions:

E Empty cuvette.

T1 Good oil sample.

T5 Moderate degraded sample.

T10 Highly contaminated sample.

Perceptual differences are apparent between the various samples shown.

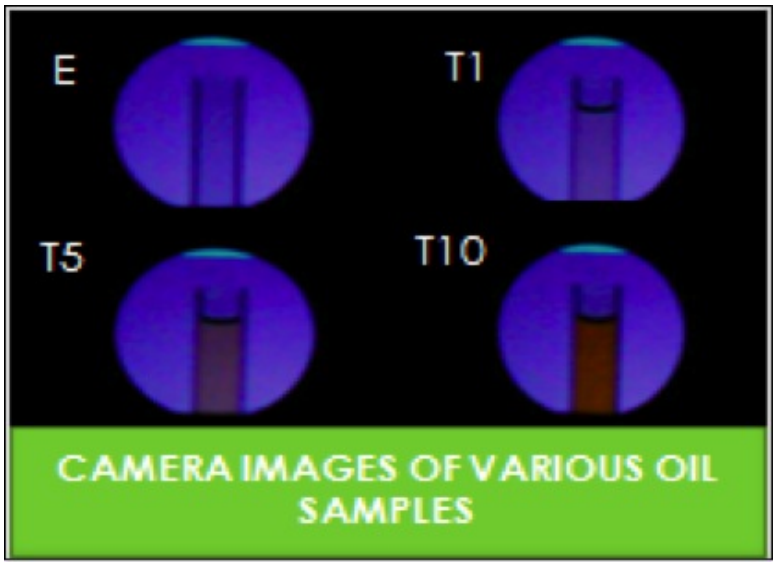

Figure 4.7: Examples of images of different oil samples images taken by a CMOS camera.

4.4.3 LED based system

A system was developed for producing light from a white LED through an optical diffuser element and a coloured transparent plastic film. The colour of the transparent film was made to form a background screen used in the PCOM system.

4.4.3.1 Spectrometer and LED based system

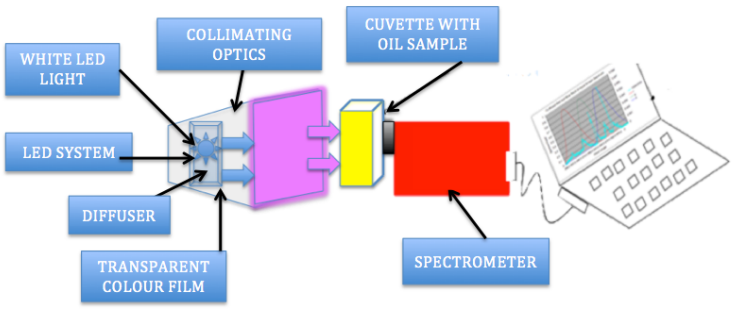

Figure 4.8: LED source with coloured transparent film and spectrum analyser.

Figure (4.8) shows a schematic diagram of the LED based system. Light pro-

duced by the LED passes through the transparent film before being transmitted through an oil sample contained in a cuvette. A spectrometer receives the signal to produce digitised data.

Spectrum analyser and LED system setup

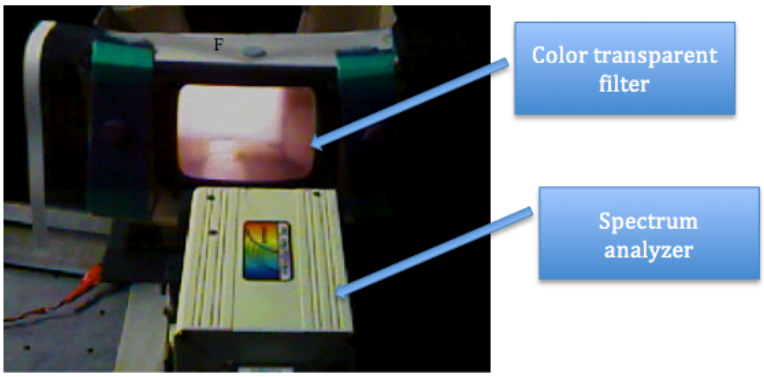

Figure 4.9: LED and spectrometer.

Figure (4.9) shows the actual setup of the system with a spectrum analyser. The image shows how the white LED based light is affected by the transparent coloured plastic.

4.4.4 LED system with CMOS camera

A CMOS camera was used to capture images of various oil samples using the background light provided by the LED system. The LED system was situated inside the portable chromatic oil monitoring system (PCOMS) figure (4.6) replacing the VDU monitor background screen.

4.4.4.1 Schematic diagram of the CMOS and LED system

Figure (4.10) shows a schematic diagram of the LED system. It shows the location of the cuvette containing different samples of degraded oil, an optical collimating unit to increase the camera resolution and a CMOS camera acting as a receiver. A coloured light filter (printed acetate) is used to introduce a similar light wavelength to that produced by a VDU screen.

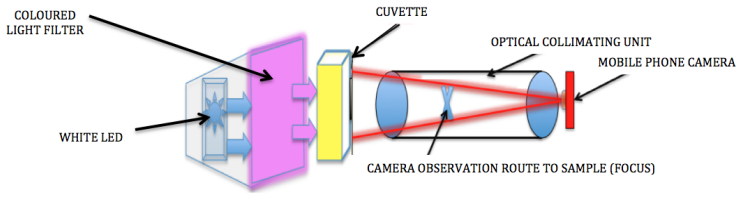

Figure 4.10: CMOS monitoring of oil using LED produced light with coloured transparent plastic filter.

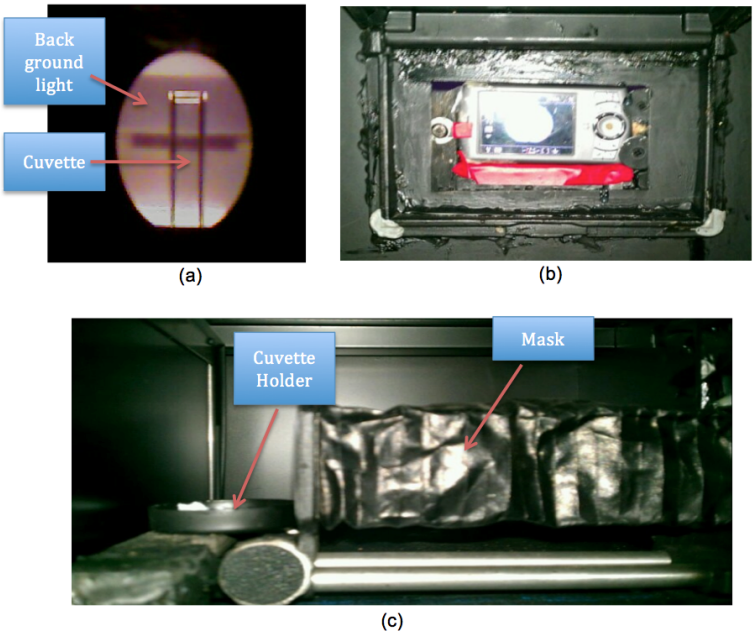

Figure 4.11: a) Components of the LED-CMOS system inside PCOMS.
b) CMOS holder on the PCOMS.
c) The mask (the camera tunnel).

4.4.4.2 CCD camera and LED system

Figure (4.11) (a) shows an empty cuvette in front of the viewing screen. Light is transmitted through the plastic coloured film and then through the cuvette, which affects the spectrum of the transmitted light. The CMOS camera figure (4.11) (b) receives the transmitted spectral signal. The collimating unit shown in figure (4.11) (c) is used to focus more on the monitored area and prevent any interference from extraneous light.

4.4.4.3 Examples of various oil samples from PCOMS with LED illumination

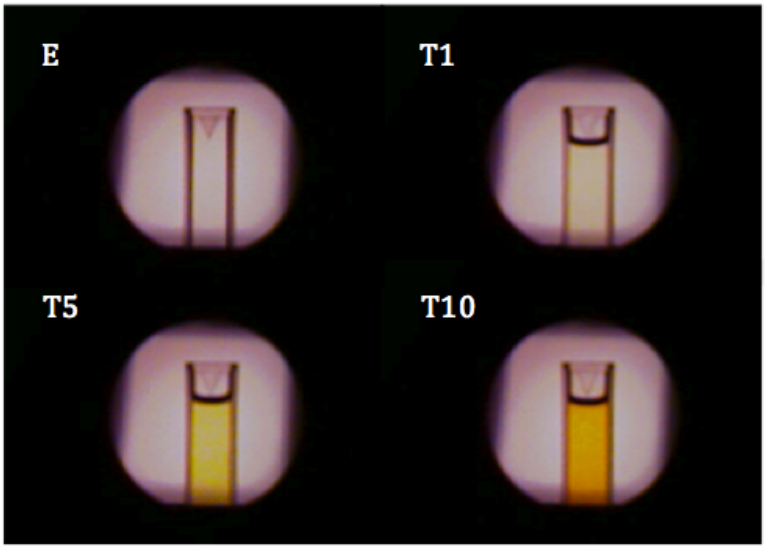

Figure 4.12: Images of different contaminated oil samples obtained with the PCOMS and LED illumination.
(E) empty cuvette.
(T1) fresh oil.
(T5) moderate degraded oil.
(T10) highly degraded oil.

Figure (4.12) shows examples of various oil sample images taken with a CMOS camera with LED illumination figure (4.10). This illustrates the kind of change in the images obtained with the LED light source.

4.4.5 Oil particles monitoring

Filter paper is a barrier with a semi permeable property, which allows liquid to pass through it and separate it from particles, sludge or any mixed compounds contained in the oil Jakob et al. (2005).A funnel is used to control the flow of liquid. It has a narrow tube connected to a wide diameter tube.

4.4.6 Funnel and filter paper system

The oil was filtered using a paper filter introduced into the cone at the top of the funnel. It was noticeable that a fresh oil sample was absorbed and passed through the filter paper more rapidly than other contaminated samples. Moderate and degraded samples took longer to be filtered depending on the contamination level.

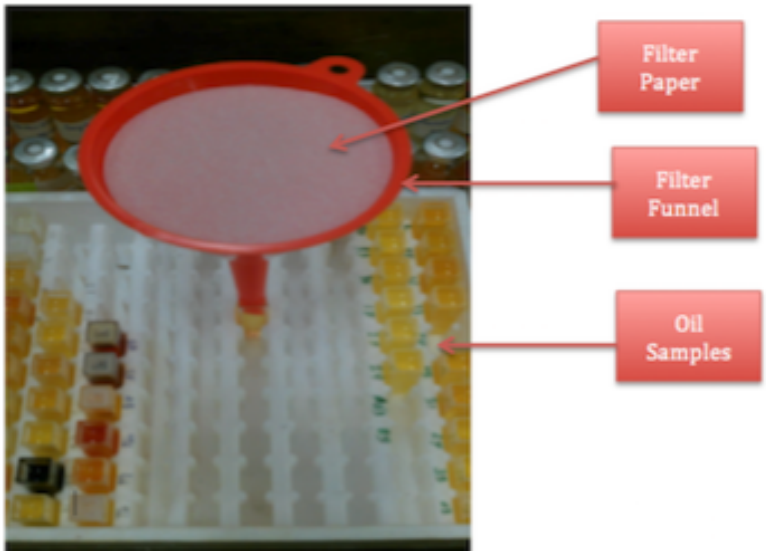

Figure 4.13: Filter paper placed in a funnel.

Figure (4.13) shows a filter funnel system used for filtering an oil samples. The oil sample was poured on to the filter paper from the top of the funnel, so that the particles in the oil were trapped on the surface of the filter paper. Once an oil sample was filtered it was introduced into the LED and monitoring system (subsection 4.4.5).

4.4.6.1 Examples of filter papers with different particles

Figure (4.14) shows different filter papers contaminated with different degraded oil samples. The filter papers used in this experiment were Qualitative filter paper. It is made from refined pulp and linters and with more than 95% alpha cellulose content which acts as a semi permeable paper barrier Sartorius (2012).These filter papers were used to remove solid particles from the liquid oil.

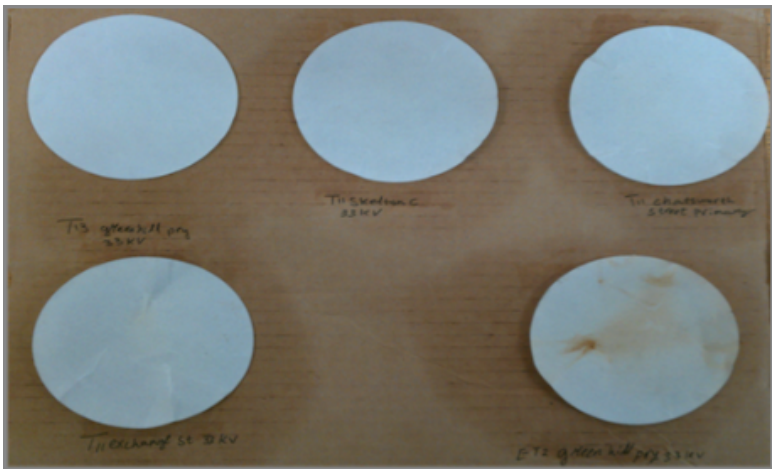

Figure 4.14: Examples of different contaminated oil sample filter papers.

4.4.7 LED light addressed filter paper

A simple approach for confirming the presence of any particles in the oil samples has been adopted. This involves pouring the oil through a filter paper (using the surface filtering technique descried in section 4.2.2) and optically examining both the filtered oil and any sediment remaining on the filter paper.

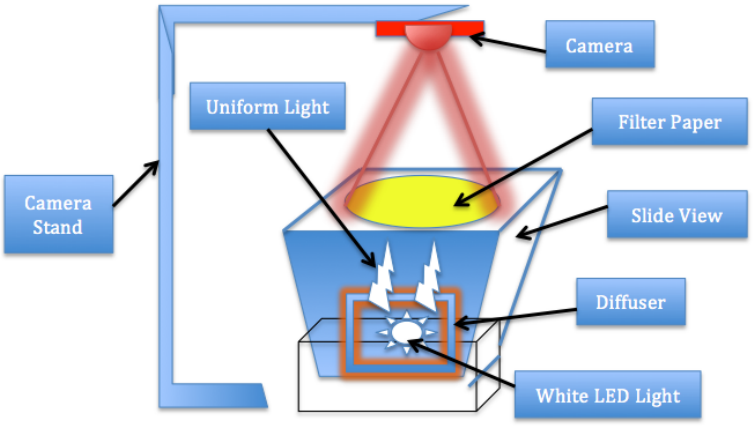

Figure 4.15: Schematic diagram of system for adding optically addressing sediment on Filter papers.

A schematic diagram of a system used for addressing a partially laden filter

paper is shown on figure (4.15). This utilizes the LED source (descried in subsection 4.4.3). Light from the LED is passed through the diffuser and then through the filter paper, which holds particles and other compounds, such sludge, dirt etc. before being captured by the CMOS camera. Once the image has been captured, software is used to analyze it in terms of R, G and B (chapter 3, subsection 3.4.1).

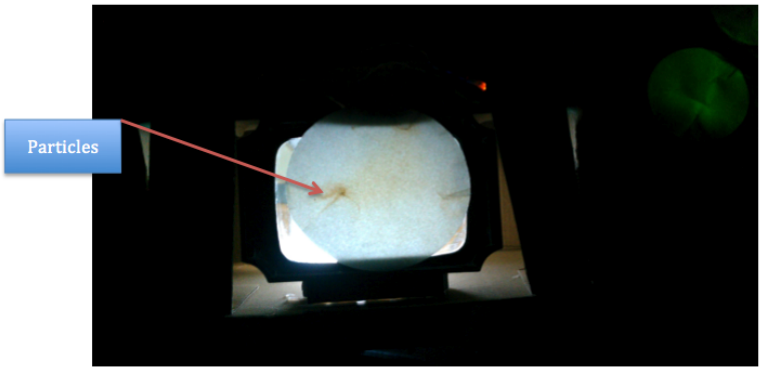

Figure 4.16: View of a filter paper placed on the screen of the LED unit.

Figure (4.16) shows an image of a backlit filter paper using the LED source. This corresponds to a highly contaminated sample (ET2 Green Hill pryb33KV) and shows clearly a trace of particles on the surface of the filtered paper.

4.5 Summary

This chapter has described the oil sample handling and processing procedures, followed by a description of three optical systems used for extracting data for chromatic processing.

The cuvette for holding oil samples to be addressed has been described, followed by a description of the method used to capture particles from the oil using filter papers for additional chromatic analysis.

The oil sample contained in a cuvette was first addressed optically using a PCOMS (Portable Chromatic Oil Monitoring System) with illumination provided by a computer screen, the spectrum of which was controlled by software from the VDU computer. A second system to illuminate the cuvette oil used a white LED whose output was collimated.

The LED spectrum system could be conveniently adapted for addressing particles captured on a filter paper using light transmission through the filter paper and the particles captured on it.

A spectrometer system was also used for addressing the VDU screen illuminated sample in order to validate the chromatic approach with respect to a sample monitored.

Chapter 5

EXPERIMENTAL RESULTS AND TEST DATA

5.1 Introduction

This chapter present raw data obtained from the optical experimental system (chapter 4) supplemented by data from conventional oil monitoring tests which include dissolved gas analysis and liquid condition (acidity, water contents and electrical strength) which were provided by Electricity North West (ENW) LTD.

5.2 Results of Optical Experiments

5.2.1 Spectrometer analysis

This method is applied to monitor different oil samples using uniform light illumination from a VDU screen transmitted through a sample cuvette and addressed by a detector (spectrometer or camera) as described in chapter 4, section 4.3.

The tests were performed to identify differences between various oil samples. In this section results are presented which have been obtained with this experimental procedure. The objective of the spectrometer results was to provide a detailed or comparison with spectral changes in the illumination from the VDU screen for different oil samples.

Examples of the spectra of the light emitted by the VDU screen viewed through various oil samples are presented in figures (5.1) (a) and (b). Figure (5.1) (a) shows the spectra for relatively normal transformer oil samples (T1, T9 and T10 samples) and an empty cuvette. Results for abnormal oil samples (84, 63 and 85) are presented in figure (5.1) (b).

These figures show the presence of a discrete band of spectral emissions extending over the wavelength range of 345 to 1000nm.

Figures (5.2) (a) and (b) show expanded scale records over limited wavelength ranges for the variously degraded oil samples T1, T9, T10 of figure 5.1 (a).

5.2.2 Spectrometer monitoring of camera images of samples

Results for the optical spectra of a number of illuminated oil samples obtained from images with a mobile phone camera (chapter 4, subsection 4.4.2) are shown on figure (5.3). There are spectra of a VDU screen showing the image captured by a camera using LED sources. They are not simply spectra of the LED source viewed through the samples.

Transmission optical spectra for samples of an empty cuvette (E), fresh oil ($T1$), moderately degraded samples ($T5$) and highly contaminant samples ($T10$) are presented. The results show the main clusters of wavelengths produced by the LED in the wavelength range $460-650$ nm and the different effect of the various oil samples in reducing the signal amplitudes at these wavelengths. The largest effects occur in the shortest wavelength range ($480-551$nm) compared with longer ones ($551-649$ nm), consistent with the VDU source results shown on figure (5.1) and (5.2).

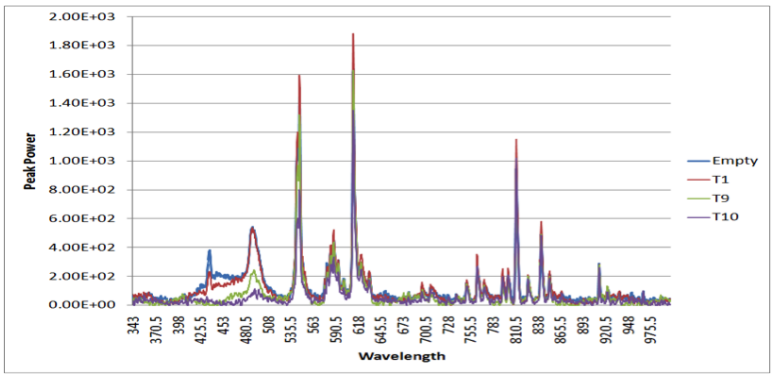

(a)

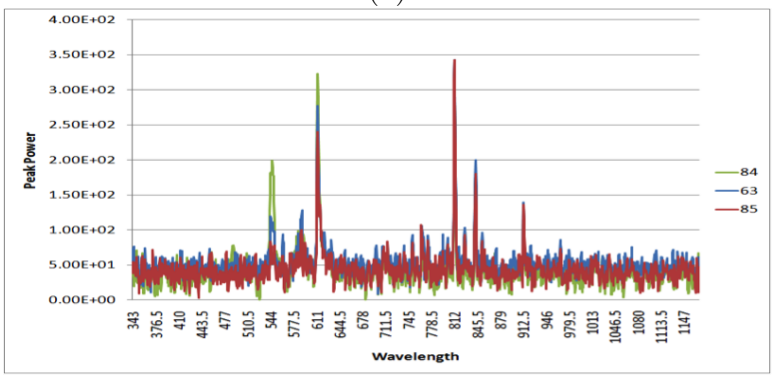

(b)

Figure 5.1: Transmission Spectra of Various Transformer Oils.
(a)Normal ($T1$), Moderately Degraded ($T9$), Heavily Degraded ($T10$)
(b)Some abnormal oil conditions.

5.2.3 R, G, B outputs from the CMOS with VDU illumination

The outputs from the CMOS camera with VDU illumination (chapter 4, subsection 4.4.4) yield the chromatic parameter R,G,B, which correspond to the spectral signals given on figure (5.1) and (5.2). The R,G,B values were of a specified area of the image. The values of R,G,B for 28 different transformer oils are shown on figure (5.4).

The results illustrate the complex variation in the R,G,B values produced by the different oil samples.

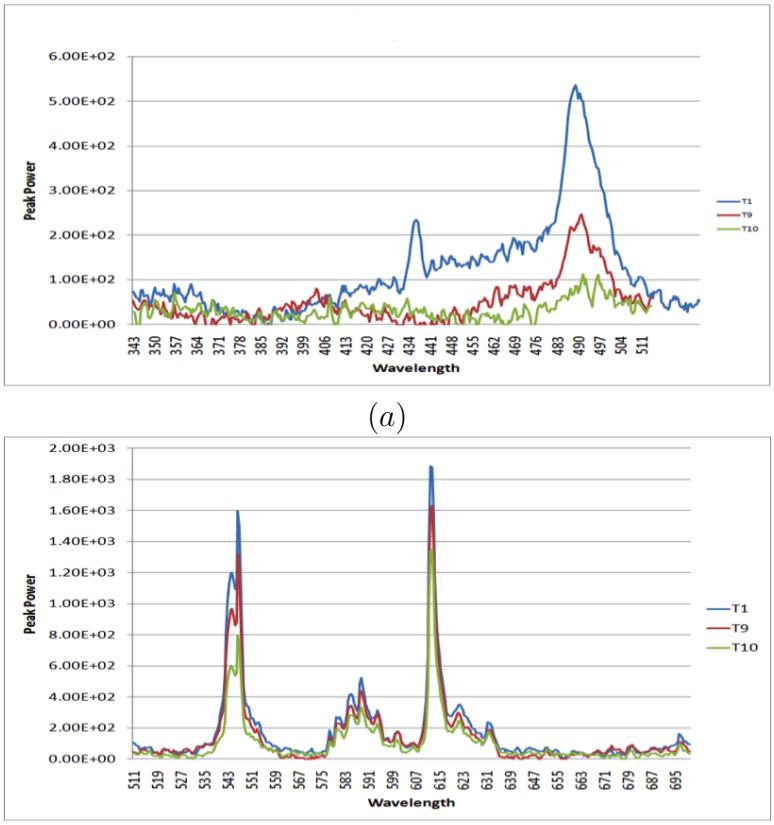

Figure 5.2: Highlighted Details of the Transformer Oil spectra (a)Short wavelength difference spectra (b)Longer wavelength expanded scale.

5.2.4 R,G,B outputs from the mobile phone camera with LED illumination for various oils

The images obtained from the mobile phone camera with LED illumination (chapter 4, subsection 4.4.4) yield values for the chromatic parameters R,G,B directly corresponding to the spectral signal given on figure (5.3). The values were for specified areas of the images using software described in appendix (drotri appendix F1). Values of R,G,B for the selected samples of oils are shown on figure (5.5) and translated in appendix B, section B.3.

The results show how the measured R,G,B vary with different oil samples.

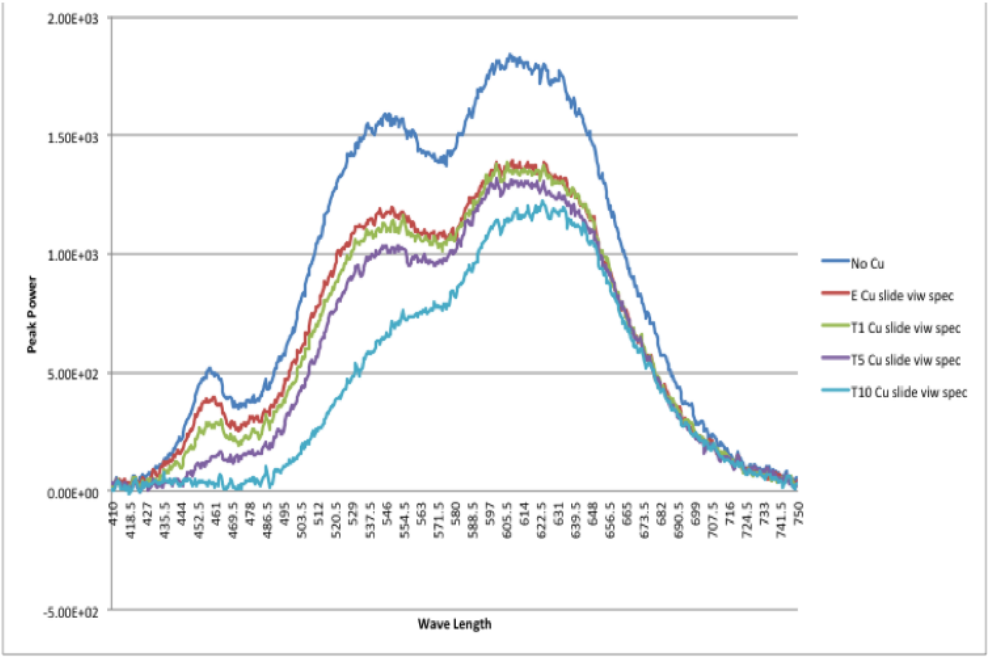

Figure 5.3: Transmission spectrum for various oil samples (LED view system).

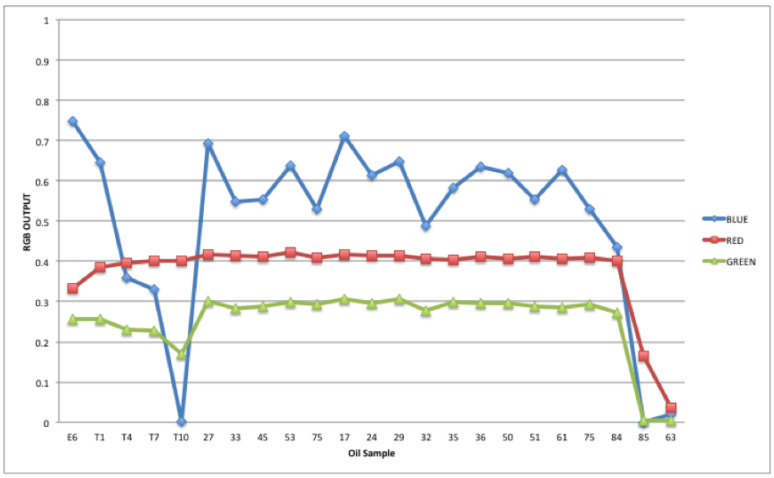

Figure 5.4: R,G,B outputs vs. oil samples from CMOS camera with screen illumination.

5.2.5 R,G,B output from camera and LED source for particles on filter paper

Figure (5.6) shows typical images of filter papers following the filtering of different kinds of oils addressed with LED backlighting as descried in chapter 4, subsection

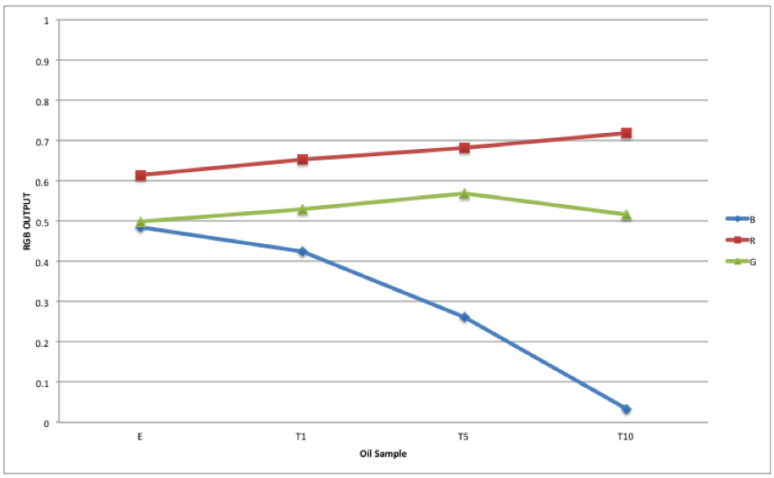

Figure 5.5: R,G,B outputs vs. oil samples from mobile phone camera with LED illumination.

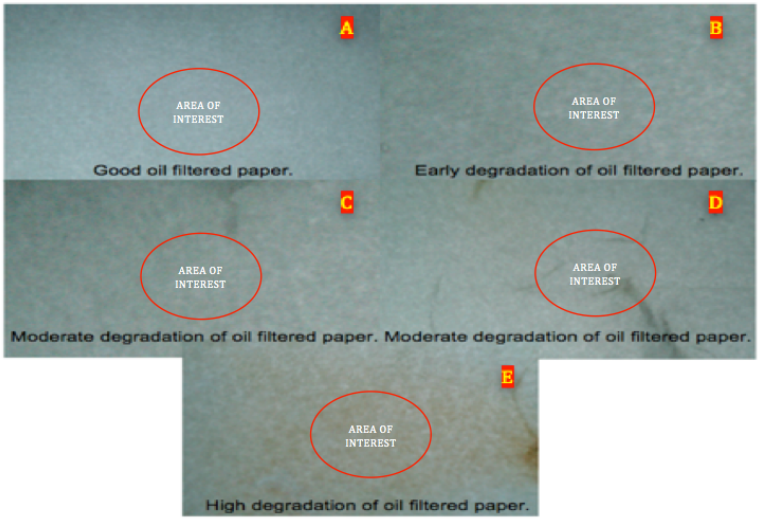

Figure 5.6: Different contaminated oil filter papers. Examples of images of LED backlight filter paper following filtering of different oil A) Fresh oil B C D) Different degradation oil E) Highly degraded oil.

4.4.4.

Specific areas on the images circled in red on the figure identify the areas of interest. Since the filter paper introduced in the funnel (chapter 4, figure (4.15)) takes the shape of the funnel, most oil sediments are concentrated on the central

area of the filter paper. Images A,B,C,D and E from the addressing mobile phone (MDA) were analysed in term of R,G,B outputs using the software described in appendix F1.

The results are shown on figure (5.7) in the form of a graph of R,G,B versus oil samples. The results indicate various changes in the R,G,B parameter values for the different conditions.

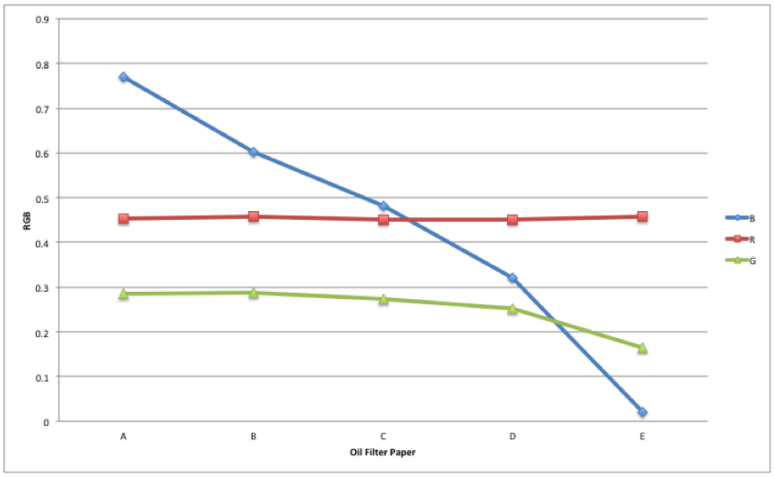

Figure 5.7: RGB values of filter paper deposits for various oil samples A) fresh oil B), C) and D) moderate degraded oil sample and E) highly contaminated oil sample.

Figure (5.7) is the raw RGB of the optically measured oil samples, which were then filtered through filter paper. The RGB values plotted on figure (5.7) are tabled on appendix D.

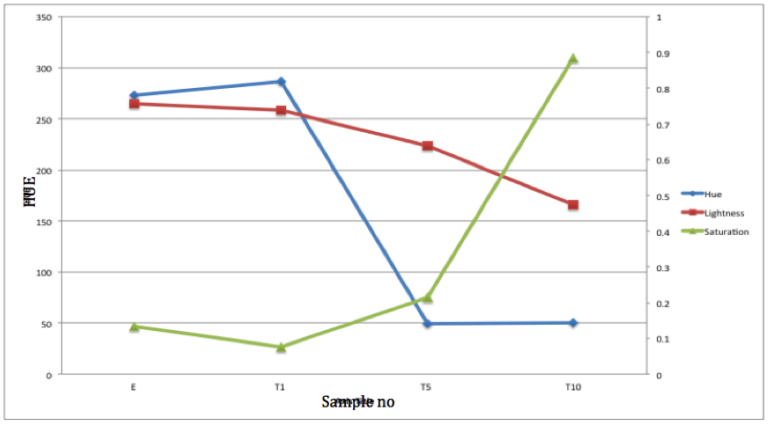

Figure 5.8: Derived HLS from raw RGB values.

The RGB on figure (5.7) were analysed chromatically (chapter 3, section 3.3) to obtain hue, lightness and saturation (appendix D) for each oil sample figure (5.8).

5.2.6 Raw R,G,B values for filtered and non filtered transformer oil samples and contaminated filter paper

The raw RGB data presented on figure (5.9) (a) and (b) represent non filtered and filtered oil samples respectively. The RGB data is extracted from a picture taken by mobile phone camera, which illuminated by backlight screen (VDU) (chapter 4, subsection 4.4.2).

The values are taken from a point of interest on the image and analysed using software (droptry). The RGB values for the filtered and non filtered oil samples shown on figure 5.9 (a) and (b) are listed on appendix D.3.

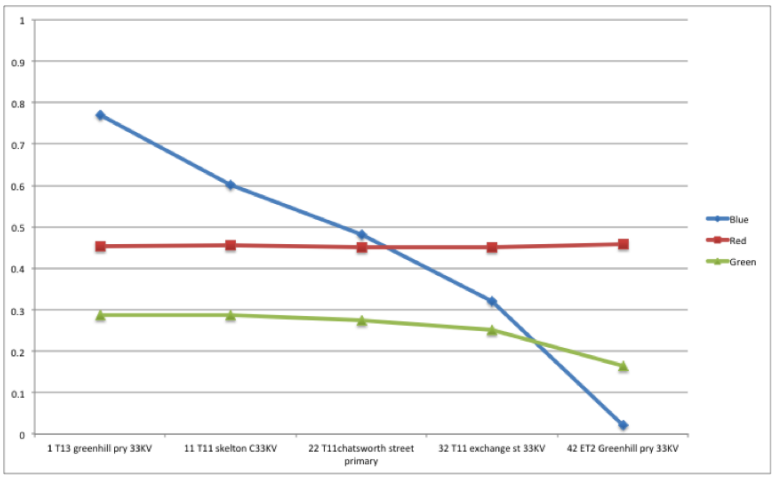

(a)

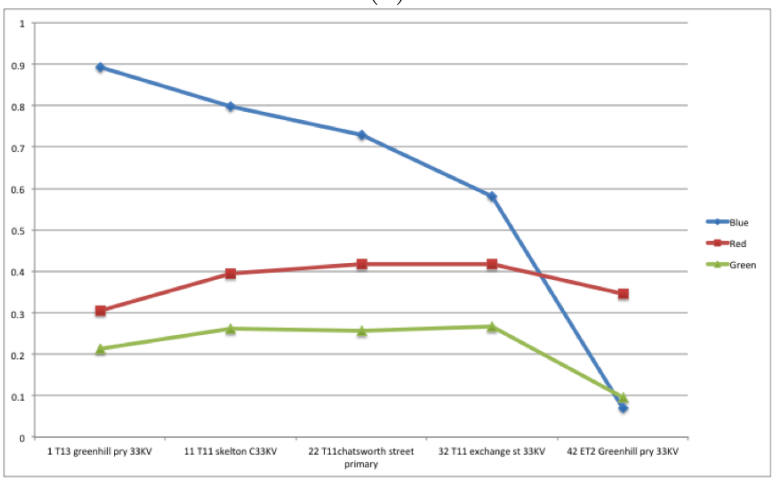

(b)

Figure 5.9: Raw RGB values of a) non filtered oil samples b) filtered oil samples.

5.3 Dissolved Gas Test Data

The results of the dissolved gas tests provided by Electricity North West (ENW) are given in appendix C.1 as tables showing the level of dissolved gases for each of the 23 oil samples investigated. The gases detected were CO,CO_2 etc. Examples of these data are shown graphically on figure (5.10) for a limited number of oil samples (T1, T9, 63, T10 and 85) representing various degrees of degradation. The gases are grouped according to the potential fault indicated (table 2.1, chapter 2, subsection 2.3.1) i.e. severe overheating, local overheating, electrical discharging (arcs, corona, spark). Figure (5.10) shows data for different gas

compounds of different degraded oil samples. The data are presented in the form of gas concentration levels for various gas types. The results illustrate the substantial and complex variations which occur in practice.

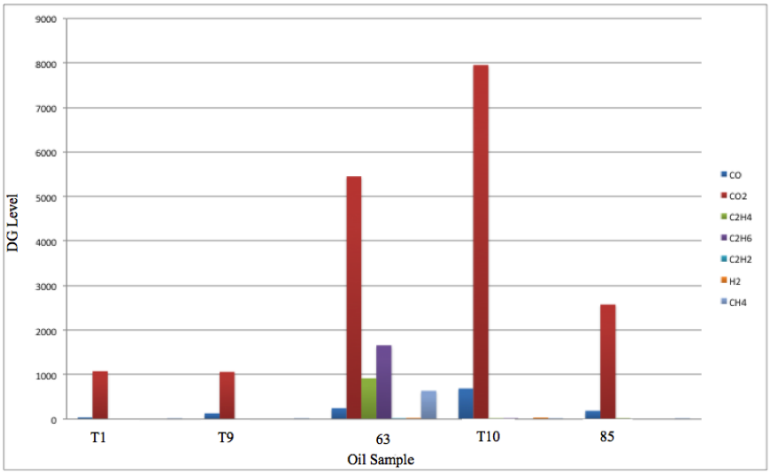

Figure 5.10: Dissolved gases levels for different transformer oil samples.

5.4 Oil Contamination Water, Acidity and Electrical Strength Data

Test data for transformer oil contaminated by water, acidity and with different electrical strengths as provided by ENW, are given in appendix C.2 , in the form of tables showing the levels of these conditions for each of the oil samples investigated. Examples of these data are shown graphically on figures (5.11) (a) and (b) for the oil samples T1, T9, 63, T10 and 85 for which dissolved gas results have been given on figure (5.11) and which represent various degrees of oil degradation. The results illustrate the complex nature of the data and the trends which they represent.

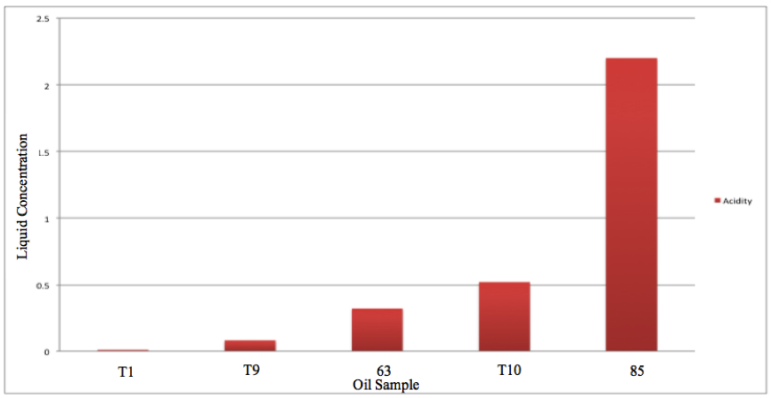

(a)

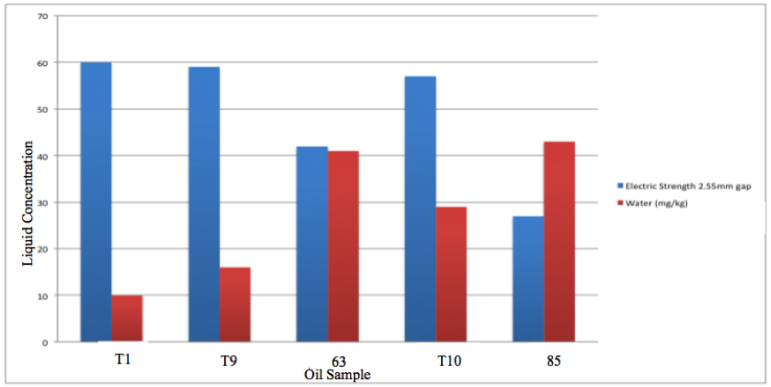

(b)

Figure 5.11: Level of water contents, acidity and electrical discharge for selected oil transformer samples a) T1, b) T9, c) 63, d) T10 e) 85. a) Acidity b) Electrical Strength and Water.

5.5 SUMMARY

The results presented in this chapter illustrate the large amount of data which are available for monitoring the degradation of a transformer oil sample. Each oil sample has seven different dissolved gases monitored along with water content, acidity and electrical strength and a substantial amount of optical spectrum data. There is therefore a need to extract relevant quantified information from all these data in a convenient and economic manner, which does not overlook significant events but provides a high level of traceability.

Chapter 6

DISCUSSION OF EXPERIMENTAL RESULTS AND TEST DATA

6.1 Introduction

The experimental and test data for the transformer oil presented in chapter 5 maybe analyzed chromatically for accommodating the large amount of data without unacceptable loss of sensitivity and for extracting meaningful information from them.

The chromatic approach is first applied for analyzing the polychromatic optical signatures of the oils and the results are compared with the colour index evaluation.

The chromatic approach is then applied independently to the dissolved gas data and the water/ acidity/ electrical strength data to provide relevant chromatic signatures for each of there two groups of data.

Finally a secondary chromatic procedure is used to provide an overall chromatic signature for the oil degradation, which combines the chromatic signatures for each of the three sets of data. The features dominating the overall degradation maybe extracted from each of the chromatic processing steps.

The procedure for chromatically analyzing and combining the experimental and test data involving data preprocessing, primary processing and secondary processing is summarized on the flow chart of figure (6.1):

The procedures has been implemented on a specially designed Matlab package (appendix G.2)

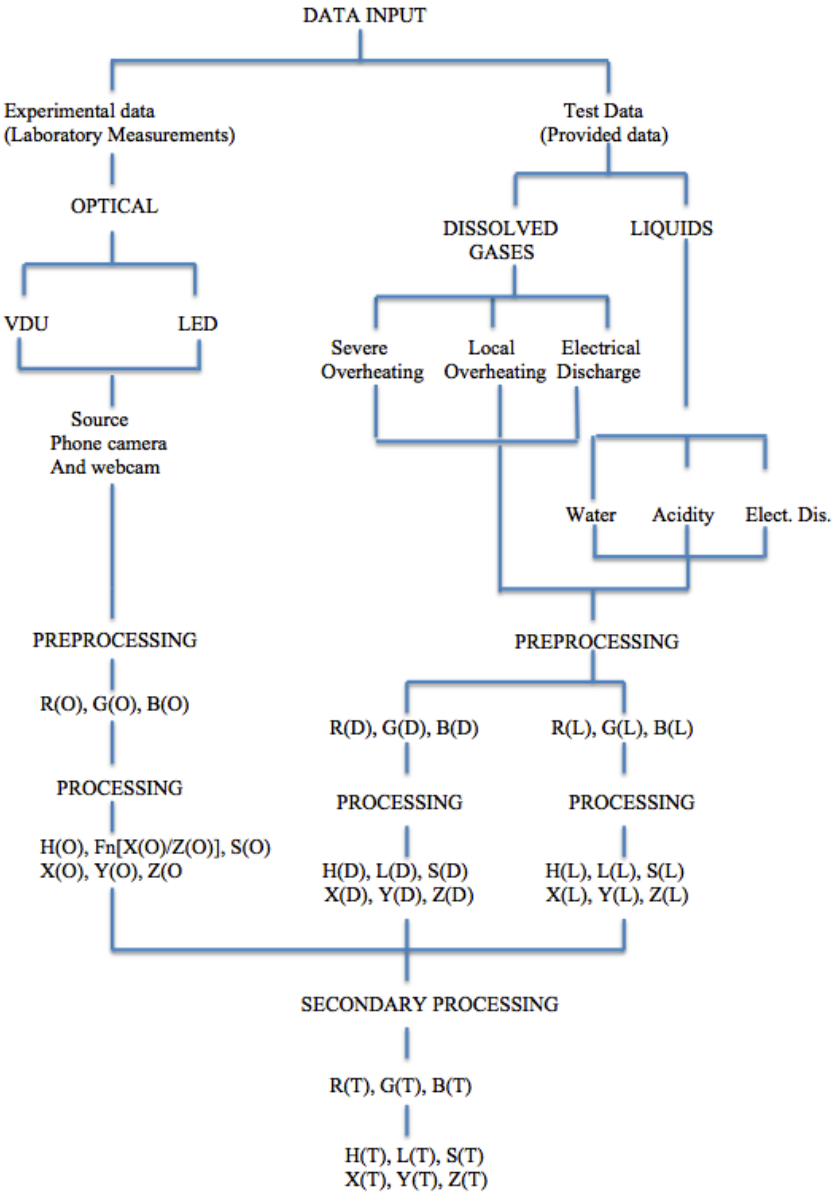

Figure 6.1: Data processing flow chart.

DATA PREPROCESSING PROCEDURES

Experimental results and test data need to be preprocessed to produce the equivalent of R, G, B outputs for chromatic processing. This section describes how this maybe achieved with the measured optical results (figure 5.2, chapter 5), the provided dissolved gases data (table C.1 appendix C.1) and the provided

water contents etc. test data (table C.2 appendix C.2).

The optical results obtained from the camera based experiments are already in the required form since the camera output are in terms of R, G, B (figure 5.6, chapter 5).

The manner in which each of these preprocessed data are then chromatically processed is described. Finally the chromatic combination of these individual data sets is described. The main two sections in this chapter will be the experimental results and the test results.

EXPERIMENTAL RESULTS

6.2 Optical Monitoring Results

6.2.1 RGB from optical spectra

Optical chromatic parameters of X, Y, Z or H, L, S (chapter 3, section 3.3.3) maybe obtained from either detailed spectra of figure (5.1 and 5.2), chapter 5, or directly from the R,G,B camera channels, figure (5.5), chapter 5. In the case of the optical spectrum results (figure 5.1 and 5.2, chapter 5), the spectral data are first subjected to preprocessing using the three non orthogonal processors figure 6.2 to yield outputs R,G,B.

Spectra of the form shown on figure (5.1 and 5.2), chapter 5 may be represented by three parameters R,G,B (similar to those of colour science) by superimposing three processors with overlapping responses upon the transmission spectrum as shown on figure (6.2). This forms the basis for interpreting the outputs of relevant R, G, B pixels from various camera images Jones et al. (2009). The region from 420 nm to 620 nm represents the visible part of the spectrum.

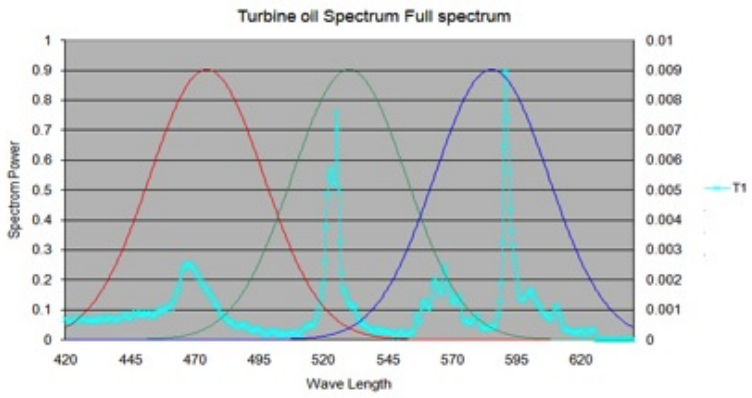

Figure 6.2: Non orthogonal chromatic processors superimposed upon an optical spectrum.

The R,G,B values obtained [(R red, G green and B blue are not a colour science)] are then transformed into the chromatic parameters X,Y,Z or H,L,S using equations 3.26, 3.27 and 3.28 for HLS and 3.20, 3.21 and 3.22 for XYZ of chapter 3 subsection 3.3.2 and 3.4.1. The procedure followed then is described in section 6.2.2 below for direct R,G,B camera output.

6.2.2 Chromatic processing for optical transmission results

6.2.2.1 Camera RGB output

The R,G,B results of the camera light transmission tests of subsection 5.2.4 chapter 5 appendix B.1, table B.1. have been analysed with both XYZ and HLS chromatic systems. The chromatic parameters for the optical signal are designated as X(O), Y(O), Z(O), H(O), L(O),S(O).

6.2.2.2 Z(O):X(O) Cartesian diagram

A chromatic representation of the oil sample data may be made in term of X (O), Y (O), Z(O) defined by the following equations:

$$Z(O) = B(O)/(3 * L(O)) \tag{6.1}$$

$$Y(O) = G(O)/(3 * L(O)) \tag{6.2}$$

$$X(O) = R(O)/(3 * L(O)) \tag{6.3}$$

$$L(O) = (B(O) + G(O) + R(O))/3 \tag{6.4}$$

i.e. Z(O), Y(O), X(O) represent the relative strength of the signal in the short, medium and long wavelength regions.

Figure (6.3) shows a Cartesian chromatic map of Z(O):X(O) for the oil sample results presented on figure (5.5) chapter 5 and RGB values of appendix B.1, table B.1. The majority of the oil samples lie on a short diagonal close to the centre of the diagram (0.33,0.33) but with a few samples (T1, T9, 63, T10, 85) more widely dispersed. Thus an oil sample may be represented to a first approximation by its long dominant wavelength region which is approximately given by the ratio of Z(O)/X(O), i.e. the gradient of the locus from the origin to the point on the Z(O):X(O) map (chapter 3, subsection 3.5.2).

6.2.2.3 Polar H-L diagram for polychromatic light transmission

The R, G, B optical oil results were also transformed into H(O), L(O), S(O) parameters using the algorithms of equations (3.20), (3.21), (3.22) (chapter 3, Section 3.4.2).

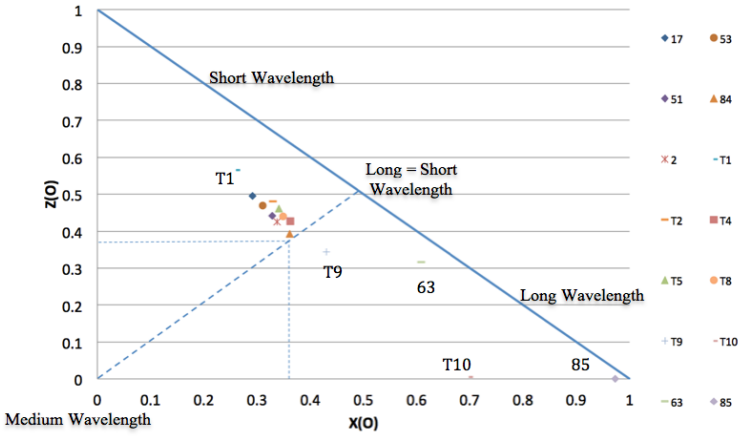

Figure 6.3: Z (O) Vs. X (O) Cartesian graph for different degraded oil sample optical tests.

Figure (6.4) shows the results for the transformed experimental data of figure (5.4) chapter 5 as a map of H (O):L (O). Figure (6.4) (a) shows the overall results whilst figure (6.4) (b) shows an expanded view for $L(O) < 0.4$.

The results on figure (6.4) (a) show most data lying at L(O) values <0.4 but with 3 samples (T10, 63, 85) with considerably higher values (>0.5). The three samples also have a greater variation of H value than the other results.

Figure (6.4) (b) for the expanded L(O) scale shows a clear trend for these data with the uncontaminated oil T1 at the origin and the other oils having L values increasing at constant H initially (H∼270 degree) before deviation towards H∼300 degree as L increasses beyond 0.15.

6.2.2.4 Combination of XYZ and HLS parameters

Particular parameters from the H,S,L and the X,Y,Z schemes may in principle be combined to produce a further chromatic map. For the optical data, a map of Z(O)/X(O) vs. S(O) can be useful. This represents a variation of a dominant wavelength (Z(O)/X(O)) as a function of a signal spread parameter S(O).

Figure (6.5) shows such a diagram where $Z(O)/X(O) > 1$ represents the dominance of the short wavelength whereas $Z(O)/X(O) < 1$ is with the long wavelengths dominant. $Z(O)/X(O) = 1$ corresponds to equal contributions from short and long wavelength ranges. The condition $S = 0$, corresponds to equal amplitudes at all wavelengths. As the $Z(O)/X(O)$ value deviates from unity by

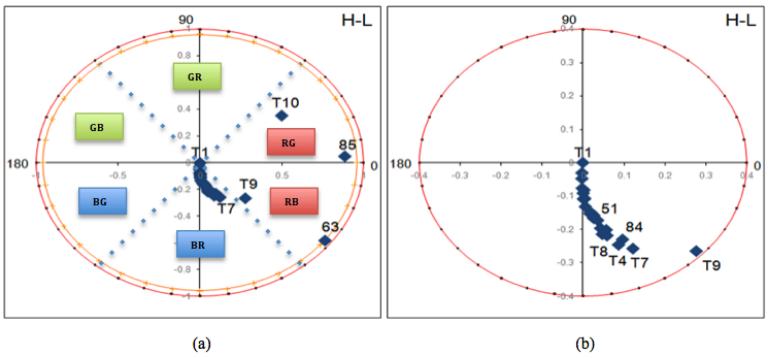

Figure 6.4: H-L polar graph for the tests with different level of degraded samples *a*)H(O) L(O) full scale *b*)H:L 0-0.4 L(O) scale.

either increasing or decreasing the signal becomes increasingly monochromatic leading to $S \rightarrow 1$.

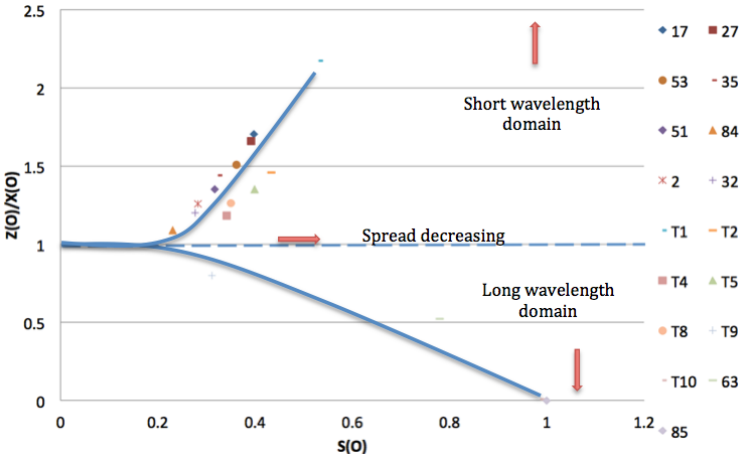

Figure 6.5: (x(O)/y(O)) : S(O) Cartesian Diagrame.

This map figure (6.5) shows that for most oil samples, the short wavelength dominates, the uncontaminated sample T1 having the highest value ($\sim$ 2.2) and being most monochromatic S($\sim$ 0.5). However for two samples (T10, 63) the long wavelength is dominant with one (63) having a particularly high value of S($\sim$ 0.8)

The combined Z(O), X(O), S(O) map of figure (6.5) may be mathematically manipulated to produce a more linearized form of map. This is achieved with the

algorithm given on table 6.1.

Table 6.1: Transformation of the $[X(O)/Z(O)] : S$ Function (dominant effect) into a Montonic Function with Range $0 - 1$

(X(O)/Z(O))	(X(O)/Z(O))n	S(O)n
<1	1/2 (X(O)/Z(O))	1/2 (1- S(O))
> 1	1/2 (1-Z(O)/X(O)))	1/2 (1+S(O))

This involves using the parameters $1/2(\frac{X(O)}{Z(O)})$, $1/2(1-S(O))$ for $(\frac{X(O)}{Z(O)}) < 1$ and the parameters $1/2(1-\frac{Z(O)}{X(O)})$,$1/2(1+S(O))$for $\frac{X(O)}{Z(O)} > 1$. Figure (6.6) shows the chromatic map obtained with this formulation.

The resulting graph of $\frac{X(O)}{Z(O)}$ n against Sn for the various oil samples shows a linear relationship between$\frac{X(O)}{Z(O)}$ n and Sn with a boundary between the normal and highly degraded oil samples (T9, 63, T10, 85) at [X (O)/Z (O)] n $\sim 1/2$, S (O) n $\sim 1/2$.

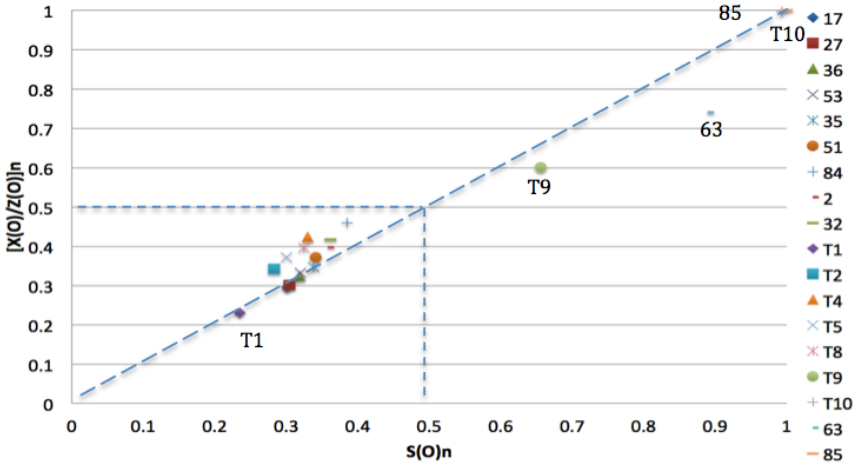

Figure 6.6: $([x(O)/z(O)]n : S(O)n$ Transformed Cartesian Diagram.

6.2.2.5 Comparison of chromatically transformed optical data with the CI index

The chromatically analysed results may be compared with the CI value appendix F.1, figure F.1. of the various oil samples tested. This may be done in two ways. Firstly the transformed Cartesian dominant wavelength $X(O)/Z(O)$ (subsection 6.2.2) may be compared with the colour index (CI). Secondly the signal strength parameter L (O) (sub subsection 6.2.2.4) may be compared with CI. These comparisons are shown on figures (6.7) (a) and (b) respectively.

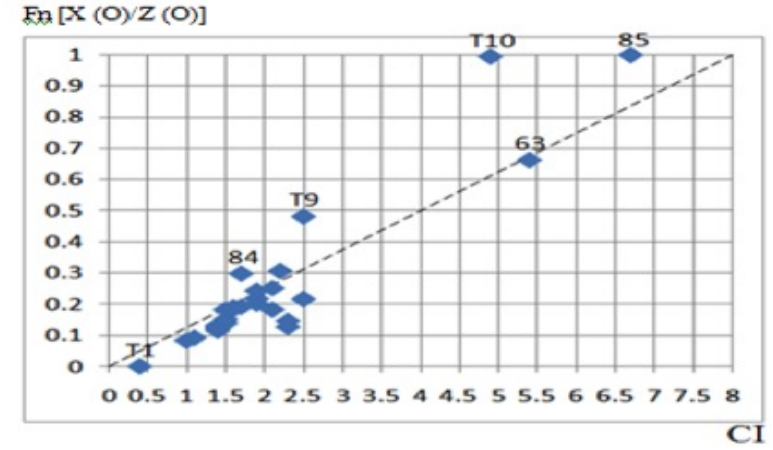

(a)

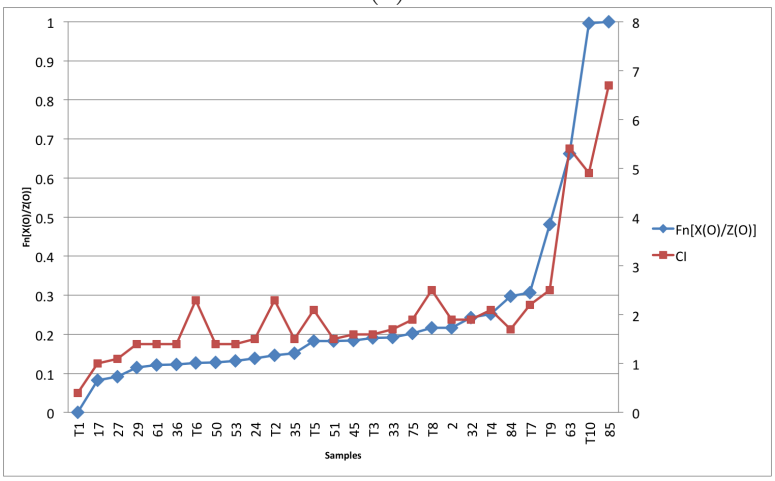

(b)

Figure 6.7: (Comparisons of the Chromatic Parameters dominate wavelength with Colour Index for Various Oil Samples (*a*) $Fn[X(O)/Z(O)]$ (*b*) Averaged long and short wavelengths $L(O)$.

The results for Fn $[X(O)/Z(O)]$ show a similar but not identical trend of the dominant wavelength with Colour Index. Both dominant wavelength and colour index identify samples T10, 63, 85 as being particularly different from the other samples with T9 also being marginally different. A comparison between the colour index appendix F.1 of the oil and the optical chromatic parameter $Fn[X(O)/Z(O)]$ as a function of oil sample (figure 6.7 (*b*)) ordered according to increasing values of $Fn[X(O)/Z(O)]$ shows a good agreement. Both parameters identify samples (85, T10, 63, T9) as having abnormally high parameter values.

In addition the CI shows samples (T6, T2, T5, T8, T10) to have marginally higher values than the $Fn[X(O)/Z(O)]$ results.

6.2.3 Effect of solid micro particles in oil samples

6.2.3.1 Filter paper particles

Experimental results obtained from the optical measurements of oil samples passed through filter papers (chapter 4, subsection 4.4.5 and chapter 5, figure 5.7 (RGB results) and the sediment remaining on the filter papers may also be chromatically assessed. The R,G,B values from the filter paper E, T1, T5 and T10 (chapter 5, figure 5.7) are transformed into the H,L,S values given on table 6.2.

Table 6.2: HLS values obtained from the raw R,G,B values chapter 5, appendix D).

filtered oil samples	R	G	B
T13	254.4	0.47	0.62
11 T11	263.66	0.48	0.5
22 T11	270.57	0.47	0.48
32 T11	278.98	0.42	0.37
42 ET2	10.38	0.17	0.67

The H and S values of different oil samples were normalised according to

$$N = (S - HDS)/(FS - HDS) \tag{6.5}$$

Where

N= normalization.

S= unknown oil sample.

HDS= high degraded oil sample.

FS= Fresh oil sample.

These values then combined according to the equation:

$$Fn(H - S) = 0.5.S + ((1 - H)/2) \tag{6.6}$$

The values of this parameter for an empty cuvette and the different oil samples (T1, T5,T10) are shown on figure (6.8).

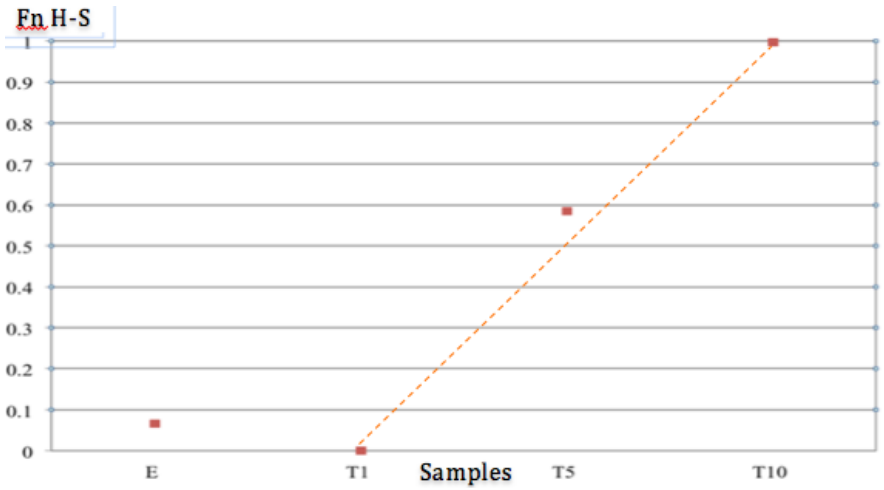

Figure 6.8: (Calibrated LED viewer results for sample points Hue and Saturation $(H-S)$.

T1 represents a fresh oil sample, which shows zero degradation on the $(Fn(H-S))$ scale. T5 shows a moderate degradation compared to T1. T10 is shown as a highly degraded oil sample on the $(Fn(H-S)$ scale.

6.2.3.2 Particles in oil

The RGB optical results obtained for 5 oil samples (T13 Greenhill, T11 Skelton, T11Chatsworth, T11 Exchange, ET2 Greenhill) with and without particle filtering (chapter 5, subsection 5.2.6) may be transformed chromatically using the X,Y,Z system for comparing trends with and without filtering. The chromatic parameter chosen for such a comparison is

$$Z_P = \frac{B}{R+G+B} \tag{6.7}$$

Since the short wavelength end of the spectrum is anticipated to be most affected by any particles. The Z parameter has been calculated taking account of the settling time for any particulate material before and after filtering according to the equation

$$Z_P = Z_P 4[\frac{Z_P(sample)}{\overline{Z_P}(1hour)}] \tag{6.8}$$

Where

Z_{P4} is the averaged corrected Z reference after 4 minutes.

Z_P (sample)is the Z for the unknown sample.

$\overline{Z_P}$ (1 hour) is the average corrected Z reference after one hour.

The Z value calculated is then normalised with respect to the benchmark samples T1 and the most heavily degraded sample 85.

$$Z_{PN} = [\frac{Z_P(sample) - Z_P(85)}{Z_P(T1) - Z_P(85)}] \tag{6.9}$$

Z_{PN} is the normalised corrected Z.

Z_P (85) is the highly contaminated reference sample.

Z_P (T1) is the fresh reference oil sample.

The chromatic signature of a filtered oil sample may be compared with its signature prior to filtering to investigate the effect of any suspended particles upon the chromaticity.

Figure (6.9) shows result for filtered and non filtered oil samples. The red square dots represent the non filtered samples and the blue diamond dots represent the filtered samples. Figure (6.9) compares the Z_PN (i.e. relative magnitude of the short wavelength component B(O)) values for a number of oil samples.

The result given on figure (6.9) shows that, for the non filtered oils samples Z_{PN} decreases from 1 for the normal sample to 0 for a heavily degraded sample (85). The values of Z_{PN} for the filtered samples also reduce as the degradation increased but at a slower rate. Thus the difference between Z_{PN} for the filtered and non filtered samples is an indication of the level of particle contamination. These trends are consistent with the change in the chromatic signature of the particles deposited on the filter paper.

Figure (6.10) shows the chromatic change between filtered and non filtered oil samples from figure (6.9) according to the following equation

$$Z_d = [\frac{ZO_Non - ZO_F}{ZO_Non}] \tag{6.10}$$

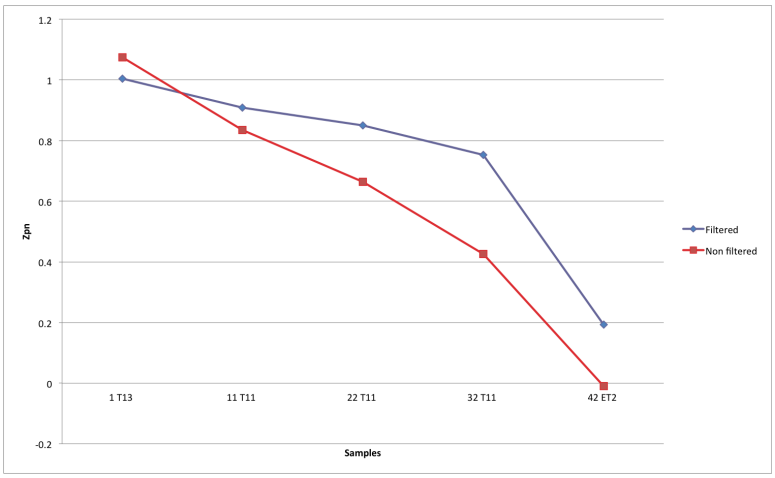

Figure 6.9: Normalised corrected (ZO_N) different oil samples.

Z_d = the difference between Z for filtered and non filtered oil samples.

ZO_{Non} = the non filtered oil samples.

ZO_F = the filtered oil sample.

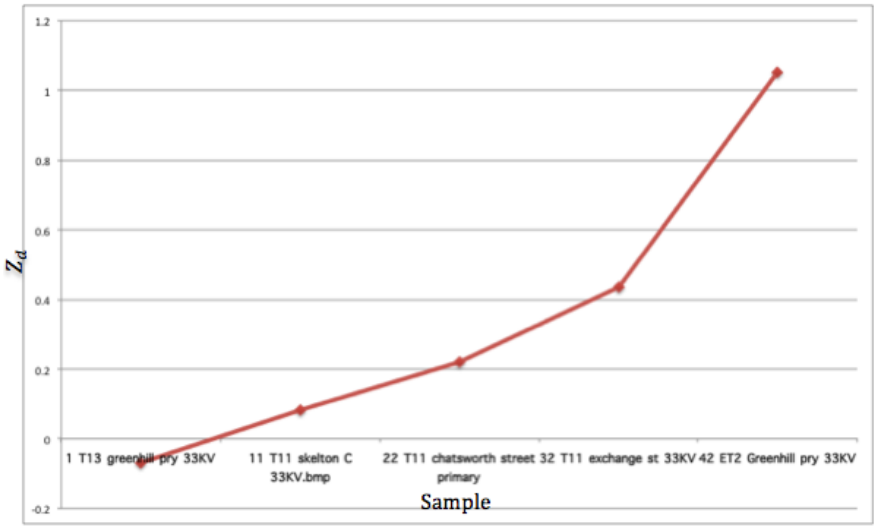

Figure 6.10: (Relative change between filtered and non filtered transformer oil.

TEST DATA

6.3 Dissolved Gas Data Processing

6.3.1 RGB for dissolved gases

The dissolved gases (chapter 5, section 5.3) may be divided into three groups (chapter 2, subsection 2.3.1 table 2.1) corresponding to the effects of severe overheating (CO2, CO, C2H4), local overheating (C2H6), and electrical discharging (H2, CH4, C2H2) Aragon-Patil et al. (2007). Conventionally, the oil degradation indicated by a dissolved gas (d (g)) may be described by two thresholds - the first (d (1)) below which the oil condition is normal, the second (d (2)) above which the oil is highly degraded and the intermediate region (d (2) $\Leftrightarrow$ d (1)) within which the oil is moderately degraded Höhlein et al. (2003). These thresholds are different for various gases and it is advantageous for a sample (d (g)) to be normalised within a common range 0-1 overall, a range of $0 - 0.33$ for the normal condition and a range 0.33 -0.66 is for the moderate degraded condition. Any (d(g)) exceeding the 0.66 boundary is considered to be highly contaminated. As a result, the normalised dissolved gas degradation, dn, can be quantified according to the following relationships

$$dn = 0.5[d(g)/(d(1))] \Longrightarrow if d(g) < d(1) \tag{6.11}$$

$$= 0.5[1 + ((d(g) - d(1))/(d(2) - d(1)))] \Longrightarrow if d(1) < d(g) < d(2) \tag{6.12}$$

For chromatic processing, the gases needed to be grouped according to the degradation with which they are associated (chapter 2 subsection 2.3.1 , table 2.2).

The three indicators (dn(SO), dn(LO), dn(ED)) for each oil sample may then be designated as the R, G, B of chromatic analysis as shown on figure (6.11). Each member of a dissolved gas group will therefore have a normalised value (dn). For example for the severe overheating group $CO2 \rightarrow dn(CO2), CO \rightarrow dn(CO), C2H4 \rightarrow dn(C2H4)$. These values are summed and divided by the number of gases in the group to yield an indication of the overall degradation associated with that group. Thus the overall degradation indicators for the severe overheating (SO), local overheating (LO), and electrical discharges (ED) groups are given respectively by

$$dn(SO) = [dn(CO2) + dn(CO) + dn(C2H4)]/3 \tag{6.13}$$

$$dn(LO) = dn(C2H6) \tag{6.14}$$

$$dn(ED) = [dn(H2) + dn(CH4) + dn(C2H2)]/3 \tag{6.15}$$

Each of these groups may be regarded as constituting a region of a spectral distribution of dissolved gases, with indication results clustering together as shown on figure (6.11). The resulting data distribution may then be addressed with three non orthogonal processors (R(D),G(D), B(D), with each of the 3 clusters of gases corresponding mainly to each of these processors (figure 6.11), and be chromatically transformed chapter 3, section 3.4 and subsection 3.4.2.

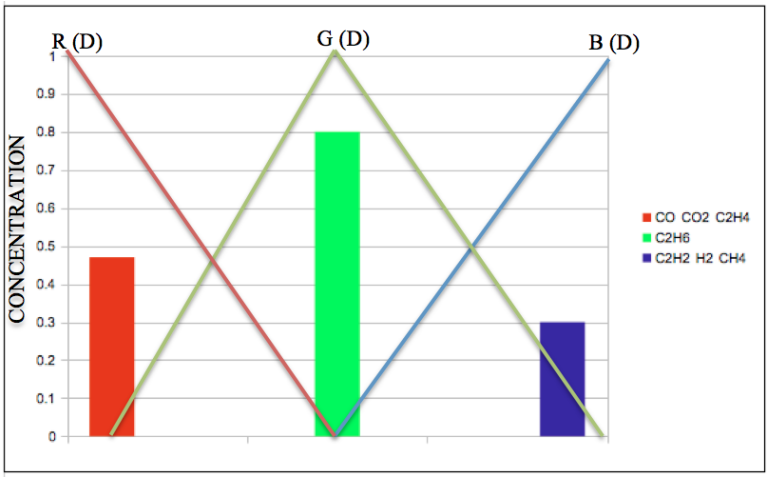

Figure 6.11: Chromatic Processors R, G, B Superimposed upon the Sum of the Normalised Levels of Dissolved Gases from Each of the Three Gas Groups (B(D) Severe Overheating, G(D) Local Overheating, R(D) Electrical Discharging.

(R red, G green and B blue are not a colour science)

6.4 Chromatic Diagrams For Dissolved Gas Monitoring

6.4.1 Dissolved gas chromatic methods

The R, G, B values for the 28 oil samples investigated are given in appendix B, table B.1.These may then be used to produce values for the chromatic parameters H(D), L(D), S(D) and Z(D), X(D), Y(D) using the following algorithms given in chapter 3 section 3.4 and subsection 3.4.2. For example, X(D), Y(D), Z(D) are given by

$$X(D) = dn(SO)/(3 * L(D)) \rightarrow Relative\ strength\ of\ Severe\ Overheating \tag{6.16}$$

$$Y(D) = dn(LO)/(3 * L(D)) \rightarrow Relative\ Strength\ of\ Local\ Overheating \tag{6.17}$$

$$Z(D) = dn(ED)/(3 * L(D)) \rightarrow Relative\ Strength\ of\ Electrical\ Discharging \tag{6.18}$$

$$L(D) = [dn(SO) + dn(LO) + dn(ED)]/3 \tag{6.19}$$

The condition of an oil sample may then be represented on either on H (D): L (D) polar diagram or a Z(D): X (D) Cartesian diagram.

6.4.2 Chromatic DG mapping

6.4.2.1 Cartesian chromatic dissolved gas

The dissolved gas data may be displayed on a Cartesian X:Y diagram by processing the RGB values (appendix E, table E.1) with equation 3.26 and 3.27 subsection 3.5.2 chapter 3. An example of such a graph is shown in figure 6.12. This figure has been produced in specially developed Matlab software (appendix G.2) as part of a demonstration package illustrating the analysis capability of chromatic approach.

Figure (6.12) gives such a Cartesian diagram for the various oil samples with different regions shown corresponding to overheating Z(D), electrical discharge X(D) and local heating Y(D). The results presented are for the more outstanding

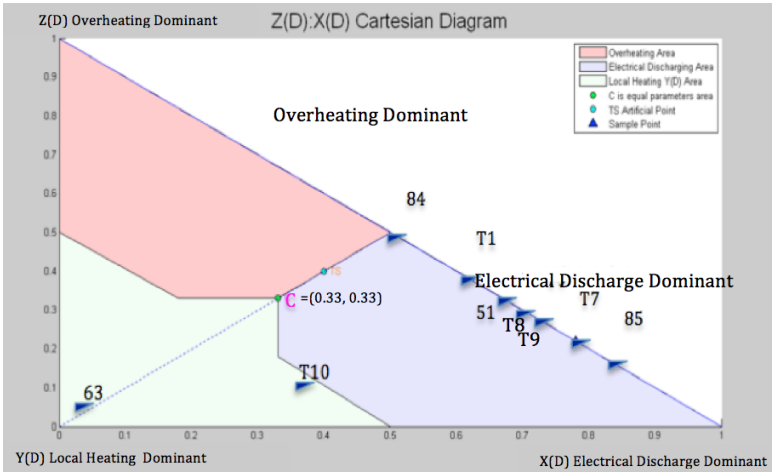

Figure 6.12: Dissolved gas Cartesian diagram.

oil samples. They indicate that for most samples there is no degradation due to local heating Y (D) ~ 0. Also, most of these samples, including the benchmark sample T1, are in the range X (D) $>$ Z (D) implying that electrical discharging dominates over severe overheating for the higher degradation samples. Sample 63 is dominated by local overheating (Y (D)) with only small contributions from severe overheating ($Z(D) \rightarrow 0$) and electrical discharging ($X(D) \rightarrow 0$). T10 is dominated more by local heating (Y (D)) and severe overheating (Z (D)) and 85 is dominated by electrical discharging ($X(D) \rightarrow 1$) Of the lower level degraded samples (L < 0.33), T7, T8, T9, 51, 85 are all dominated by relatively higher levels of electrical discharging than severe overheating ($X(D) \rightarrow 1$), whilst 84 is affected equally by severe overheating and electrical discharging ($Z(D) \sim X(D), Z(D) \sim 0$).

A difference between the Duval triangle (chapter 2, subsecection 2.4.4, reference Akbari et al. (2008),Singh and Bandyopadhyay (2010)) and the chromatic Cartesian diagram is that the Duval triangle depends on three main gases to determine the condition of the dissolved gases in the oil sample. On the other hand, the chromatic Cartesian diagram takes all key gases into consideration to give an accurate indication of the condition of the dissolved gases in the oil sample and where it is located on the Cartesian map.

6.4.2.2 Dissolved Gas Chromatic Polar Map

A polar map for dissolved gas indication of degradation obtained with equation 6.13 − 6.15 in combination with equation 3.20 and 3.21, chapter 3 for H,L,S using the R, G, B values given in appendix D is shown on figure (6.13) for the 28 transformer oil samples.

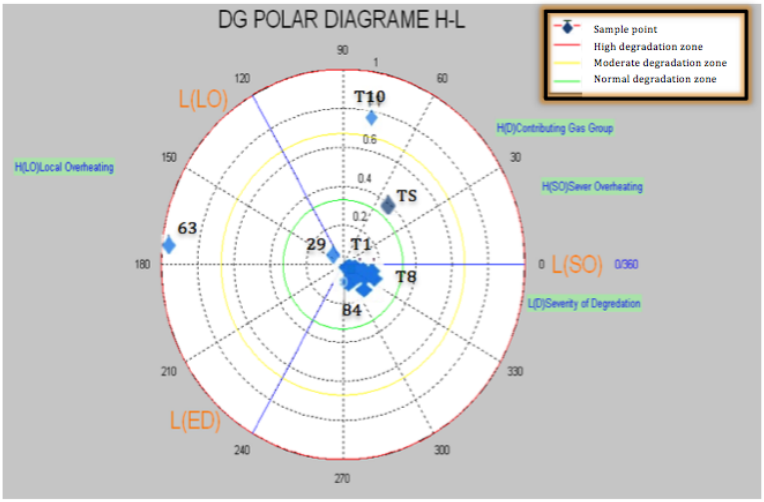

Figure 6.13: Dissolved gas polar chromatic diagram created by Matlab.

For this case L (D) represents the amount of oil degradation according to the relationship

$$L(D) = [dn(SO) + dn(LO) + dn(ED)]/3 \tag{6.20}$$

The L (D) scale may be divided into three ranges, 0−0.33 corresponding to a normal condition, 0.33− 0.66 corresponding to moderate degradation, and 0.66−1 corresponding to high degradation. This subdivision is based upon the fact that if only one of the group of gases (SO, LO, ED) has a value dn= 1 then L (D) = 1/3 and a degradation flag needs to be shown; if two groups have a value of dn = 1, L (D) = 2/3 and a high degradation flag needs to be shown. The azimuthal coordinate H (D) indicates the group of dissolved gases which dominates the degradation, 0 degrees → severe overheating, 120 degrees → local overheating, 240 degrees → electrical discharges. For example an oil sample Ts is indicated to have suffered moderate degradation either due to only local overheating or due to a combination of equal contributions from severe overheating and electrical

discharges plus some contribution from local overheating. Based upon this interpretation sample 63 is a highly contaminated sample and is dominated by local overheating and the electrical discharging region, but more dominated by the local overheating. Sample T10 is also highly degraded being located between local overheating and severe overheating, but it is dominated by local overheating. It might be considered that an indication of electrical discharge ED within a sample represents a more severe condition than overheating as the insulation materials of the oil tends to be lost Lewand (2006).

Magnitude of L (D) dissolved gases

Whereas the Cartesian Z(D):X(D) and Polar H(D):L(D) diagrams provide an indication of the relative magnitude of components, they do not highlight clearly an overall absolute magnitude. This may be achieved by using the chromatic parameter L(D) (equation 6.19) as the comparator.

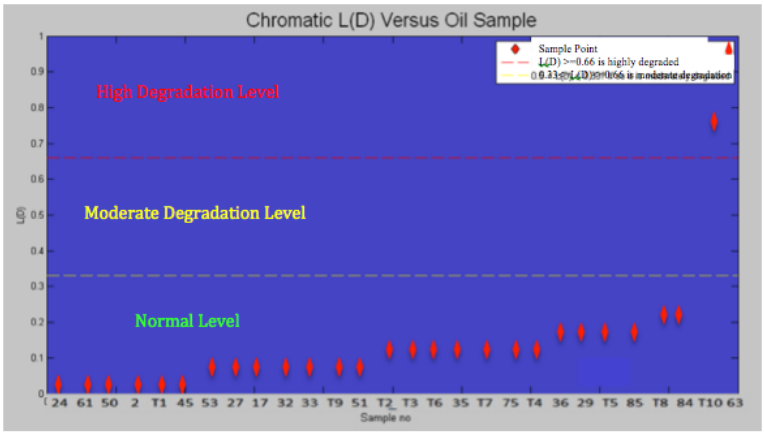

Figure 6.14: Total magnitude of dissolved gas.

Figure (6.14) shows L(D) as a function of oil sample type arranged in increasing level of L(D). This shows that all samples except T10 and 63 lie below the level $L(O) < 0.33$.

Summary of procedures for obtaining dissolved gas chromatic analysis

A procedure based upon the various analyses given in subsection 6.4.2 maybe used to give an indication of the overall dissolved gas condition. The route for

tracing the dominant components is summarised on figure 6.15. The steps involved in this procedure are as follows:

I. Determine the L (D) value of the sample.

II. If L (D) > 0.66 then it is highly degraded.

III. If $0.33 <$ L (D) < 0.66 then it is moderately degraded.

IV. If condition (II) or (III) is satisfied then examine X (D): Y (D) map.

V. Determine from X (D): Y (D) map which dissolved gas group dominates.

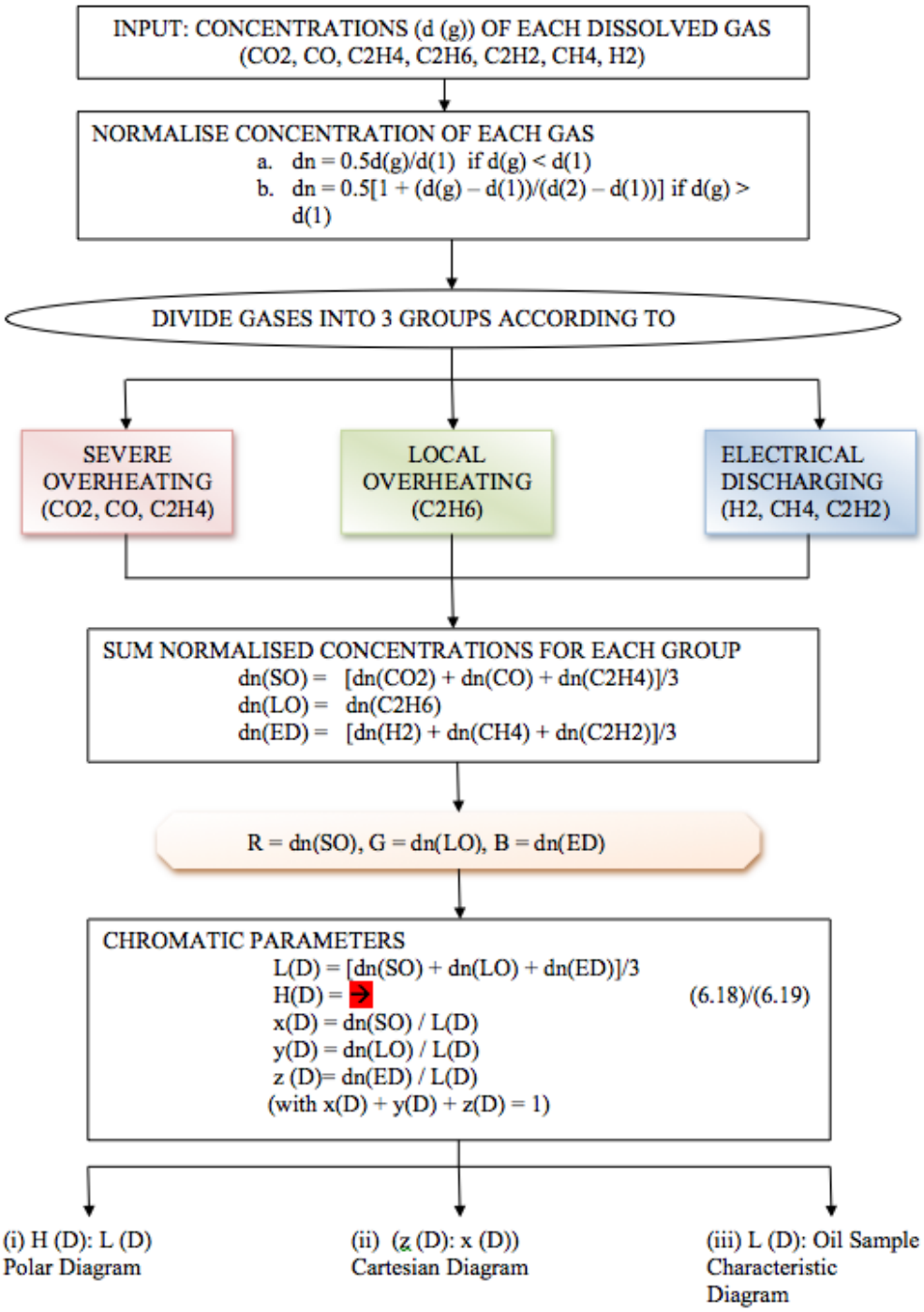

Figure 6.15: Flow chart of the overall dissolved gas procedure.

6.5 Water, Acidity And Electrical Strength Data Processing

Each of the oil degradation factors acidity, water content, loss of electric strength (chapter 2 subsection 2.3.1), may be quantified in terms of these various chromatic parameters. The first step in this procedure is to normalise each factor on a scale $0-1$ and to establish critical levels of degradation according to established protocols.

For example the measured acidity may be normalised based upon the fact that an acidity level greater than 0.3 units can lead to sludge formation in the oil Meshkatoddini (2008).whilst oil sample T1 (L (a, T1)) represents a normal oil condition (Chapter 5 subsection 5.2.4 figure 5.5). Thus the normalised acidity level (L (a, N)) of an oil sample (L (a, sample)) maybe defined as;

$$L(a,N) = [L(a,sample) - L(a,T1)]/[0.3 - L(a,T1)] \tag{6.21}$$

Values of $R(\ell), G(\ell), B(\ell)$ were calculated in this manner for the 28 oil samples tested using the data presented in chapter 5, section 5.4, appendix C.2. Some samples values are given on figure (6.16) for a small selection of oils (T1, T10, 63, 85, T9, 84, T9).

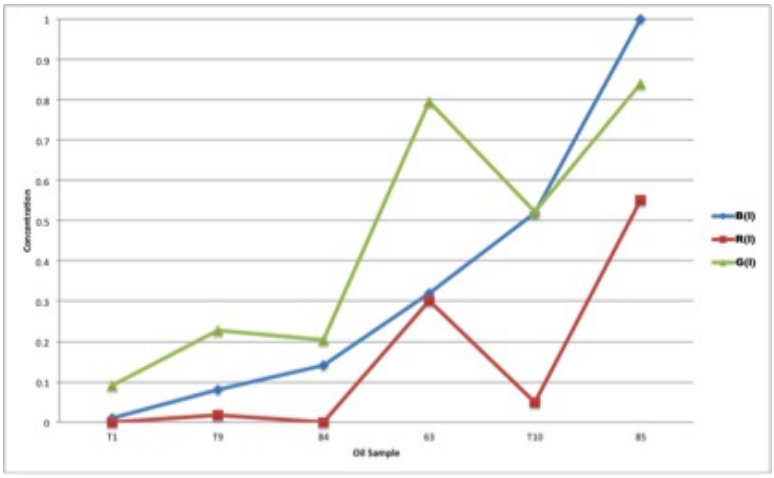

Figure 6.16: $R(\ell), G(\ell), B(\ell)$ versus oil type for a selection of oils tested.

The values $R(\ell), G(\ell), B(\ell)$ are raw values which are transformed into the chromatic parameters $X(\ell), Y(\ell), Z(\ell)$ and $H(\ell), S(\ell), L(\ell)$ using equations 3.20, 3.21 and 3.22 for HLS; 3.26, 3.27 and 3.28 for XYZ, chapter 3.

The water content may be normalised with respect to oil samples 17 and 27 which have equal water content that is considered to be normal (L (w, 17) = 6 mg/kg. L(w, U) = 50) a severe degradation level may be regarded as that of one sample (L(w, 85)= 43) *Leibfriedet al.* (2002).

The normalised water content level (L(w, N)) of a sample L(w, sample), may then be given by

$$L(w, N) = [L(w, sample) - L(w, 17)]/[L(w, U) - L(w, 17)] \tag{6.22}$$

The loss of electric strength (L (es, sample) maybe normalised with respect to a number of oil samples, including T1, which have a full strength of 60 kV Luksich (2004).The normalised loss of electric strength L (es, N) is then expressed as

$$L(es, N) = [L(es, T1) - L(es, sample)]/L(es, T1) \tag{6.23}$$

so that L(es,N) ranges from 0 (no loss of strength) to 1 (complete loss of strength). As a result, the worst sample, 85, has lost just over half of its electric strength (L(es, 85N) = 0.55). Figure (6.17) shows each of the normalised values for acidity (L (a)), water (L (w)) and electrical strength (L(es)) (calculated with equations 6.21, 6.22, 6.23) for a number of typical oil samples.

The chromatic analysis procedure was then to treat each of the three parameters L (a), L (w) and L (es) as the chromatic inputs R (ℓ),G (ℓ),B (ℓ) (chapter 5, section 5.4).

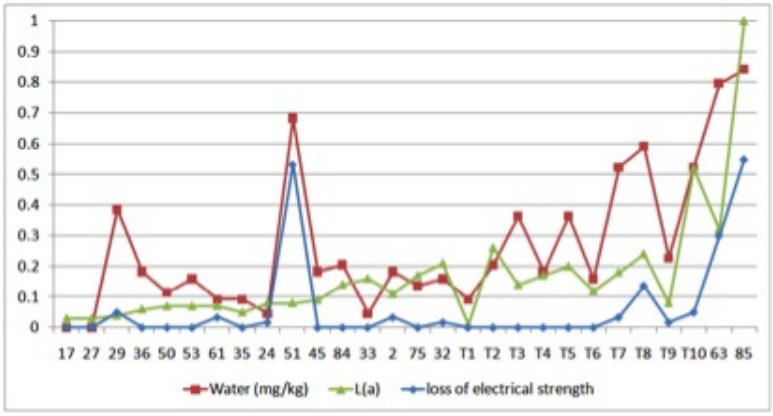

Figure 6.17: Normalised values of acidity level L(a), water content L(w) and loss of electric strength (L(es) for various Oil Samples.

6.6 Chromatic Diagram For Acidity, Water Content And Electrical Strength

There are three aspects, which need to be addressed in order to discuss the liquid results. These aspects are as follow:

- Water (w)
- Acidity (a)
- Electrical Stress (es)

6.6.1 Chromatic analysis methodology

Values of the chromatic parameters $H(\ell), L(\ell)$ and $X(\ell), Y(\ell)$ may be calculated using the $R(\ell), G(\ell), B(\ell)$ parameters and algorithms given in chapter 3, equations 3.26, 3.27 and 3.28 so that

$$L(\ell) = (L(a) + L(w) + L(es))/3 \tag{6.24}$$

$$X = L(w)/3L(\ell) \tag{6.25}$$

$$Y = L(a)/3L(\ell) \tag{6.26}$$

$$Z = L(es)/3L(\ell) \tag{6.27}$$

The results may then be presented on a chromatic polar diagram H(ℓ) : L(ℓ) and a Cartesian diagram X(ℓ): Y(ℓ).

6.6.2 Cartesian chromatic diagram for water, acidity and electrical strength

Figure (6.18) shows a $Y(\ell)$:$X(\ell)$ Cartesian diagram on which the $X(\ell)$ coordinate indicates the fraction of the total degradation for the group of three members which is due to the water content whilst the $Y(\ell)$ coordinate indicates the fraction due to acidity.

The fraction of overall degradation due to the third member, loss of electric strength (Z(ℓ)), is also apparent on figure (6.18) (equation 6.28).

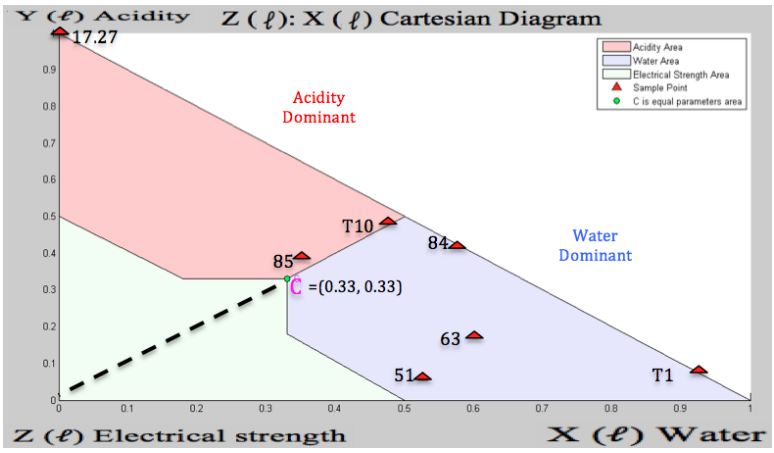

Figure 6.18: Cartesian diagrams of chromatic parameters $Y(\ell)$ versus $X(\ell)$.

$$Z(\ell) = 1 - (X(\ell) + Y(\ell)) \tag{6.28}$$

This implies that the origin of the $X(\ell)$: $Y(\ell)$ Cartesian diagram corresponds to all the degradation being due to the loss of electric strength if L (A) is not zero. Conversely the locus (chapter 3 subsection 3.5.2).

$$X(\ell) + Y(\ell) = 1 \tag{6.29}$$

corresponds to no loss of electric strength ($Z(\ell)$ =0). A sample with coordinates 0.33, 0.33 corresponds to equal contributions from each of the three members of the group.

Loci of constant loss of electric strength (Z (ℓ) = constant) may also be displayed on the Cartesian diagram. As an example, T (S), located is approximately at $X(\ell) \sim Y(\ell)$ and with $Z(\ell)$> 0 implying approximately equal degradation due to acidity and water content plus some contribution from the loss of electric strength. Sample 85 has a moderate degraded level in this liquid domain but it is still of concern because all three components of the liquid group are of equal magnitude but loss of electrical strength is considered to be more severe [1].

Sample 63 is a degraded sample since two parameters (water and electrical strength) show high degradation levels, but it is dominated by the water parameter.

[1]Loss of electrical strength is considered to be more severe as the oil tends to lose its electrical insulation property and start to conduct current between the live parts of the transformer and the insulation paper Looms (1988).

6.6.3 Polar chromatic maps for water, acidity and electrical strength

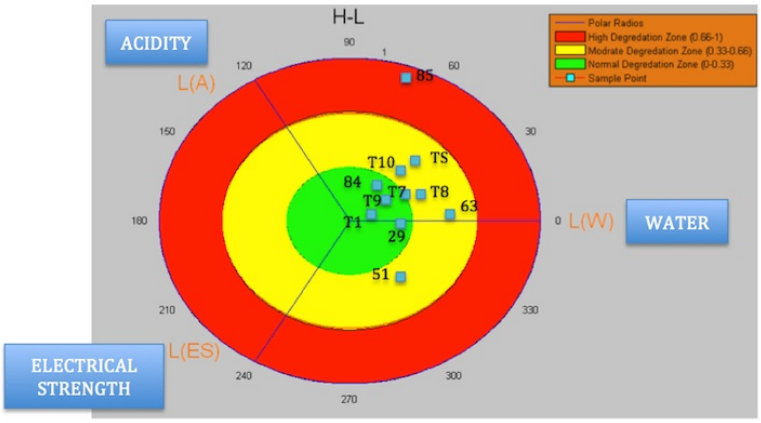

Figure 6.19: Polar diagrams of chromatic parameters H (ℓ) versus L (ℓ) for various oil samples.

Figure (6.19) shows a schematic of a H (ℓ): L (ℓ) polar diagram, where the radius, L (ℓ), is a measure of the overall severity of degradation due to all three members of the group (acidity, water content, electric strength) according to

$$L(\ell) = [L(aN) + L(wN) + L(esN)]/3 \tag{6.30}$$

H (ℓ) is defined by equation 3.20 chapter 3, subchapter 3.4.2.
Water

$$w = ((w/50) - (minw/50))/(1 - (minw/50)) \tag{6.31}$$

Acidity

$$a = acidity$$

$$acidity \geq 1 \Longrightarrow a = 1 \tag{6.32}$$

$$0 \leq a \leq 1$$

Electrical strength

$$es = (1 - (electrical\ strength/60)) \tag{6.33}$$

Where (a) is acidity, (w) is water content, (es) is electrical discharge. For example a H (ℓl) value (equation 3.20 chapter 3, subchapter 3.4.2) approaching 90 degrees is indicative of relatively high contributions from at least the acidity and water content factors.

Samples 63, 51, T10, are in the range (0.33< L < 0.66), which indicates a relatively high level of degradation. The degradation of each of these samples is governed by different members of the three degradation factors. The T10 degradation is governed mainly by acidity and water content, 63 by water content and 51 by water content and loss of electric strength but not acidity. On the other hand, samples T8, T7 are approaching the intermediate degradation threshold (L $\sim$ 0.33) and with degradation dominated by water content.

6.6.4 L (ℓ) Liquid chromatic parameter

An alternative diagram is to specifically relate L (ℓ) to the particular transformation equation 6.30.

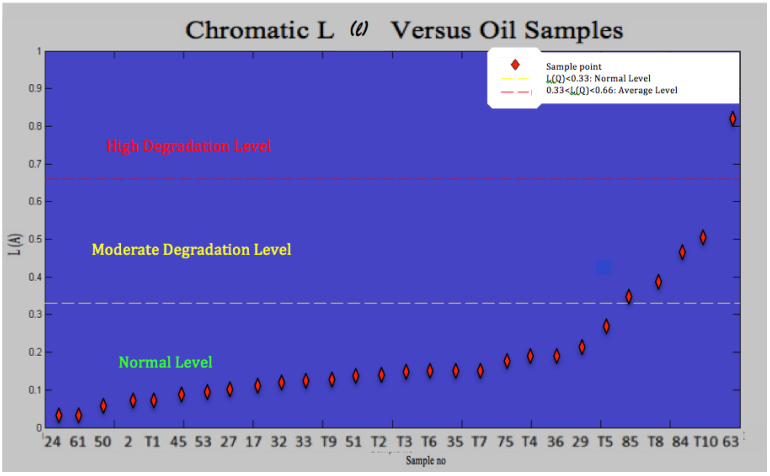

Figure 6.20: Combined acidity, water, and electrical strength for various samples.

Figure (6.20) shows the combined degradation indicator L (ℓ) for the various samples. Two thresholds maybe identified on the L (ℓ) graph namely at 0.33 and 0.66. Any sample in the range 0.33−0.66 is regarded as moderately degraded. Any samples above 0.66 are regarded as highly degraded.

SECONDARY PROCESSING

6.7 Combination Of (Optical, Dissolved Gas And Acidity) Effects

6.7.1 Chromatic analysis procedures

The chromatic values of the optical, dissolved gas and liquids parameters may be further chromatically processed to provide a cumulative quantification of overall degradation. For this purpose the most dominant chromatic parameter for each factor needs to be identified and then each of these regarded as R, G, B inputs into the chromatic algorithm (Chapter 3 subsection 3.4).

The most suitable chromatic parameter for the optical case is Fn(X(O)/Z(O)) (L(OT) = Fn(X(O)/Z(O))) (section 6.2.2) dissolved gas L(D) (subsection 6.4.2) and for liquid L(ℓ) (subsection 6.6.4).

A chromatic polar map (H(T);L(T)) may then be analysed to indicate the dominant degradation factor. Alternatively a Cartesian X(T):Y(T) diagram may be produced to quantify the contribution for each degradation facet. Finally the chromatic L(T) factor maybe presented as a function of oil sample to illustrate the magnitude of the overall degradation. L(T) is defined by equation 6.34.

$$L(T) = [L(OT) + L(D) + L(\ell)]/3 \tag{6.34}$$

Two L(T) degradation thresholds maybe established (L (T) = 0.33, 0.66) corresponding respectively to moderate and high degradation levels. These threshold values derive from the fact that if any of the three indicators L (OT), L (D), L (ℓ) tended to a maximum value whilst the others were zero, this would translate into L(T) = 0.33 (moderate degradation threshold); if two of the three indicators possessed maximum values and the other zero, then L(T) = 0.66. Thus the levels L (T) = 0.33, 0.66 represent approximate thresholds for progressive oil degradation.

6.7.2 Cartesian chromatic diagram for overall oil degradation

The total degradation results may be displayed on a Cartesian X(T), Y(T), Z(T) chromatic map figure (6.21).

The regions dominated by dissolved gases, optical, and liquid are distinguished on this figure so that samples dominated by each effect can be identified. The benchmark sample T1 is mainly liquid/ dissolved gas. Sample 63 is a mixture of optical, gas and acidity but it is dominated by gas. Sample 85 is a mixture of

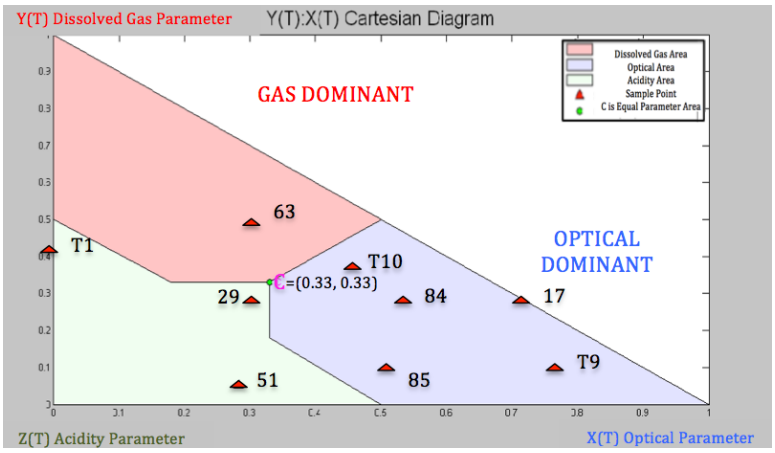

Figure 6.21: Cartesian diagrams of chromatic parameters Y (T), Z (T) and X (T).

acidity and optical but it is dominated by optical etc. Of course this map only indicates relative levels and not magnitude.

6.7.3 H-L Polar chromatic map of the combined degradation

Figure (6.22) shows the total polar chromatic H-L map for the combination of dissolved gas, optical and liquid components.

On this map the benchmark oil (T1), which is a good oil sample is located at the origin of the polar map. Sample T10 (H$\simeq$45 degree, L$\simeq$0.7) for example is shown to be degraded predominantly due to the optical indicator (Fn(X (O)/Z (O))

plus the dissolved gases factor (L (D); 63 (H$\simeq$120, L$\simeq$0.7) is degraded mainly due to the dissolved gases (L(D)); 85 (H$\simeq$290 degree, L$\simeq$0.48) is degraded due to a combination of liquid (L(ℓ)) and optical effects (L(OT)= (Fn(X(O)/Z(O))). The oil samples showing most signs of approaching a moderate degradation boundary (L$\sim$0.33) are 51, T8, T7, T9, 84, all having values of L (T)$\sim 0.15 - 0.2$ compared with a threshold of 0.33.

6.7.4 Overall magnitude parameter L (T)

In order to obtain an indication of how severe the overall oil condition is, recourse has to be made to the strength parameter L(T). This parameter value maybe

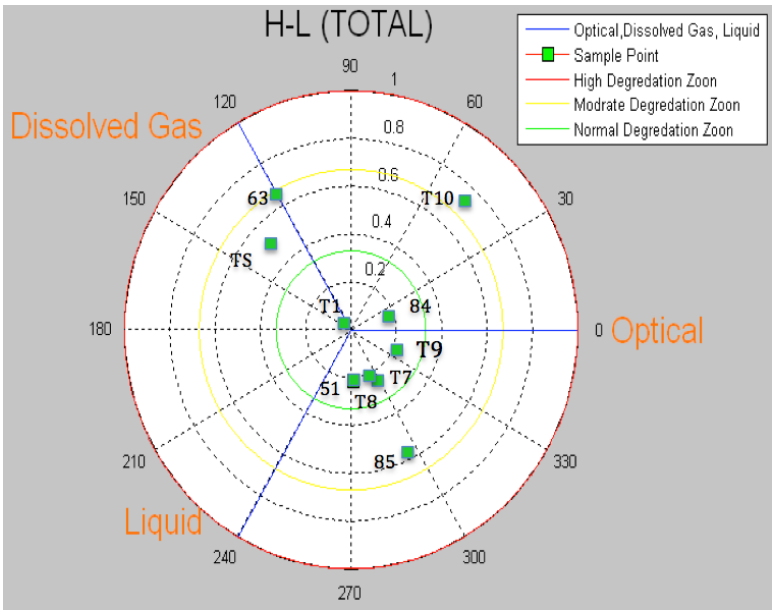

Figure 6.22: Polar diagram of chromatic parameters H (T) versus L (T).

calculated from the three components values (gas, Liquid, optical) according to equation 6.35.

$$L(T) = [L(OT) + L(DG) + L(\ell))]/3 \tag{6.35}$$

Figure (6.23) shows the individual magnitudes of the gas, liquid, optical components for each of 28 oil samples, which need to be processed to give the overall condition. All components of the L(T) parameter are normalised in the range 0−1 (equation 6.35). The graph shows a general agreement between each component in indicating critical levels. For example all three components indicates oil sample T10, 63 to have particularly high levels although there are examples of deviation from this (sample 85).

Figure (6.24) shows the overall magnitude parameter L(T) (equation 6.35) for various oil samples in increasing value order.

The two degradation thresholds of the L(T): oil sample map at L(T)=0.33 and 0.66 are shown. This diagram shows that samples T10, 63 and 85 are clearly the most degraded, lying around the severe degradation threshold (L(T)=0.66). They are followed by samples T8, 51, T7, T9, 84 but all are below the moderate degradation threshold of 0.33. Most of the remaining oil samples have L(T) 0.1 (i.e 10% full range).

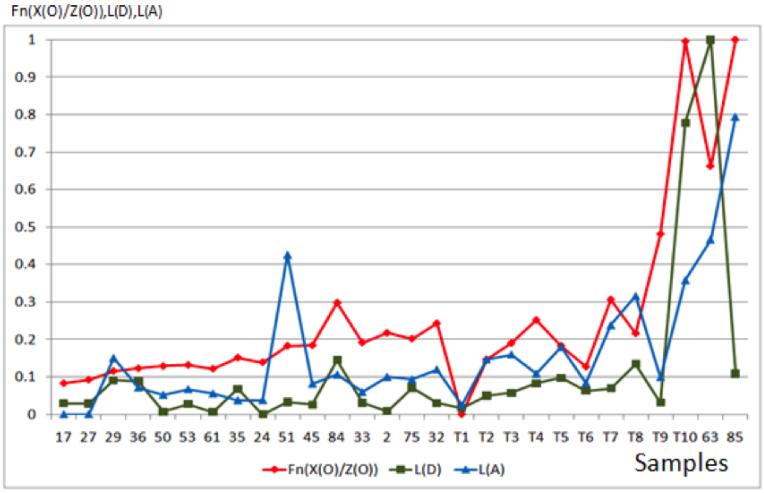

Figure 6.23: Optical (Fn(x(O)/z(O))), Dissolved Gases (L(D)) and Liquids/ Electric Strength.

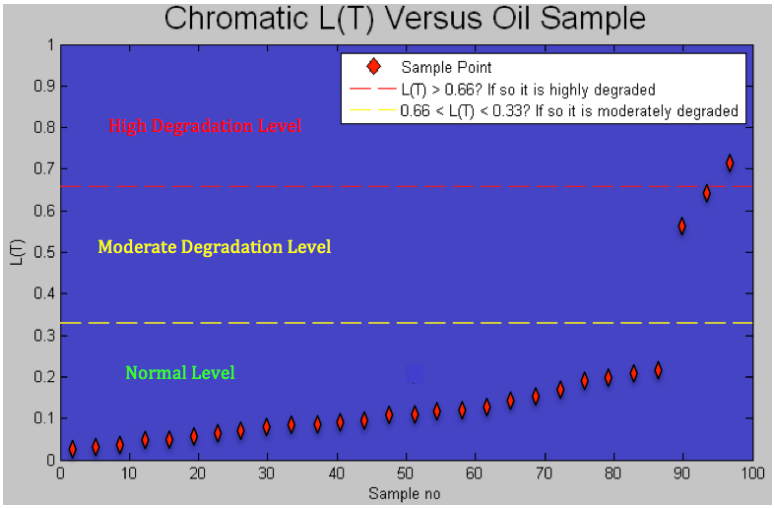

Figure 6.24: Overall magnitude parameter L(T) for various oil samples.

6.8 SUMMARY

This chapter has presented a description of the various ways in which chromatic transforms can be used for analysing the experimental results presented in chapter 5. Such transforms have been produced for

a) Optical transmission through oil samples using VDU light source.

b) Dissolved gas measurement for the oil samples.

c) Water contents, acidity, and electrical strength for the oil samples.

In each case Cartesian (X,Y,Z) and polar (H,L,S) chromatic maps have been produced and the chromatic parameter which dominates the identification of oil degradation has been determined. In the case of the optical results (a) above it has been shown that a chromatic parameter Z(O)/X(O) can be identified which closely resembles variation in colour index used conventionally.

Using the dominant chromatic parameters for the three different oil tests (a) optical (b) dissolved gas (c) liquid it has been shown how the test results can be further transformed chromatically to provide overall chromatic parameters which quantify the overall degradation condition of an oil sample.

It has been further explained how this overall chromatic parameter enables the source of degradation to be traced back to various levels of detail i.e. optical, dissolved gas etc. at the next level, water, acidity etc. as required by the end user.

Finally it has been shown that the chromatic optical approach has the capability of being adapted for indicating the extent to which suspended sediment may exist in the oil and affect the first level optical measurement.

Chapter 7

CONCLUSIONS

7.1 Project Achievements

Investigations have been conducted into the degradation of transformer oils which result in losses in performance of a utility transformer. These studies were performed on degraded oil samples provided by an industrial organisation. A new optical monitoring technique based upon a chromatic method has been developed and a new approach to analysing data from different types of tests, also based upon chromatic methods, has been developed and tested.

As a result of the study, a more versatile optical monitoring approach than hitherto available has been demonstrated. It has also been shown how complex sets of data from several different test dissolved gases, water contents, acidity, electrical discharging and optical transmission can be conveniently combined and correlated to yield an overall oil degradation indication. Software for performing this analysis has been specially developed in Matlab and tested and a user friendly system for site use demonstrated. Implementation of the approach on a portable P.C. has indicated the possibility of producing a portable system for site use. The outline Matlab code is included in appendix G.2. The test preformed with the VDU screen show that a portable system enclosed in a box that is light proof is feasible although the system is quite bulky. Tests preformed with LED illumination also show that this may be focusable for particle monitoring.

The project has shown how chromatic techniques are able to provide details about the degradation of an oil sample and the ability to combine different chromatic parameters to give details about the condition of the sample and also reasons for the degradation. In comparison with the Duval technique the chromatic

techniques provides more detailed results by utilising more factors e.g. dissolved gases, optical and liquid.

The work presented here has led to a number publications and outcomes. These are listed and described in appendix A.

7.2 Recommendations for Further Work

The developed system is capable of further evaluation through the acquisition of additional test data and empirical knowledge regarding oil degradation. For example, preliminary experiments have indicated a capability to monitor micro solid particles within an oil sample using a chromatic optical approach. This requires further refinement and development via additional extensive sample testing. Other types of test data can be accommodated into the developed scheme as future experience of the power industry grows and new testing approaches evolve. Effort will be needed to produce the extended software and develop further the user friendly data visualisation.

Bibliography

Adedipe, A. (2010). Toxins in lake Erie. Master's thesis, Case Western Reserve University.

AIST (2005). Information technology on five senses. Number 3. Public Relations Department.

Akbari, A., Setayeshmehr, A., Borsi, H., and Gockenbach, E. (2008). A software implementation of the Duval triangle method. In *ESEI* 2008. ISEI 2008. Conference Record of the 2008 IEEE International Symposium on *Electrical Insulation*, pp. 124-127.

Alshabben, S. (2012). Introduction to HCI: Human I/O, http://embots.dfki.de/doc/seminar_ss09/SandraAlshabben_HumanIO.pdf, last checked 22 November 2012.

Andreev, E. N. and Chubraeva, L. I. (2007). Investigation of a model HTSC transformer with amorphous alloy cores. *Journal of Materials Processing Technology* 181, 25-30.

Aragon-Patil, J., Fischer, M., and Tenbohlen, S. (2007). Improvement of interpretation of dissolved gas analysis for power transformers. In *International Conference on Advances in Processing, Testing and Application of Dielectric Materials*. Oficyna Wydawn. Politechn., 2009

Arivazhagan, S., Shebiah, R., Nidhyanandhan, S., and Ganesan, L., (2010). Fruit recognition using color and texture features. *Journal of Emerging Trends in Computing and Information Sciences* **1** (**2**), 90-94.

ARNO, S. (2006). Dissolved gas analysis of transformer oils: Effects of electric arc. *In Proceedings of the 6th WSEAS International Conference on Power Systems.* WSEAS.

Arvind, D., Khushdeep, S., Deepak, K. (2012). Condition monitoring of power transformer by analysing dissolved gas analysis and oil contamination test. *Journal Of Information*, Knowledge And Research In Electrical Engineering **1** (**2**), 103-111.

Apollo America Corp. (2012). Color comparison, http://www.greatlakesgeartech.com/apollo2.html, last checked 18 November 2012.

Apple Developer. (2005). Color management

overview,https://developer.apple.com/library/mac/documentation/graphicsimaging/conceptual/csintro/csintro last checked 24 November 2012.

Axis (2010). Ccd and Cmos sensor technology, http://www.axis.com/files/whitepaper/wp_ccd_cmos_40722_en_1010_lo.pdf Last checked 22 June 2013. Technical report, Axis communications.

Bartley, P. (2003). Analysis of transformer failures. In *International association of engineering insurers* 36th annual conference, Stockholm, pp. 1-12.

Bartley, W. (2002). Life cycle management of utility transformer assets. Hartford Steam Boiler Inspection & Insurance Company.

Bates, D. (2006). Dga in a box. A utility's perspective. Alabama Power Company, Alabama, USA.

Bergström, Kaplan, D. A., and Powell J., (2005). Laser absorption measurements in opaque solids. *The Absorptance of Metallic Alloys to Nd: YAG and Nd: YLF Laser Light*, 39.

Blackstock, D. (2000). *Fundamentals of physical acoustics*. Wiley-Interscience, 187.

Boser, K. J. (2003). Power transformer design, construction and field assembly. *Electricity Today* 4.

Bresch, H., Wassermann, B., Langer, B., Graf, C., Flesch, R., Becker, U., , Österreicher, B., Leisner, T., and Rhl, E., (2008). Elastic light scattering from free sub-micron particles in the soft x-ray regime. *Faraday discussions* 137, 389-402.

Brian, D. and Sparling, J. A., (2012). Power transformer life extension through better monitoring, http://site.ge-energy.com/prod_serv/plants_td/en/downloads/powergrid_europe07.pdf, last checked 25 June 2013.

Bureau of Reclamation. (2003). Transformer diagnostics. *Facilities Instructions, Standards, And Techniques* **3** (**13**).

Cargol, T. (2005). An overview of online oil monitoring technologies. In *Fourth Annual Weidmann-ACTI Technical Conference*, San Antonio.

Castleberry, G. W. (2008). Power plant electrical distribution systems.

PDH Center, 2410 Dakota Lakes Drive Herndon, VA 20171-2995.

Chen, A. (2009). Environmental energy technologies division news. http:// eetd.lbl.gov/newsletter/, Last checked 23 December 2012. 7 (4).

Chiesa, N. (2010). Power Transformer Modeling for Inrush Current Calculation. Ph. D. thesis, Norwegian University of Science and Technology, ISBN 978-82-471-2086-6.

Choi, S., Enjeti, P., and Pitel I. (1996). Autotransformer configurations to enhance utility power quality of high power ac/dc rectifier systems. *Proc. Particle Accelerator Conf.',95,* pp.1985 -1987 1995.

Chong, H., Gortler, S., and Zickler, T. (2008). A perception-based color space for illumination-invariant image processing. In *ACM Transactions on Graphics (TOG)*, Volume **27**, pp. 61. ACM.

Circutor (2012). Dielectric strength tester for isolating oils. Technical report, CIRCU-TOR S.A,: Código: P60311.

Cunningham, D. (1999). Expert system for transformer fault diagnosis. B.Sc Thesis. The University of Queensland.

David, I. G. and Rajaram, M. (2012). Separation of faults in oil immersed power transformers using fuzzy Rogers method. *European Journal of Scientific Research* Volume **80** (**4**), pp 423-429.

Dervos, C., Paraskevas, C., Skafidas, P., and Vassiliou, P. (2005a). A complex permittivity based sensor for the electrical characterization of high-voltage transformer oils. *Sensors* Volume **5** (**4**), pp 302-316.

Dervos, C., Paraskevas, C., Skafidas, P., and Vassiliou, P. (2005b). Dielectric characterization of power transformer oils as a diagnostic life prediction method. *Electrical Insulation Magazine, IEEE* Volume **21** (**1**), pp 11-19.

DiGiorgio, J. (2005). Dissolved gas analysis of mineral oil insulating fluids. DGA Expert System: A Leader in Quality, *Value and Experience* Volume **1**, 1-17.

Digital SLR photography (2012). Digital SLR Technology. http://digitalslrphotography.50webs.com, Last checked 24 November 2012.

Donaldson (2012). Surface iteration versus depth iteration, http://www.emea.donaldson.com/en/ltermedia/support/datalibrary/0

60171.pdf, last checked 26 November 2012.

DSI Ventures (2008). Dissolved gas analysis guide for transformers filled with beta fluid. *DSI Ventures*, Inc. http://n.b5z.net/i/u/10009217/f/DGA_for_Beta.pdf. Last checked 26 Jun 2013.

Electrical Construction Maintenance. (2003). The basics of transformers. http://ecmweb.com/archive/basics-transformers, Last checked 18 November 2012.

Fairman, H., Brill, M., and Hemmendinger, H. (1997). How the CIE 1931 color-matching functions were derived from Wright-Guild data. *Color Research & Application* Volume **22** (**1**), pp 11-23.

Faust, B. (1997). Modern Chemical Techniques. Number 978-1-87034-319-0.

Ferri, D. (2012). Uv-vis spectroscopy, http://www.vanbokhoven.ethz.ch/education/UV-Vis_-_D._Ferri; last checked 20 November 2012.

Foot, J. and Kilsby, C. (1989). Absorption of light by aerosol particles: An inter-comparison of techniques and spectral observations. *Atmospheric Environment (1967)* Volume **23** (**2**), PP 489-495.

Ford, A. and Roberts, A. (1998). Colour space conversions. *Westminster University*, London, pp 1-31.

Friedman, K., Hoffman, P., Bryan, W. (2012). Large power transformers and the U.S electric grid. The U.S. Department of Energy.

Garza, C., (2010). Measurement of mechanical strain using chromatic monitoring of photoelasticity. *Applied mechanics and materials*. **24-25**, 123-128.

Ghoneim, S., and Ward, S., (2012). Dissolved gas analysis as a diagnostic tools for early detection of transformer faults. *Advances in Electrical Engineering Systems* **1** (**3**), 152-156.

Gierlinger, F. (2005). Color spaces in modern multimedia environments. *EBU Technical Review*.

Golden, S., Craft, S., and Villalanti, D. (1995). Refinery analytical techniques optimize unit performance. *Hydrocarbon Processing* 74, 85-

106.

Gunter, M. and Light, I. (1992). Optical mineralogy. *Encyclopedia of earth system science* 3, 467.

Hamrick, L. (2009a). Dissolved gas analysis for transformers. Winter 2009-2010
Neta World.

Hamrick, L. (2009b). Transformer oil sampling. Summer 2009 Vol 31 (2) pp 23 *Neta World*.

Hanbury, A. (2002). The taming of the hue, saturation and brightness colour space. In *Proceedings of the 7th Computer Vision Winter Workshop*, Bad Aussee, Austria, pp. 234-243.

Hanbury, A. (2008). Constructing cylindrical coordinate colour spaces. *Pattern Recognition Letters* **29** (**4**), 494-500.

Harlow, J. H. I. (2004). *Electric Power Transformer Engineering* (1 ed.). Number 0-8493-1704-5 in 9. CRC Press LLC.

Hart, D. (2012). Dielectric fluids for transformer cooling history and types.
http://www.nttworldwide.com/docs/001_Dielectric_Fluids_for_Transformer_Cooling.pdf, last checked 26 Jun 2013.

Helmers, H. and M. Schellenberg (2003). Cmos vs. ccd sensors in speckle interferometry. *Optics & Laser Technology* **35** (**8**), 587-595.

Höhlein, I., Kachler, A., Stach, M., Tenbohlen, S., and Leibfried, T. (2003). Transformer life management, german experience with condition assessment. In *Contribution for Cigr SC12/A2-Merida Kolloquium*.

Horn, R. (2009). Script to lecture: Raman spectroscopy. Lecture Series, Modern Methods in Heterogeneous Catalysis.

Jacobs, D. (2007). Computer graphics, http://www.cs.umd.edu/~djacobs/CMSC427/Color.pdf, last checked 22 November 2012.

Jakob, F., Sacramento, C., and Bensalem, P. (2005). Oil: The four r's: retain, recondition, reclaim, replace. *Analytical ChemTech International, Inc*.

Jianjun, C., Peilin, Z., Guoquan, R. and Jianping, F. (2007). Decentralized

and overall condition monitoring system for large-scale mobile and complex equipment. *Journal of Systems Engineering and Electronics* **18** (**4**), 758-763.

Jones, G., Deakin, A., and Spencer, J., (2009). Chromatic signatures of broadband optical spectra for liquor discrimination. *Measurement Science and Technology* **20** (**2**), 025304.

Khan, N. (2010, December). Daylight simulation for design and compliance.

King, T. (2005). Human color perception, cognition, and culture: why red is always red. In *Proc. SPIE*, Volume 5667, pp. 234-242.

Kirtley Jr, J., Hagman, W., Lesieutre, B., Boyd, M., Warren, E., Chou, H., and Tabors, R. (1996). Monitoring the health of power transformers. *Computer Applications in Power*, *IEEE* **9** (**1**), 18-23.

Kodak (2012). The nature of light and color. http://motion.kodak.com, Last checked 22 November 2012.

Koehler (2008). Koehler petroleum testing equipment catalog. In *2008 Koehler Catalog*, pp. 43-77. Koehler Instrument Company, Inc.

Koirala, P. (2007). Rgb color spaces. http://www.cs.joensuu.fi/~pkoirala/article/RGB-space.pdf, Last checked 10 June 2013

Kolb, H., Fernandez, E., and Nelson, R. (2005). Simple anatomy of the retina. http://webvision.med.utah.edu/book/part-i-foundations/simple-anatomy-of-the-retina/, last checked 20 Jun 2013.

Konica Minolta. (2007). Precise Color Communication. Number 9242-4830-92. Japan: Konica Minolta Sensing. INC.

Krzywinski, M. (2012). Color palettes matter. http://mkweb.bcgsc.ca, Last checked 23 November 2012.

Laborelec (2012). Oil analyses condition assessment of transformers and rotating machinery. http://www.smartsignal.com, Last checked 19 November 2012.

Lee, J. C., Seo, H. S., and Kim, Y. J. (2012). The increased dielectric breakdown voltage of transformer oil based nanofluids by an external magnetic field. *International Journal of Thermal Sciences* **62** (**0**), 29-33.

Leibfried, T., Kachler, A., Zaengl, W., Der Houhanessian, V., Kchler, A., and Breiten-bauch, B. (2002). Ageing and moisture analysis of power transformer insulation systems. *CIGRE Session*, Paris, 1-6.

Lewand, L. (2006). Practical experience gained from furanic compound analysis. In *Proceedings of the 2006 International Conference of Doble Clients*, Boston, MA (USA).

Lim, S., Choi, H., Chung, D., Ko, S., and Han, B. (2005). Impedance variation of a flux-lock type SFCL dependent on winding direction between coil 1 and coil 2. *IEEE transaction on Applied Superconductivity*. Volume 15, issue 2.

Litwiller, D. (2001). Ccd vs. cmos. *Photonics Spectra* **35** (**1**), 154-158.

Looms, J. (1988). Insulators for high voltages. Peter Peregrinus Limited 7.

Lucas, J. (2000). Historical development of the transformer. The Institution of Electrical Engineers, Sri Lanka Centre, Chairman's Lecture 1, 14.

Luksich, J. (2004). Evaluating new and in-service vegetable oil dielectric fluids. In *Weidmann-ACTI 3rd Annual Technical Conference*, Sacramento, CA.

Malm, W. (1999). Introduction to visibility, Volume 40. Cooperative Institute for Research in the Atmosphere, NPS Visibility Program, Colorado State University.

Manahan, S. (2000). Environmental chemistry. Lewis, ISBN 1-56670-492-8.

Meister, D. and Sheedy, J. (2000). Introduction to Ophthalmic Optics. SOLA Optical USA.

Meng, L. W. (2009, May). Dissolved gas analysis (dga) of mineral oil used in transformers.

Meshkatoddini, M. (2008). Aging study and lifetime estimation of transformer mineral oil. *American J. of Engineering and Applied Sciences* **1** (**4**), 384-388.

Mihai, D. and Străjescu, E. (2007). From wavelength to rgb filter. *U.P.B. Sci. Bull. Series D*, Vol. 69, No. 2, 2007 ISSN1453-2358.

Muhamad, N., Phung, B., Blackburn, T., and Lai, K. (2007). Comparative

study and analysis of dga methods for transformer mineral oil. In *Power Tech*, 2007 IEEE Lausanne, pp. 45-50.

Murthy, T. (1996). Assessment of transformer insulation condition by evaluation of paper-oil system. In *Electrical Insulation and Dielectric Phenomena, 1996*., *IEEE 1996 Annual Report of the Conference on*, Volume 1, pp. 332-335.

Micro Spectral Analysis. (2012). Petroleum and oil color spectrometer i-lab vrv-300 for ASTM d1500 method.

Neumann, M. (1983). Dipole moment fluctuation formulas in computer simulations of polar systems. *Molecular Physics* **50** (**4**), 841-858.

Nunes, S., de Zea Bermudez, V., Silva, M., Smith, M., Ostrovskii, D., Ferreira, R., Carlos, L., Rocha, J., Goncalves, A., and Fortunato, E. (2007). Sol-gel-derived potassium-based di-ureasils for smart windows. *Journal of Materials Chemistry* **17** (**40**), 4239-4248.

Otto, G. (2000). Color Theory and 2D Image Representation. http://viz.aset.psu.edu/gho/sem_notes/color_2d/index.html, Last checked 24 November 2012.

Parraman, C. and Rizzi, A. (2011). Colour coded. *Society of Dyers and Colourists*. ISBN 978-0-90156-93-4.

Poynton, C. (1995). A guided tour of color space. In *SMPTE Advanced Television and electronic imaging conference*, pp. 167-180.

Puentes, G. et al. (2007). Classical and quantum scattering in optical systems. Physics Department/Huygens Laboratory/Quantum Optics Group, Faculty of Mathematics and Natural Sciences, Leiden University.

Power Electronical. (2012). Transformer oil testing and oil analysis, http://www.oil-testers.com/Transformer_Oil_Testing_Laboratory.html; last checked 18 November 2012.

Perfector Scientific. (2012). Disposable Cuvettes. http://www.perf-sci.com, Last checked 26 November 2012.

Ragaa, M., Spencer, J. W., Jones, G., and Deakin, A. (2010). Characterisation of partial dis-charge signals using a chromatic approach. In *18th International Conference on Gas Discharges and Their Applications*. GD Greifswald, Germany.

Rojas, R. (2012). Global Computer Vision. Freie Universität Berlin, Takustraβe 9 14195 Berlin, Germany.

Ryer, A. (1997). *Light measurement handbook*. International Light 17 Graf Road Newburyport, MA 01950. ISBN 0-9658356-9-3.

Sahin, F. (1997). A radial basis function approach to a color image classification problem in a real time industrial application. Ph. D. thesis, Virginia Polytechnic Institute and State University.

Sartorius (2012). Filter Papers (Including Thimbles, Glass and Quartz Microfiber Filters), http://www.analytics-shop.com, Last checked 26 November 2012. pp 123.

Scarso, L. (2010). Introduction to colours in context mkiv. *TUGboat-TeX Users Group* **31** (**3**), 203.

Shaban, K., El-Hag, A., and Matveev, A. (2009). A cascade of artificial neural networks to predict transformers oil parameters. *Dielectrics and Electrical Insulation*, *IEEE Transactions on* **16** (*2*), 516-523.

Shankar, V., Saurabh, V. and Prashant (2011). Transformer's history and its insulating oil. In *Proceedings of the 5th National Conference; INDIACom-2011 Computing For Nation Development*, March 10 – 11, 2011 Bharati Vidyapeeth's Institute of Computer Applications and Management, New Delhi.

Shoureshi, R., Norick, T., and Swartzendruber, R. (2004). Intelligent transformer monitoring system utilizing neuro-fuzzy technique approach. *Intelligent Substation Final Project Report*, 4-26. Colorado School of Mines

Siemens AG. (2010). Gas-guard R 8. Energy Sector.

Singh, S., and Bandyopadhyay, M. (2010). Duval triangle: A noble technique for dga in power transformers. International Journal of Electrical and Power Engineering **4** (**3**), 193-197.

Smith, B. (2001). Oil mist detection as an aid to monitoring an engine's condition. AIMarEST, MIDGTE. *PSERC Publication* (2004): 4-26.

Snyder, J. (1996). Area light sources for real-time graphics. Technical Report MSR-TR-96-11, Microsoft Research Advanced Technology Division, Microsoft Corporation One Microsoft Way Redmond, WA 98052.

Souza, G. and Miller, J. (2012). Elastic light scattering of biopolymer/gold nanoparticles fractal aggregates. *Reviews in Plasmonics 2010* , 39-68.

Stockman, M. (2007). Criterion for negative refraction with low optical losses from a fundamental principle of causality. *Physical Review Letters* **98** (**17**), 177404.

Stone, M. (2003). *A field guide to digital color*, Vol 3. AK Peters Natick, MA.

Strobel, N. (2011). Electromagnetic radiation, http://www.astronomynotes.com, last checked 18 December 2012.

Taylor, A. E. F. (2000). *Illumination Fundamentals*. Rensselaer Polytechnic Institute.

Terrell Croft, Wilford I., Summers, F. H. (2008). *American Electricians' Handbook* (15 ed.). Number 0071494626. McGraw-Hill.

Texas Instruments Incorporated (2001). Section 4 power transformer design, www.ti.com/lit/ml/slup126/slup126.pdf, last checked 19 December 2012.

TOSHIBA (2012). Transformers corporation power system. Shibaura 1-Chome, Minato-Ku, Tokyo 105-8001, Japan.

Turcotte, R. (2011). Transformer oil testing. The Locomotive. " *Process Safety Progress* 15, no. 1 (1996): 2-4.

Tutorvista (2012). Laws of Refraction. http://www.tutorvista.com, Last checked 22 November 2012.

U.S. Department of the Interior. (2005). *Transformers: Basics, Maintenance and Diagnostics*. Books Express Publishing.

U.S. Department of Energy. (2005). Large power transformers. Technical Report AK-0509, Mitsubishi Denki Bldg,.2-2-3. Marunouchi, Chiyod-KU, Tokyo 100-8310. Japan.

Verma, P. (2005). Condition monitoring of transformer oil and paper. http://dspace.thapar.edu:8080/dspace/bitstream/123456789/91/3/T91.pdf last checked 22 Jun 2013.

Wang, M. (2003). A novel extension method for transformer fault diagnosis. *Power Delivery, IEEE Transactions on*, **18** (**1**).

Wang, M., Vandermaar, A., and Srivastava, K. (2002). Review of condition assessment of power transformers in service. *Electrical Insulation Magazine*, IEEE **18** (**6**), 12-25.

Wang, Z. (2000). Artificial intelligence applications in the diagnosis of power trans-former incipient faults.

Whatman (2009). Cellulose filters, http://www.whatman.com/references/iterationsimplified.pdf, last checked 26 November 2012.

Williams, D.B., & Carter, C. (2009). *Transmission Electron Microscopy*, 4, Springer.

Williamson, S., and Cummins, H. (1983). Light and color in nature and art. *Light and Color in Nature and Art*, by Samuel J. Williamson, Herman Z. Cummins, pp. 512. ISBN 0-471-08374-7. Wiley-VCH, February 1983. 1.

Willson, R. and Shafer, S. (1991). Dynamic lens compensation for active color imaging and constant magnification focusing. No. CMU-RI-TR-91-26. Carnegie-Mellon Univ Pittsburgh Pa Robotics Inst, 1991.

Wimmer, B. (2009). Megapixel Video. http://www.securitysales.com/resources/ss3dumies.pdf, last checked 20 June 2013

Woodham, R. (2008). Colour is a Medium as well as a Message. In *Colour Perception: Philosophical, Psychological, Artistic and Computational Perspectives* (S. Davis, ed.), vol. 9 of Vancouver Studies in Cognitive Science, pp. 117–140, Oxford University Press, 2000.

Yuliastuti, E. (2010). Analysis of dielectric properties comparison between mineral oil and synthetic ester oil. Master's thesis, Delft University of Technology.

Yun, Y., Chen, W., Wang, Y., and Pan, C. (2008). Photoacoustic detection of dissolved gases in transformer oil. *European Transactions on Electrical Power* **18** (**6**), 562-576.

Zemplen, G. (2002). An Eye For Optical Theory? Bmge Gtk Technika-Mernok es Tudomnytorte net Doktori Iskola, 2002.

Zurich, N. (2001). Ccd versus cmos. Has ccd imaging come to an end? In *Photogrammetric Week* 01.

Appendix A

List of Publication

A concise overview of the work presented here is in the process of being published in High Voltage Engineering and Testing, 3rd Edition
Author: Hugh M. Ryan
Year: 2012
ISBN: 978-1-84919-263-7

A presentation of the work was made in the IOP (Institute of Physics) conference at the Department of Mechanical Engineering in the University of Liverpool in 2010.
It was also included in the following presentation:

Chromatic Monitoring of Electric Power Systems with Examples of Applications, G. R. Jones, J. W. Spencer, A. G. Deakin, D. H. Smith, E. Elzagzoug, M. Ragaa ,2012 EuroDoble Colloquium, 15-17 October, 2012, Manchester UK.
The software was demonstrated to Mr. Jones from ENW Warrington.

A paper on the subject of chromatic oil monitoring is also in progress. The details are as follow:

Provisional title: CONDITION MONITORING OF HIGH VOLTAGE TRANSFORMER OILS USING OPTICAL CHROMATICITY

Author: Ezzaldeen Elzagzoug

Appendix B

VDU and LED Transmitted Light RGB Values

B.1 Raw RGB Values From VDU

B.2 Raw RGB Values From LED

B.3 Spectra Data From VDU

Table B.1: Raw RGB values for different transformer oil samples.

	R	G	B
E6	0.33	0.26	0.75
T1	0.39	0.26	0.64
T4	0.40	0.23	0.36
T7	0.40	0.23	0.33
T10	0.40	0.17	0.00
27	0.42	0.30	0.69
33	0.41	0.28	0.55
45	0.41	0.29	0.55
53	0.42	0.30	0.64
75	0.41	0.29	0.53
17	0.42	0.31	0.71
24	0.41	0.30	0.61
29	0.41	0.31	0.65
32	0.41	0.28	0.49
35	0.40	0.30	0.58
36	0.41	0.30	0.64
50	0.41	0.30	0.62
51	0.41	0.29	0.55
61	0.41	0.28	0.63
75	0.41	0.29	0.53
84	0.40	0.27	0.44
85	0.17	0.00	0.00
63	0.04	0.00	0.02

Table B.2: Early transformer oil samples raw RGB values from LED illumination.

	R	G	B
E	0.61	0.50	0.48
T1	0.65	0.53	0.42
T5	0.68	0.57	0.26
T10	0.72	0.52	0.03

Table B.3: Spectra data for different transformer oil samples.

		E	T1	T5	T9	T10
300		1.00E-009	1.00E-009	1.00E-009	1.00E-009	1.00E-009
303		1.00E-009	1.00E-009	1.00E-009	1.00E-009	1.00E-009
306		1.00E-009	1.00E-009	1.00E-009	1.00E-009	1.00E-009
309		1.00E-009	1.00E-009	1.00E-009	1.00E-009	1.00E-009
312		1.00E-009	1.00E-009	1.00E-009	1.00E-009	1.00E-009
315		1.00E-009	1.00E-009	1.00E-009	1.00E-009	1.00E-009
318		1.00E-009	1.00E-009	1.00E-009	1.00E-009	1.00E-009
321		1.00E-009	1.00E-009	1.00E-009	1.00E-009	1.00E-009
324		1.00E-009	1.00E-009	1.00E-009	1.00E-009	1.00E-009
326.9		1.00E-009	1.00E-009	1.00E-009	1.00E-009	1.00E-009
329.9		1.00E-009	1.00E-009	1.00E-009	1.00E-009	1.00E-009
332.9		1.00E-009	1.00E-009	1.00E-009	1.00E-009	1.00E-009
335.9		1.00E-009	1.00E-009	1.00E-009	1.00E-009	1.00E-009
338.9		1.00E-009	1.00E-009	1.00E-009	1.00E-009	1.00E-009
341.9		1.00E-009	1.00E-009	1.00E-009	1.00E-009	1.00E-009
344.9		1.00E-009	1.00E-009	1.00E-009	1.00E-009	1.00E-009
347.9		1.00E-009	1.00E-009	1.00E-009	1.00E-009	1.00E-009
350.9		2.52E-007	2.35E-007	2.48E-007	2.51E-007	2.27E-007
353.9		2.60E-007	2.43E-007	2.60E-007	2.64E-007	2.35E-007
356.9		2.75E-007	2.53E-007	2.74E-007	2.80E-007	2.52E-007
359.9		2.92E-007	2.68E-007	2.93E-007	2.95E-007	2.68E-007
362.9		2.95E-007	2.80E-007	3.14E-007	3.09E-007	2.76E-007
365.9		3.02E-007	2.87E-007	3.20E-007	3.13E-007	2.86E-007
368.9		3.09E-007	2.84E-007	3.16E-007	3.07E-007	2.94E-007
371.9		3.07E-007	2.64E-007	2.93E-007	2.87E-007	2.79E-007
374.9		2.77E-007	2.13E-007	2.54E-007	2.36E-007	2.48E-007
377.8		2.57E-007	1.59E-007	1.94E-007	1.78E-007	2.12E-007
380.8		2.02E-007	1.26E-007	1.35E-007	1.23E-007	1.53E-007
383.8		1.38E-007	8.29E-008	8.14E-008	8.62E-008	9.32E-008
386.8		7.65E-008	4.93E-008	4.20E-008	4.45E-008	4.89E-008
389.8		4.36E-008	3.84E-008	1.53E-008	2.97E-008	1.97E-008
392.8		7.48E-009	3.35E-008	3.43E-009	2.21E-008	1.00E-009
395.8		1.00E-009	1.26E-008	8.77E-009	2.12E-008	1.00E-009
398.8		1.00E-009	4.34E-009	9.09E-009	3.89E-009	5.81E-009
401.8		1.10E-008	1.83E-008	1.58E-008	3.89E-009	2.15E-008
404.8		1.10E-008	2.46E-008	1.58E-008	1.17E-008	2.15E-008
407.8		1.10E-008	2.31E-008	1.58E-008	1.17E-008	3.66E-008
410.8		1.10E-008	2.13E-008	8.00E-009	2.30E-008	3.66E-008
413.8		1.80E-008	3.37E-008	7.68E-009	4.35E-008	3.84E-008

		E	T1	T5	T9	T10
416.8		8.03E-009	1.98E-008	1.00E-009	4.35E-008	2.27E-008
419.8		8.03E-009	1.34E-008	1.00E-009	3.57E-008	2.27E-008
422.8		8.39E-009	1.34E-008	1.00E-009	3.86E-008	9.60E-009
425.7		1.39E-008	1.34E-008	1.00E-009	2.44E-008	1.07E-008
428.7		6.84E-009	2.72E-009	2.02E-008	3.86E-008	4.12E-009
431.7		6.84E-009	2.72E-009	2.02E-008	4.07E-008	4.12E-009
434.7		6.84E-009	2.72E-009	2.02E-008	4.07E-008	4.12E-009
437.7		1.92E-008	1.09E-008	1.37E-008	2.69E-008	4.32E-009
440.7		3.16E-008	1.96E-008	1.98E-008	3.11E-008	5.65E-009
443.7		4.65E-008	2.85E-008	2.57E-008	3.65E-008	6.94E-009
446.7		5.92E-008	3.53E-008	3.30E-008	4.20E-008	1.05E-008
449.7		7.80E-008	4.54E-008	3.15E-008	2.98E-008	1.69E-008
452.7		9.83E-008	5.81E-008	4.10E-008	3.83E-008	2.09E-008
455.7		1.20E-007	7.33E-008	5.21E-008	4.78E-008	2.76E-008
458.7		1.42E-007	8.99E-008	6.30E-008	5.89E-008	3.28E-008
461.7		1.58E-007	1.04E-007	7.33E-008	6.79E-008	3.57E-008
464.7		1.78E-007	1.13E-007	8.74E-008	7.82E-008	4.86E-008
467.7		1.86E-007	1.27E-007	9.27E-008	8.46E-008	4.64E-008
470.7		1.92E-007	1.35E-007	9.68E-008	8.62E-008	4.06E-008
473.7		1.94E-007	1.38E-007	1.02E-007	8.53E-008	3.90E-008
476.6		1.93E-007	1.37E-007	1.04E-007	8.52E-008	3.55E-008
479.6		1.94E-007	1.37E-007	1.09E-007	8.73E-008	2.80E-008
482.6		2.01E-007	1.45E-007	1.19E-007	9.24E-008	3.15E-008
485.6		2.07E-007	1.50E-007	1.27E-007	1.03E-007	3.48E-008
488.6		2.14E-007	1.65E-007	1.38E-007	1.12E-007	3.97E-008
491.6		2.24E-007	1.83E-007	1.53E-007	1.26E-007	3.77E-008
494.6		2.41E-007	1.96E-007	1.70E-007	1.39E-007	4.85E-008
497.6		2.60E-007	2.11E-007	1.88E-007	1.56E-007	5.80E-008
500.6		2.75E-007	2.24E-007	2.12E-007	1.75E-007	6.85E-008
503.6		3.01E-007	2.41E-007	2.36E-007	2.02E-007	8.42E-008
506.6		3.36E-007	2.64E-007	2.69E-007	2.34E-007	1.17E-007
509.6		3.71E-007	2.96E-007	3.04E-007	2.70E-007	1.46E-007
512.6		3.97E-007	3.22E-007	3.32E-007	3.01E-007	1.69E-007
515.6		4.24E-007	3.42E-007	3.53E-007	3.25E-007	1.85E-007
518.6		4.41E-007	3.56E-007	3.64E-007	3.47E-007	1.97E-007
521.6		4.45E-007	3.61E-007	3.66E-007	3.61E-007	1.95E-007
524.6		4.51E-007	3.68E-007	3.72E-007	3.68E-007	1.98E-007
527.5		4.63E-007	3.79E-007	3.78E-007	3.81E-007	1.97E-007
530.5		4.76E-007	3.98E-007	3.91E-007	3.91E-007	2.07E-007
533.5		4.91E-007	4.18E-007	4.13E-007	4.11E-007	2.22E-007
536.5		5.11E-007	4.45E-007	4.42E-007	4.37E-007	2.45E-007

		E	T1	T5	T9	T10
539.5		5.32E-007	4.64E-007	4.63E-007	4.60E-007	2.65E-007
542.5		5.62E-007	4.86E-007	4.92E-007	4.90E-007	2.91E-007
545.5		5.77E-007	5.09E-007	5.20E-007	5.20E-007	3.16E-007
548.5		6.01E-007	5.28E-007	5.45E-007	5.44E-007	3.36E-007
551.5		6.21E-007	5.46E-007	5.65E-007	5.56E-007	3.56E-007
554.5		6.38E-007	5.74E-007	5.91E-007	5.76E-007	3.78E-007
557.5		6.54E-007	5.93E-007	6.13E-007	5.94E-007	4.08E-007
560.5		6.89E-007	6.20E-007	6.45E-007	6.20E-007	4.36E-007
563.5		7.25E-007	6.53E-007	6.78E-007	6.49E-007	4.65E-007
566.5		7.60E-007	6.79E-007	7.15E-007	6.80E-007	4.92E-007
569.5		7.92E-007	6.95E-007	7.52E-007	7.14E-007	5.15E-007
572.5		8.18E-007	7.14E-007	7.83E-007	7.42E-007	5.38E-007
575.4		8.44E-007	7.31E-007	8.08E-007	7.67E-007	5.62E-007
578.4		8.63E-007	7.50E-007	8.31E-007	7.84E-007	5.89E-007
581.4		8.95E-007	7.72E-007	8.57E-007	8.13E-007	6.17E-007
584.4		9.25E-007	7.94E-007	8.76E-007	8.45E-007	6.53E-007
587.4		9.56E-007	8.31E-007	9.07E-007	8.71E-007	6.77E-007
590.4		9.86E-007	8.56E-007	9.35E-007	9.09E-007	7.09E-007
593.4		1.02E-006	8.81E-007	9.70E-007	9.56E-007	7.43E-007
596.4		1.04E-006	9.12E-007	9.91E-007	9.89E-007	7.77E-007
599.4		1.07E-006	9.43E-007	1.02E-006	1.02E-006	7.99E-007
602.4		1.10E-006	9.71E-007	1.05E-006	1.07E-006	8.32E-007
605.4		1.14E-006	1.01E-006	1.08E-006	1.11E-006	8.62E-007
608.4		1.17E-006	1.05E-006	1.10E-006	1.14E-006	8.98E-007
611.4		1.20E-006	1.09E-006	1.13E-006	1.18E-006	9.21E-007
614.4		1.23E-006	1.12E-006	1.15E-006	1.21E-006	9.56E-007
617.4		1.24E-006	1.14E-006	1.18E-006	1.24E-006	9.75E-007
620.4		1.27E-006	1.17E-006	1.20E-006	1.27E-006	1.00E-006
623.4		1.29E-006	1.19E-006	1.23E-006	1.30E-006	1.03E-006
626.3		1.32E-006	1.21E-006	1.26E-006	1.33E-006	1.06E-006
629.3		1.35E-006	1.24E-006	1.29E-006	1.36E-006	1.08E-006
632.3		1.37E-006	1.27E-006	1.33E-006	1.39E-006	1.11E-006
635.3		1.40E-006	1.30E-006	1.36E-006	1.42E-006	1.14E-006
638.3		1.44E-006	1.33E-006	1.39E-006	1.45E-006	1.18E-006
641.3		1.47E-006	1.36E-006	1.42E-006	1.48E-006	1.22E-006
644.3		1.51E-006	1.40E-006	1.47E-006	1.50E-006	1.25E-006
647.3		1.55E-006	1.44E-006	1.48E-006	1.55E-006	1.29E-006
650.3		1.59E-006	1.48E-006	1.51E-006	1.59E-006	1.32E-006
653.3		1.63E-006	1.51E-006	1.55E-006	1.64E-006	1.35E-006
656.3		1.67E-006	1.54E-006	1.61E-006	1.68E-006	1.39E-006
659.3		1.71E-006	1.59E-006	1.65E-006	1.75E-006	1.43E-006

		E	T1	T5	T9	T10
662.3		1.75E-006	1.62E-006	1.71E-006	1.78E-006	1.45E-006
665.3		1.79E-006	1.66E-006	1.77E-006	1.84E-006	1.49E-006
668.3		1.84E-006	1.70E-006	1.80E-006	1.87E-006	1.54E-006
671.3		1.88E-006	1.74E-006	1.84E-006	1.93E-006	1.58E-006
674.3		1.92E-006	1.76E-006	1.89E-006	1.97E-006	1.62E-006
677.2		1.96E-006	1.79E-006	1.93E-006	2.01E-006	1.66E-006
680.2		2.00E-006	1.82E-006	1.97E-006	2.04E-006	1.73E-006
683.2		2.04E-006	1.86E-006	2.03E-006	2.07E-006	1.77E-006
686.2		2.10E-006	1.90E-006	2.09E-006	2.09E-006	1.83E-006
689.2		2.15E-006	1.95E-006	2.16E-006	2.12E-006	1.87E-006
692.2		2.20E-006	1.99E-006	2.21E-006	2.16E-006	1.92E-006
695.2		2.26E-006	2.04E-006	2.27E-006	2.21E-006	1.97E-006
698.2		2.31E-006	2.10E-006	2.32E-006	2.28E-006	1.99E-006
701.2		2.33E-006	2.15E-006	2.37E-006	2.32E-006	2.03E-006
704.2		2.35E-006	2.21E-006	2.39E-006	2.37E-006	2.06E-006
707.2		2.38E-006	2.27E-006	2.42E-006	2.40E-006	2.09E-006
710.2		2.40E-006	2.33E-006	2.43E-006	2.46E-006	2.10E-006
713.2		2.44E-006	2.39E-006	2.48E-006	2.53E-006	2.16E-006
716.2		2.50E-006	2.46E-006	2.53E-006	2.62E-006	2.20E-006
719.2		2.57E-006	2.51E-006	2.59E-006	2.69E-006	2.27E-006
722.2		2.65E-006	2.57E-006	2.64E-006	2.76E-006	2.33E-006
725.1		2.72E-006	2.59E-006	2.73E-006	2.82E-006	2.41E-006
728.1		2.77E-006	2.61E-006	2.79E-006	2.85E-006	2.44E-006
731.1		2.83E-006	2.64E-006	2.85E-006	2.88E-006	2.49E-006
734.1		2.87E-006	2.69E-006	2.90E-006	2.92E-006	2.54E-006
737.1		2.91E-006	2.78E-006	2.94E-006	3.00E-006	2.57E-006
740.1		2.97E-006	2.82E-006	3.01E-006	3.05E-006	2.63E-006
743.1		3.03E-006	2.87E-006	3.07E-006	3.10E-006	2.69E-006
746.1		3.07E-006	2.94E-006	3.11E-006	3.15E-006	2.72E-006
749.1		3.13E-006	2.99E-006	3.17E-006	3.22E-006	2.78E-006
752.1		3.19E-006	3.06E-006	3.22E-006	3.28E-006	2.84E-006
755.1		3.24E-006	3.11E-006	3.28E-006	3.33E-006	2.88E-006
758.1		3.31E-006	3.16E-006	3.34E-006	3.38E-006	2.94E-006
761.1		3.37E-006	3.21E-006	3.40E-006	3.44E-006	3.00E-006
764.1		3.41E-006	3.25E-006	3.44E-006	3.48E-006	3.04E-006
767.1		3.47E-006	3.30E-006	3.49E-006	3.55E-006	3.10E-006
770.1		3.51E-006	3.36E-006	3.55E-006	3.59E-006	3.15E-006
773.1		3.56E-006	3.39E-006	3.61E-006	3.65E-006	3.20E-006
776		3.59E-006	3.43E-006	3.65E-006	3.71E-006	3.24E-006
779		3.64E-006	3.47E-006	3.70E-006	3.74E-006	3.28E-006
782		3.69E-006	3.51E-006	3.77E-006	3.80E-006	3.34E-006

		E	T1	T5	T9	T10
785		3.71E-006	3.56E-006	3.80E-006	3.85E-006	3.36E-006
788		3.75E-006	3.60E-006	3.84E-006	3.88E-006	3.41E-006
791		3.81E-006	3.64E-006	3.88E-006	3.94E-006	3.48E-006
794		3.84E-006	3.71E-006	3.92E-006	3.98E-006	3.51E-006
797		3.89E-006	3.74E-006	3.98E-006	4.01E-006	3.57E-006
800		3.95E-006	3.79E-006	4.01E-006	4.06E-006	3.60E-006
803		3.98E-006	3.85E-006	4.06E-006	4.10E-006	3.64E-006
806		4.03E-006	3.88E-006	4.13E-006	4.14E-006	3.68E-006
809		4.07E-006	3.92E-006	4.15E-006	4.20E-006	3.70E-006
812		4.10E-006	3.97E-006	4.19E-006	4.22E-006	3.72E-006
815		4.15E-006	4.00E-006	4.24E-006	4.27E-006	3.78E-006
818		4.17E-006	4.05E-006	4.27E-006	4.30E-006	3.80E-006
821		4.21E-006	4.08E-006	4.32E-006	4.34E-006	3.84E-006
824		4.28E-006	4.12E-006	4.36E-006	4.41E-006	3.90E-006
826.9		4.31E-006	4.19E-006	4.41E-006	4.46E-006	3.95E-006
829.9		4.37E-006	4.21E-006	4.47E-006	4.51E-006	4.01E-006
832.9		4.43E-006	4.27E-006	4.50E-006	4.58E-006	4.06E-006
835.9		4.46E-006	4.32E-006	4.55E-006	4.60E-006	4.10E-006
838.9		4.51E-006	4.35E-006	4.61E-006	4.64E-006	4.14E-006
841.9		4.53E-006	4.38E-006	4.62E-006	4.68E-006	4.16E-006
844.9		4.56E-006	4.42E-006	4.67E-006	4.70E-006	4.20E-006
847.9		4.61E-006	4.45E-006	4.71E-006	4.75E-006	4.24E-006
850.9		4.62E-006	4.50E-006	4.73E-006	4.78E-006	4.26E-006
853.9		4.67E-006	4.52E-006	4.78E-006	4.82E-006	4.30E-006
856.9		4.74E-006	4.57E-006	4.82E-006	4.88E-006	4.35E-006
859.9		4.77E-006	4.62E-006	4.85E-006	4.90E-006	4.37E-006
862.9		4.81E-006	4.64E-006	4.91E-006	4.92E-006	4.42E-006
865.9		4.85E-006	4.66E-006	4.91E-006	4.97E-006	4.44E-006
868.9		4.85E-006	4.69E-006	4.93E-006	4.96E-006	4.45E-006
871.9		4.88E-006	4.69E-006	4.97E-006	4.97E-006	4.48E-006
874.9		4.89E-006	4.71E-006	4.96E-006	4.99E-006	4.47E-006
877.8		4.92E-006	4.71E-006	4.97E-006	5.00E-006	4.48E-006
880.8		4.98E-006	4.73E-006	5.00E-006	5.03E-006	4.52E-006
883.8		5.01E-006	4.78E-006	5.03E-006	5.06E-006	4.53E-006
886.8		5.06E-006	4.79E-006	5.07E-006	5.09E-006	4.56E-006
889.8		5.10E-006	4.81E-006	5.07E-006	5.13E-006	4.59E-006
892.8		5.13E-006	4.85E-006	5.09E-006	5.11E-006	4.59E-006
895.8		5.17E-006	4.82E-006	5.10E-006	5.10E-006	4.60E-006
898.8		5.19E-006	4.80E-006	5.04E-006	5.10E-006	4.56E-006
901.8		5.21E-006	4.76E-006	5.00E-006	5.03E-006	4.53E-006
904.8		5.28E-006	4.70E-006	4.98E-006	4.99E-006	4.52E-006

		E	T1	T5	T9	T10
907.8		5.27E-006	4.67E-006	4.91E-006	4.95E-006	4.45E-006
910.8		5.31E-006	4.62E-006	4.89E-006	4.91E-006	4.43E-006
913.8		5.37E-006	4.62E-006	4.89E-006	4.92E-006	4.45E-006
916.8		5.39E-006	4.67E-006	4.89E-006	4.92E-006	4.45E-006
919.8		5.42E-006	4.68E-006	4.93E-006	4.94E-006	4.47E-006
922.8		5.47E-006	4.73E-006	4.95E-006	4.99E-006	4.50E-006
925.7		5.49E-006	4.80E-006	4.99E-006	5.02E-006	4.54E-006
928.7		5.53E-006	4.83E-006	5.07E-006	5.06E-006	4.60E-006
931.7		5.52E-006	4.89E-006	5.10E-006	5.13E-006	4.62E-006
934.7		5.53E-006	4.95E-006	5.16E-006	5.18E-006	4.68E-006
937.7		5.55E-006	4.99E-006	5.24E-006	5.25E-006	4.76E-006
940.7		5.50E-006	5.04E-006	5.27E-006	5.29E-006	4.79E-006
943.7		5.48E-006	5.06E-006	5.32E-006	5.32E-006	4.82E-006
946.7		5.47E-006	5.07E-006	5.34E-006	5.36E-006	4.86E-006
949.7		5.41E-006	5.10E-006	5.33E-006	5.34E-006	4.85E-006
952.7		5.38E-006	5.07E-006	5.35E-006	5.35E-006	4.85E-006
955.7		5.34E-006	5.07E-006	5.31E-006	5.37E-006	4.85E-006
958.7		5.29E-006	5.07E-006	5.31E-006	5.33E-006	4.83E-006
961.7		5.29E-006	5.05E-006	5.33E-006	5.33E-006	4.85E-006
964.7		5.26E-006	5.07E-006	5.31E-006	5.35E-006	4.83E-006
967.7		5.25E-006	5.07E-006	5.33E-006	5.34E-006	4.85E-006
970.7		5.29E-006	5.08E-006	5.35E-006	5.37E-006	4.88E-006
973.7		5.29E-006	5.12E-006	5.36E-006	5.38E-006	4.89E-006
976.6		5.32E-006	5.12E-006	5.40E-006	5.40E-006	4.92E-006
979.6		5.35E-006	5.13E-006	5.41E-006	5.44E-006	4.95E-006
982.6		5.35E-006	5.17E-006	5.42E-006	5.43E-006	4.96E-006
985.6		5.38E-006	5.15E-006	5.45E-006	5.44E-006	4.98E-006
988.6		5.37E-006	5.15E-006	5.41E-006	5.46E-006	4.96E-006
991.6		5.37E-006	5.15E-006	5.40E-006	5.42E-006	4.94E-006
994.6		5.41E-006	5.13E-006	5.42E-006	5.43E-006	4.96E-006
997.6		5.39E-006	5.14E-006	5.39E-006	5.43E-006	4.92E-006
1000.6		5.42E-006	5.13E-006	5.40E-006	5.41E-006	4.93E-006
1003.6		5.47E-006	5.13E-006	5.41E-006	5.43E-006	4.96E-006
1006.6		5.47E-006	5.16E-006	5.40E-006	5.41E-006	4.94E-006
1009.6		5.49E-006	5.12E-006	5.41E-006	5.39E-006	4.93E-006
1012.6		5.58E-006	5.19E-006	5.45E-006	5.45E-006	4.98E-006
1015.6		5.66E-006	5.25E-006	5.51E-006	5.50E-006	5.03E-006
1018.6		5.77E-006	5.30E-006	5.58E-006	5.58E-006	5.10E-006
1021.6		5.84E-006	5.38E-006	5.63E-006	5.63E-006	5.15E-006
1024.6		5.93E-006	5.43E-006	5.71E-006	5.68E-006	5.20E-006
1027.5		6.01E-006	5.49E-006	5.76E-006	5.76E-006	5.26E-006

		E	T1	T5	T9	T10
1030.5		6.08E-006	5.57E-006	5.82E-006	5.81E-006	5.31E-006
1033.5		6.16E-006	5.63E-006	5.91E-006	5.87E-006	5.39E-006
1036.5		6.24E-006	5.70E-006	5.97E-006	5.96E-006	5.45E-006
1039.5		6.22E-006	5.69E-006	5.96E-006	5.94E-006	5.44E-006
1042.5		6.20E-006	5.69E-006	5.95E-006	5.95E-006	5.43E-006
1045.5		6.19E-006	5.68E-006	5.95E-006	5.94E-006	5.44E-006
1048.5		6.18E-006	5.67E-006	5.95E-006	5.94E-006	5.44E-006
1051.5		6.15E-006	5.67E-006	5.94E-006	5.94E-006	5.43E-006
1054.5		6.14E-006	5.67E-006	5.94E-006	5.94E-006	5.43E-006
1057.5		6.14E-006	5.67E-006	5.94E-006	5.93E-006	5.44E-006
1060.5		6.11E-006	5.66E-006	5.93E-006	5.93E-006	5.43E-006
1063.5		6.10E-006	5.65E-006	5.93E-006	5.93E-006	5.43E-006
1066.5		6.09E-006	5.65E-006	5.94E-006	5.93E-006	5.44E-006
1069.5		6.05E-006	5.64E-006	5.92E-006	5.92E-006	5.43E-006
1072.5		6.05E-006	5.64E-006	5.92E-006	5.92E-006	5.43E-006
1075.4		6.05E-006	5.64E-006	5.93E-006	5.93E-006	5.44E-006
1078.4		6.03E-006	5.65E-006	5.93E-006	5.93E-006	5.43E-006
1081.4		6.01E-006	5.64E-006	5.93E-006	5.92E-006	5.43E-006
1084.4		6.01E-006	5.65E-006	5.94E-006	5.93E-006	5.45E-006
1087.4		5.98E-006	5.65E-006	5.93E-006	5.93E-006	5.43E-006
1090.4		5.96E-006	5.64E-006	5.92E-006	5.92E-006	5.43E-006
1093.4		5.96E-006	5.64E-006	5.92E-006	5.92E-006	5.43E-006
1096.4		5.94E-006	5.63E-006	5.92E-006	5.91E-006	5.42E-006
1099.4		5.92E-006	5.61E-006	5.90E-006	5.88E-006	5.40E-006
1102.4		5.92E-006	5.59E-006	5.89E-006	5.87E-006	5.40E-006
1105.4		5.89E-006	5.57E-006	5.86E-006	5.84E-006	5.36E-006
1108.4		5.86E-006	5.53E-006	5.82E-006	5.80E-006	5.33E-006
1111.4		5.83E-006	5.49E-006	5.77E-006	5.76E-006	5.30E-006
1114.4		5.78E-006	5.44E-006	5.72E-006	5.71E-006	5.24E-006
1117.4		5.73E-006	5.36E-006	5.64E-006	5.63E-006	5.17E-006
1120.4		5.66E-006	5.26E-006	5.55E-006	5.54E-006	5.09E-006
1123.4		5.57E-006	5.15E-006	5.42E-006	5.41E-006	4.96E-006
1126.3		5.44E-006	4.97E-006	5.25E-006	5.23E-006	4.80E-006
1129.3		5.29E-006	4.75E-006	5.03E-006	5.00E-006	4.60E-006
1132.3		5.09E-006	4.49E-006	4.77E-006	4.74E-006	4.34E-006
1135.3		4.90E-006	4.20E-006	4.47E-006	4.44E-006	4.07E-006
1138.3		4.74E-006	3.90E-006	4.18E-006	4.13E-006	3.80E-006
1141.3		4.63E-006	3.64E-006	3.92E-006	3.87E-006	3.55E-006
1144.3		4.62E-006	3.43E-006	3.71E-006	3.67E-006	3.36E-006
1147.3		4.70E-006	3.31E-006	3.59E-006	3.55E-006	3.26E-006
1150.3		4.83E-006	3.27E-006	3.54E-006	3.51E-006	3.22E-006

		E	T1	T5	T9	T10
1153.3		5.00E-006	3.27E-006	3.52E-006	3.49E-006	3.22E-006
1156.3		5.15E-006	3.27E-006	3.51E-006	3.48E-006	3.22E-006
1159.3		5.25E-006	3.25E-006	3.46E-006	3.44E-006	3.18E-006
1162.3		5.31E-006	3.17E-006	3.36E-006	3.34E-006	3.09E-006
1165.3		5.34E-006	3.03E-006	3.20E-006	3.19E-006	2.96E-006
1168.3		5.32E-006	2.85E-006	3.00E-006	3.00E-006	2.78E-006
1171.3		5.29E-006	2.63E-006	2.77E-006	2.78E-006	2.57E-006
1174.3		5.25E-006	2.39E-006	2.52E-006	2.52E-006	2.34E-006
1177.2		5.18E-006	2.10E-006	2.21E-006	2.23E-006	2.06E-006
1180.2		5.11E-006	1.79E-006	1.89E-006	1.91E-006	1.76E-006
1183.2		5.06E-006	1.49E-006	1.58E-006	1.60E-006	1.47E-006
1186.2		5.01E-006	1.24E-006	1.31E-006	1.33E-006	1.23E-006
1189.2		4.98E-006	1.05E-006	1.12E-006	1.15E-006	1.05E-006
1192.2		4.98E-006	9.75E-007	1.03E-006	1.05E-006	9.66E-007
1195.2		4.95E-006	9.71E-007	1.01E-006	1.03E-006	9.47E-007
1198.2		4.93E-006	1.01E-006	1.03E-006	1.04E-006	9.62E-007
1201.2		4.91E-006	1.05E-006	1.06E-006	1.05E-006	9.85E-007
1204.2		4.88E-006	1.09E-006	1.08E-006	1.06E-006	1.00E-006
1207.2		4.86E-006	1.12E-006	1.10E-006	1.07E-006	1.02E-006
1210.2		4.86E-006	1.17E-006	1.13E-006	1.11E-006	1.05E-006
1213.2		4.86E-006	1.26E-006	1.22E-006	1.19E-006	1.13E-006
1216.2		4.88E-006	1.39E-006	1.35E-006	1.32E-006	1.25E-006
1219.2		4.91E-006	1.56E-006	1.53E-006	1.51E-006	1.42E-006
1222.2		4.92E-006	1.76E-006	1.75E-006	1.73E-006	1.62E-006
1225.1		4.93E-006	1.97E-006	1.99E-006	1.97E-006	1.84E-006
1228.1		4.93E-006	2.18E-006	2.23E-006	2.22E-006	2.07E-006
1231.1		4.90E-006	2.38E-006	2.46E-006	2.45E-006	2.28E-006
1234.1		4.88E-006	2.56E-006	2.66E-006	2.66E-006	2.47E-006
1237.1		4.84E-006	2.72E-006	2.84E-006	2.84E-006	2.63E-006
1240.1		4.78E-006	2.85E-006	2.98E-006	2.99E-006	2.77E-006
1243.1		4.73E-006	2.96E-006	3.11E-006	3.12E-006	2.88E-006
1246.1		4.70E-006	3.07E-006	3.23E-006	3.23E-006	2.99E-006
1249.1		4.65E-006	3.16E-006	3.33E-006	3.33E-006	3.07E-006
1252.1		4.63E-006	3.25E-006	3.42E-006	3.42E-006	3.16E-006
1255.1		4.63E-006	3.34E-006	3.52E-006	3.50E-006	3.25E-006
1258.1		4.61E-006	3.42E-006	3.60E-006	3.58E-006	3.32E-006
1261.1		4.60E-006	3.48E-006	3.67E-006	3.66E-006	3.39E-006
1264.1		4.60E-006	3.55E-006	3.75E-006	3.72E-006	3.45E-006
1267.1		4.57E-006	3.60E-006	3.80E-006	3.78E-006	3.50E-006
1270.1		4.56E-006	3.65E-006	3.85E-006	3.83E-006	3.54E-006
1273.1		4.55E-006	3.68E-006	3.89E-006	3.86E-006	3.58E-006

		E	T1	T5	T9	T10
1276		4.53E-006	3.72E-006	3.92E-006	3.90E-006	3.61E-006
1279		4.51E-006	3.73E-006	3.94E-006	3.91E-006	3.63E-006
1282		4.49E-006	3.75E-006	3.96E-006	3.93E-006	3.65E-006
1285		4.46E-006	3.76E-006	3.96E-006	3.94E-006	3.65E-006
1288		4.44E-006	3.76E-006	3.96E-006	3.94E-006	3.65E-006
1291		4.42E-006	3.75E-006	3.96E-006	3.93E-006	3.65E-006
1294		4.38E-006	3.75E-006	3.95E-006	3.92E-006	3.64E-006
1297		4.36E-006	3.73E-006	3.95E-006	3.91E-006	3.63E-006
1300		4.34E-006	3.73E-006	3.94E-006	3.91E-006	3.63E-006
1303		4.31E-006	3.72E-006	3.94E-006	3.90E-006	3.62E-006
1306		4.29E-006	3.71E-006	3.93E-006	3.89E-006	3.62E-006
1309		4.27E-006	3.70E-006	3.92E-006	3.88E-006	3.61E-006
1312		4.23E-006	3.68E-006	3.90E-006	3.86E-006	3.59E-006
1315		4.20E-006	3.65E-006	3.88E-006	3.84E-006	3.56E-006
1318		4.16E-006	3.62E-006	3.84E-006	3.80E-006	3.53E-006
1321		4.11E-006	3.58E-006	3.80E-006	3.76E-006	3.49E-006
1324		4.06E-006	3.53E-006	3.75E-006	3.71E-006	3.45E-006
1326.9		4.01E-006	3.48E-006	3.69E-006	3.65E-006	3.40E-006
1329.9		3.93E-006	3.42E-006	3.62E-006	3.59E-006	3.33E-006
1332.9		3.87E-006	3.34E-006	3.55E-006	3.51E-006	3.26E-006
1335.9		3.81E-006	3.27E-006	3.47E-006	3.43E-006	3.19E-006
1338.9		3.73E-006	3.18E-006	3.38E-006	3.34E-006	3.10E-006
1341.9		3.67E-006	3.08E-006	3.29E-006	3.24E-006	3.02E-006
1344.9		3.61E-006	2.96E-006	3.16E-006	3.12E-006	2.90E-006
1347.9		3.53E-006	2.81E-006	2.99E-006	2.95E-006	2.75E-006
1350.9		3.46E-006	2.60E-006	2.78E-006	2.75E-006	2.56E-006
1353.9		3.39E-006	2.37E-006	2.54E-006	2.51E-006	2.34E-006
1356.9		3.30E-006	2.14E-006	2.30E-006	2.28E-006	2.12E-006
1359.9		3.22E-006	1.93E-006	2.07E-006	2.06E-006	1.92E-006
1362.9		3.13E-006	1.73E-006	1.86E-006	1.85E-006	1.73E-006
1365.9		3.02E-006	1.56E-006	1.67E-006	1.67E-006	1.56E-006
1368.9		2.90E-006	1.39E-006	1.49E-006	1.48E-006	1.39E-006
1371.9		2.73E-006	1.20E-006	1.28E-006	1.28E-006	1.20E-006
1374.9		2.52E-006	1.00E-006	1.07E-006	1.07E-006	1.00E-006
1377.8		2.32E-006	8.34E-007	8.86E-007	8.89E-007	8.35E-007
1380.8		2.10E-006	6.86E-007	7.29E-007	7.28E-007	6.84E-007
1383.8		1.89E-006	5.66E-007	5.98E-007	6.00E-007	5.61E-007
1386.8		1.70E-006	4.79E-007	5.04E-007	5.08E-007	4.71E-007
1389.8		1.53E-006	4.21E-007	4.45E-007	4.45E-007	4.14E-007
1392.8		1.35E-006	3.76E-007	3.96E-007	3.96E-007	3.69E-007
1395.8		1.19E-006	3.42E-007	3.61E-007	3.60E-007	3.38E-007

		E	T1	T5	T9	T10
1398.8		1.05E-006	3.19E-007	3.36E-007	3.32E-007	3.17E-007
1401.8		9.43E-007	3.02E-007	3.18E-007	3.14E-007	2.99E-007
1404.8		8.66E-007	2.81E-007	2.95E-007	2.91E-007	2.80E-007
1407.8		8.13E-007	2.62E-007	2.75E-007	2.70E-007	2.63E-007
1410.8		7.80E-007	2.52E-007	2.63E-007	2.60E-007	2.52E-007
1413.8		7.63E-007	2.54E-007	2.64E-007	2.60E-007	2.50E-007
1416.8		7.58E-007	2.63E-007	2.73E-007	2.66E-007	2.58E-007
1419.8		7.62E-007	2.80E-007	2.91E-007	2.82E-007	2.73E-007
1422.8		7.83E-007	3.02E-007	3.11E-007	3.02E-007	2.90E-007
1425.7		8.11E-007	3.23E-007	3.32E-007	3.20E-007	3.10E-007
1428.7		8.53E-007	3.48E-007	3.57E-007	3.42E-007	3.32E-007
1431.7		9.00E-007	3.74E-007	3.82E-007	3.71E-007	3.57E-007
1434.7		9.60E-007	4.08E-007	4.16E-007	4.05E-007	3.86E-007
1437.7		1.02E-006	4.44E-007	4.59E-007	4.45E-007	4.26E-007
1440.7		1.09E-006	4.87E-007	5.04E-007	4.92E-007	4.69E-007
1443.7		1.15E-006	5.32E-007	5.54E-007	5.42E-007	5.16E-007
1446.7		1.22E-006	5.77E-007	6.11E-007	5.91E-007	5.65E-007
1449.7		1.27E-006	6.21E-007	6.63E-007	6.41E-007	6.15E-007
1452.7		1.32E-006	6.68E-007	7.13E-007	6.90E-007	6.60E-007
1455.7		1.37E-006	7.07E-007	7.62E-007	7.32E-007	7.03E-007
1458.7		1.41E-006	7.40E-007	8.04E-007	7.73E-007	7.41E-007
1461.7		1.45E-006	7.74E-007	8.37E-007	8.09E-007	7.74E-007
1464.7		1.48E-006	8.06E-007	8.71E-007	8.41E-007	8.03E-007
1467.7		1.50E-006	8.32E-007	9.01E-007	8.72E-007	8.29E-007
1470.7		1.52E-006	8.61E-007	9.27E-007	9.00E-007	8.55E-007
1473.7		1.53E-006	8.90E-007	9.51E-007	9.25E-007	8.78E-007
1476.6		1.54E-006	9.09E-007	9.76E-007	9.48E-007	8.98E-007
1479.6		1.55E-006	9.28E-007	9.92E-007	9.69E-007	9.16E-007
1482.6		1.55E-006	9.43E-007	1.01E-006	9.82E-007	9.28E-007
1485.6		1.55E-006	9.53E-007	1.02E-006	9.95E-007	9.39E-007
1488.6		1.55E-006	9.58E-007	1.03E-006	1.00E-006	9.47E-007
1491.6		1.55E-006	9.69E-007	1.03E-006	1.01E-006	9.57E-007
1494.6		1.54E-006	9.78E-007	1.05E-006	1.02E-006	9.66E-007
1497.6		1.53E-006	9.87E-007	1.06E-006	1.03E-006	9.73E-007
1500.6		1.52E-006	9.92E-007	1.06E-006	1.04E-006	9.77E-007
1503.6		1.50E-006	1.00E-006	1.07E-006	1.04E-006	9.79E-007
1506.6		1.47E-006	1.00E-006	1.07E-006	1.04E-006	9.78E-007
1509.6		1.45E-006	9.98E-007	1.07E-006	1.04E-006	9.75E-007
1512.6		1.42E-006	9.96E-007	1.06E-006	1.04E-006	9.75E-007
1515.6		1.40E-006	9.93E-007	1.06E-006	1.03E-006	9.68E-007
1518.6		1.38E-006	9.88E-007	1.05E-006	1.02E-006	9.66E-007

		E	T1	T5	T9	T10
1521.6		1.35E-006	9.80E-007	1.04E-006	1.01E-006	9.59E-007
1524.6		1.33E-006	9.70E-007	1.03E-006	1.00E-006	9.49E-007
1527.5		1.31E-006	9.56E-007	1.02E-006	9.87E-007	9.37E-007
1530.5		1.28E-006	9.43E-007	1.00E-006	9.74E-007	9.29E-007
1533.5		1.26E-006	9.29E-007	9.89E-007	9.62E-007	9.15E-007
1536.5		1.23E-006	9.16E-007	9.76E-007	9.47E-007	8.99E-007
1539.5		1.20E-006	8.99E-007	9.65E-007	9.33E-007	8.85E-007
1542.5		1.17E-006	8.86E-007	9.50E-007	9.20E-007	8.68E-007
1545.5		1.14E-006	8.68E-007	9.32E-007	9.06E-007	8.52E-007
1548.5		1.11E-006	8.50E-007	9.14E-007	8.88E-007	8.33E-007
1551.5		1.08E-006	8.29E-007	8.95E-007	8.69E-007	8.15E-007
1554.5		1.05E-006	8.10E-007	8.71E-007	8.50E-007	7.95E-007
1557.5		1.02E-006	7.87E-007	8.48E-007	8.25E-007	7.74E-007
1560.5		9.92E-007	7.61E-007	8.25E-007	7.98E-007	7.53E-007
1563.5		9.61E-007	7.38E-007	7.95E-007	7.75E-007	7.30E-007
1566.5		9.27E-007	7.16E-007	7.66E-007	7.49E-007	7.06E-007
1569.5		8.92E-007	6.91E-007	7.39E-007	7.23E-007	6.83E-007
1572.5		8.65E-007	6.65E-007	7.09E-007	6.97E-007	6.58E-007
1575.4		8.33E-007	6.43E-007	6.80E-007	6.72E-007	6.30E-007
1578.4		8.00E-007	6.11E-007	6.57E-007	6.45E-007	6.02E-007
1581.4		7.70E-007	5.83E-007	6.30E-007	6.19E-007	5.73E-007
1584.4		7.41E-007	5.58E-007	6.01E-007	5.92E-007	5.47E-007
1587.4		7.07E-007	5.31E-007	5.75E-007	5.64E-007	5.22E-007
1590.4		6.78E-007	5.02E-007	5.47E-007	5.37E-007	4.94E-007
1593.4		6.51E-007	4.82E-007	5.22E-007	5.09E-007	4.73E-007
1596.4		6.22E-007	4.58E-007	4.95E-007	4.81E-007	4.50E-007
1599.4		5.93E-007	4.31E-007	4.69E-007	4.53E-007	4.27E-007
1602.4		5.62E-007	4.09E-007	4.44E-007	4.28E-007	4.03E-007
1605.4		5.34E-007	3.87E-007	4.18E-007	4.02E-007	3.81E-007
1608.4		5.03E-007	3.57E-007	3.89E-007	3.72E-007	3.56E-007
1611.4		4.75E-007	3.30E-007	3.59E-007	3.46E-007	3.30E-007
1614.4		4.44E-007	3.02E-007	3.30E-007	3.13E-007	3.00E-007
1617.4		4.12E-007	2.71E-007	3.00E-007	2.86E-007	2.71E-007
1620.4		3.76E-007	2.39E-007	2.64E-007	2.54E-007	2.44E-007
1623.4		3.40E-007	2.13E-007	2.31E-007	2.25E-007	2.13E-007
1626.3		3.04E-007	1.87E-007	2.03E-007	1.98E-007	1.88E-007
1629.3		2.75E-007	1.64E-007	1.78E-007	1.77E-007	1.64E-007
1632.3		2.50E-007	1.44E-007	1.54E-007	1.59E-007	1.45E-007
1635.3		2.28E-007	1.29E-007	1.41E-007	1.42E-007	1.26E-007
1638.3		2.11E-007	1.19E-007	1.30E-007	1.29E-007	1.13E-007
1641.3		1.98E-007	1.09E-007	1.14E-007	1.20E-007	1.02E-007

		E	T1	T5	T9	T10
1644.3		1.84E-007	1.03E-007	1.06E-007	1.13E-007	9.48E-008
1647.3		1.68E-007	9.19E-008	9.82E-008	9.97E-008	8.76E-008
1650.3		1.53E-007	8.46E-008	8.85E-008	8.88E-008	7.91E-008
1653.3		1.36E-007	7.35E-008	7.65E-008	7.72E-008	6.96E-008
1656.3		1.14E-007	5.72E-008	6.64E-008	6.01E-008	5.49E-008
1659.3		8.93E-008	4.32E-008	4.96E-008	4.27E-008	4.36E-008
1662.3		6.78E-008	3.26E-008	3.81E-008	3.12E-008	3.34E-008
1665.3		4.63E-008	2.14E-008	2.39E-008	1.96E-008	2.75E-008
1668.3		2.83E-008	1.45E-008	1.46E-008	1.41E-008	2.10E-008
1671.3		1.62E-008	1.40E-008	1.08E-008	1.04E-008	2.54E-008
1674.3		1.68E-008	9.38E-009	9.39E-009	1.05E-008	2.02E-008
1677.2		1.70E-008	1.01E-008	3.40E-009	7.58E-009	1.46E-008
1680.2		1.59E-008	8.08E-009	3.40E-009	1.32E-008	1.04E-008
1683.2		1.59E-008	4.52E-009	3.40E-009	1.12E-008	7.18E-009
1686.2		2.09E-008	4.10E-009	4.61E-009	1.04E-008	4.75E-009
1689.2		1.51E-008	1.40E-008	3.42E-009	8.76E-009	9.30E-009
1692.2		9.63E-009	2.98E-008	3.42E-009	2.94E-008	9.30E-009
1695.2		3.07E-008	3.90E-008	3.42E-009	2.38E-008	2.64E-008
1698.2		3.07E-008	3.90E-008	1.20E-008	2.65E-008	2.64E-008
1701.2		2.85E-008	3.95E-008	9.59E-009	2.99E-008	2.26E-008
1704.2		2.88E-008	2.94E-008	1.29E-008	2.85E-008	2.96E-008
1707.2		3.49E-008	1.17E-008	1.42E-008	7.89E-009	3.60E-008
1710.2		1.34E-008	3.99E-009	3.78E-008	7.89E-009	1.89E-008
1713.2		1.34E-008	3.99E-009	3.63E-008	4.41E-009	1.89E-008
1716.2		8.97E-009	1.53E-008	5.42E-008	1.00E-009	2.12E-008
1719.2		9.99E-009	4.42E-008	6.75E-008	1.63E-008	9.78E-009
1722.2		3.82E-009	4.42E-008	6.62E-008	1.63E-008	6.98E-009
1725.1		1.19E-008	4.27E-008	4.26E-008	1.63E-008	6.98E-009
1728.1		1.19E-008	4.27E-008	3.96E-008	1.98E-008	6.98E-009
1731.1		1.76E-008	2.99E-008	2.18E-008	1.98E-008	1.40E-008
1734.1		1.47E-008	2.96E-008	2.29E-008	1.34E-008	1.40E-008
1737.1		1.47E-008	9.53E-008	2.29E-008	1.34E-008	1.04E-008
1740.1		6.14E-008	9.53E-008	7.65E-008	1.34E-008	1.04E-008
1743.1		1.12E-007	1.08E-007	7.24E-008	1.97E-008	1.04E-008
1746.1		1.67E-007	1.17E-007	7.24E-008	2.38E-008	1.00E-009
1749.1		1.00E-009	1.00E-009	1.00E-009	1.00E-009	1.00E-009
1752.1		1.00E-009	1.00E-009	1.00E-009	1.00E-009	1.00E-009
1755.1		1.00E-009	1.00E-009	1.00E-009	1.00E-009	1.00E-009
1758.1		1.00E-009	1.00E-009	1.00E-009	1.00E-009	1.00E-009
1761.1		1.00E-009	1.00E-009	1.00E-009	1.00E-009	1.00E-009
1764.1		1.00E-009	1.00E-009	1.00E-009	1.00E-009	1.00E-009

		E	T1	T5	T9	T10
1767.1		1.00E-009	1.00E-009	1.00E-009	1.00E-009	1.00E-009
1770.1		1.00E-009	1.00E-009	1.00E-009	1.00E-009	1.00E-009
1776		1.00E-009	1.00E-009	1.00E-009	1.00E-009	1.00E-009
1779		1.00E-009	1.00E-009	1.00E-009	1.00E-009	1.00E-009
1782		1.00E-009	1.00E-009	1.00E-009	1.00E-009	1.00E-009
1785		1.00E-009	1.00E-009	1.00E-009	1.00E-009	1.00E-009
1788		1.00E-009	1.00E-009	1.00E-009	1.00E-009	1.00E-009
1791		1.00E-009	1.00E-009	1.00E-009	1.00E-009	1.00E-009
1794		1.00E-009	1.00E-009	1.00E-009	1.00E-009	1.00E-009
1797		1.00E-009	1.00E-009	1.00E-009	1.00E-009	1.00E-009

Appendix C

Raw Test Data For Dissolved Gas, Acidity, Electrical Strength and Water

C.1 Dissolved Gas Raw Values

C.2 Water, Acidity, Colour Index And Electrical Strength Raw Values

Table C.1: Raw dissolved gases values for different transformer oil samples.

Sample no	17	27	29	36	50	53	61	35	24	51	45	84	33	2	75	32	63	85	T1	T2	T3	T4	T5	T6	T7	T8	T9	T10
CO	54	47	73	83	28	82	14	71	10	70	72	220	52	56	140	70	250	190	43	115	135	142	214	131	117	220	135	690
CO2	1410	1390	1480	1590	1310	730	1330	1360	850	1130	1210	1780	1900	760	1340	1660	5450	2580	1082	1908	1258	2374	2177	1383	2572	3903	1066	7951
C2H4	0	0	0	0	0	0.8	0	0	0	2.3	1.3	2.7	1.8	0	1.7	1.2	920	6.8	0	1.35	0	2.11	1.81	0	3.37	3.71	0	7.88
C2H6	0	0	1.8	0	0	0	0	0	0	0	0	0	0	0	0	0	1660	0	0	0	0	0	0	0	0	0	0	15.6
C2H2	0	1.5	0	6.3	0	0	0	5	0	0	0	0	0	0	0	0	3.8	0	0	0	0	0	0	0	0	0	0	0
H2	12	0	10	15	0	11	0	11	0	0	0	84	0	0	30	0	30	0	0	0	17.4	22.9	28	31.2	0	33.9	0	39.4
CH4	2.7	2.5	2	2.9	1.4	1.7	1.8	2.4	1.9	2.6	2	3.6	1.7	1.6	2.6	2	640	4	3.28	3.21	4.4	3.24	2.88	3.19	3.24	3.1	2.06	13.5

Courtesy Electrical North West (ENW).

Table C.2: Raw water, acidity, colour index and electrical strength values for different transformer oil samples.

Sample no	17	27	29	36	50	53	61	35	24	51	45	84	33	2	75	32	T1	T2	T3	T4	T5	T6	T7	T8	T9	T10	63	85
Electrical Strength	60	60	57	60	60	60	58	60	59	28	60	60	60	58	60	59	60	60	60	60	60	60	58	51.8	59	57	42	27
Water (mg/kg)	6	6	23	14	11	13	10	10	8	36	14	15	8	14	12	13	10	15	22	14	22	13	29	32	16	29	41	43
Acidity	0.03	0.03	0.04	0.06	0.07	0.07	0.07	0.05	0.08	0.08	0.09	0.14	0.16	0.11	0.17	0.21	0.01	0.26	0.14	0.17	0.2	0.12	0.18	0.24	0.08	0.52	0.32	1
CI	1	1.1	1.4	1.4	1.4	1.4	1.4	1.5	1.5	1.5	1.6	1.7	1.7	1.9	1.9	1.9	0.4	2.3	1.6	2.1	2.1	2.3	2.2	2.5	2.5	4.9	5.4	6.7

Courtesy Electrical North West (ENW).

Appendix D

Chromatic Data For Filtered Oil

D.1 Raw R,G,B Values For Contaminated Filter Paper

Table D.1: Raw RGB values for different contaminated filter papers.

	R	G	B
E	0.74	0.66	0.87
T1	0.75	0.68	0.79
T5	0.75	0.68	0.49
T10	0.79	0.59	0.05

D.2 HLS Generated From Raw R,G,B Values For Contaminated Filter Paper table C.1

Table D.2: HLS for different contaminated filter papers.

	H	L	S
E	272.75	0.76	0.13
T1	286.97	0.74	0.08
T5	49.31	0.64	0.21
T10	50.52	0.47	0.88

D.3 Different Filtered And Non Filtered Oil Samples

Table D.3: Different filtered oil samples.

filtered oil samples	R	G	B
T13	0.31	0.21	0.89
11 T11	0.39	0.26	0.80
22 T11	0.42	0.26	0.73
32 T11	0.42	0.27	0.58
42 ET2	0.35	0.10	0.07

Table D.4: Different non filtered oil samples.

Non filtered oil samples	R	G	B
T13	0.45	0.29	0.77
11 T11	0.46	0.29	0.60
22 T11	0.45	0.27	0.48
32 T11	0.45	0.25	0.32
42 ET2	0.46	0.16	0.02

Appendix E

Chromatic Parameters XY For Various Oil Samples

E.1 Calculated Cartesian X:Y Values For Oil Samples

Table E.1: Different dissolve gas groups based on different condition faults. table (a) and (b) represent the dissolved gases which divided into the three groups corresponding to the effects of severe overheating (CO2, CO, C2H4), local overheating (C2H6), and electrical discharging (H2, CH4, C2H2).

Sample no		17	27	29	36	50	53	61	35	24	51	45	84	33	2
RN	CO+CO2+C2H4	0.08	0.08	0.10	0.11	0.06	0.09	0.05	0.09	0.04	0.12	0.11	0.25	0.13	0.06
GN	C2H6	0.00	0.00	0.18	0.00	0.00	0.00	0.00	0.00	0.00	0.00	0.00	0.00	0.00	0.00
BN	CH4+H2+C2H2	0.06	0.07	0.05	0.21	0.02	0.05	0.02	0.17	0.03	0.03	0.03	0.23	0.02	0.02

(a)

Continue

Sample no		75	32	63	85	T1	T2	T3	T4	T5	T6	T7	T8	T9	T10
RN	CO+CO2+C2H4	0.17	0.12	2.99	0.33	0.06	0.16	0.13	0.21	0.25	0.13	0.22	0.34	0.13	0.86
GN	C2H6	0.00	0.00	67.00	0.00	0.00	0.00	0.00	0.00	0.00	0.00	0.00	0.00	0.00	1.22
BN	CH4+H2+C2H2	0.10	0.03	4.21	0.05	0.04	0.04	0.10	0.09	0.10	0.11	0.04	0.12	0.03	0.27

(b)

Courtesy Electrical North West (ENW).

Appendix F

Colour Index

F.1 Comparison Between colour index And Optical Chromatic Parameters

A comparison between the colour index of the oil and the optical chromatic Fn$[x(O)/z(O)]$ n as a function of oil sample represented in figure E.1.The trend shown by both the chromatic and Colour Index results is similar with only a few samples (T6, T2, T5, T8, 84 and T10) somewhat different. This difference could be due to accuracy of the purely visible colour index test, which is based on comparing the actual colour of the oil to a set of standard.

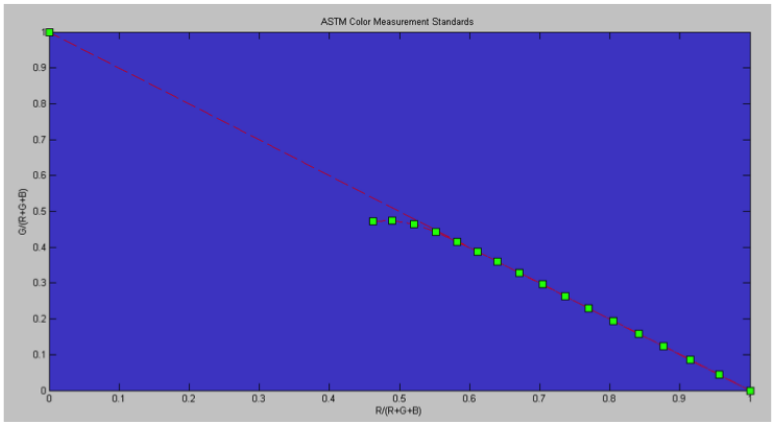

Figure F.1: Colour index standard diagram.

The colour index test is a purely visible test. It compares the actual colour of the oil to a set of standards. The darker the oil, the more contamination is present. The colour index test is reported as a numerical value between 0.5 and 5.0 with 5.0 being the worst Shaban et al. (2009) On the other hand, the

chromatic representation of oil sample is based on analysis of measured data that is sensitive to any change in these data RGB.

Appendix G

Chromatic Software

G.1 Droptri

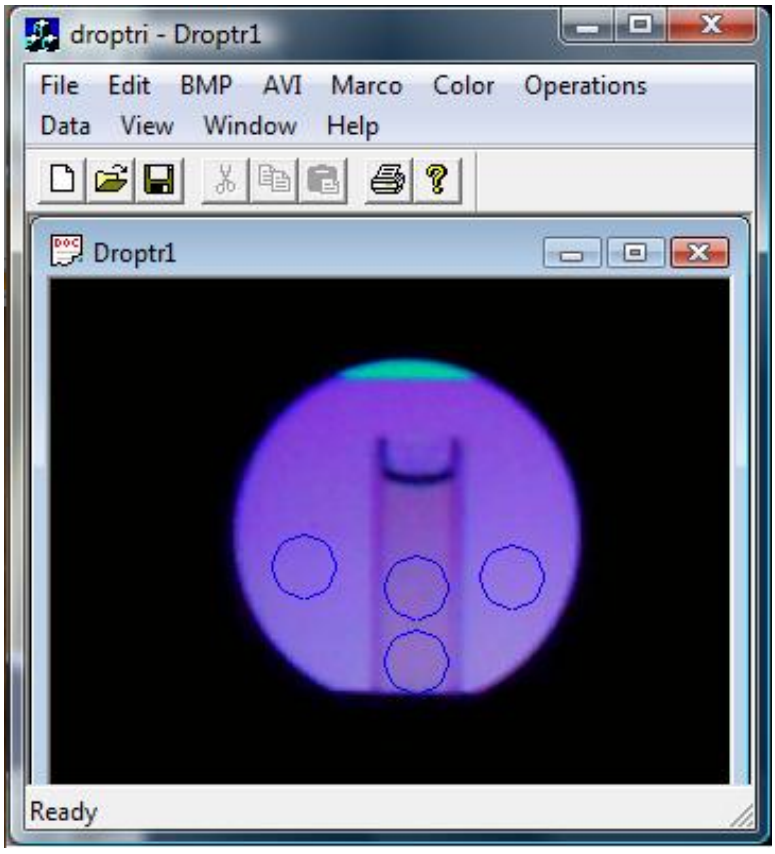

Figure G.1: Droptri analysis window.

The primary function of Droptri chromatic software figure F.1 , alongside many additional functions, specially developed at CIMS by Deakin C. (2010)

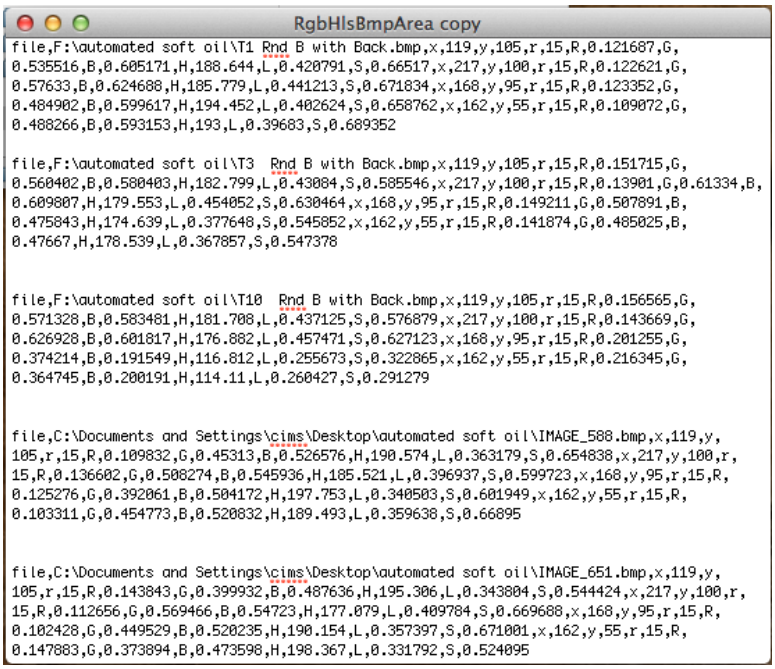

Figure G.2: RGB and HLS extracted text file from the Droptri analysis points .

for use in numerous applications, enables r, g and b values from an images pixel regions selected by the user to be obtained and logged together with their chromatic transformations into, for example, hue, lightness and saturation. The log file serves as input for further chromatic analyses and graphing outputs, for example polar plotting of hue-lightness and hue−saturation and transformation and graphing of r, g, b in terms of X, Y, Z. Space averaged r, g ,b values (700 pixels extent [$75mm2$] over $10 * 45$ mm actual cuvette area) were obtained from each oil samples image 4 pixel areas (2 sample points and 2 reference points) using Droptri chromatic software running on the laptop and transformed into corresponding values of the chromatic parameters X, Y, Z and L for each pixel area using the algorithms.

The text file (figure F.2) contain the raw values of RGB and HLS extracted from the analysed areas highlighted in circular (figure F.1).

G.2 Automated Oil Monitoring Using Matlab

Matlab as a package was used to develop a user friendly software that able to automate the chromatic oil monitoring methodology.

G.2.1 Main Input Window

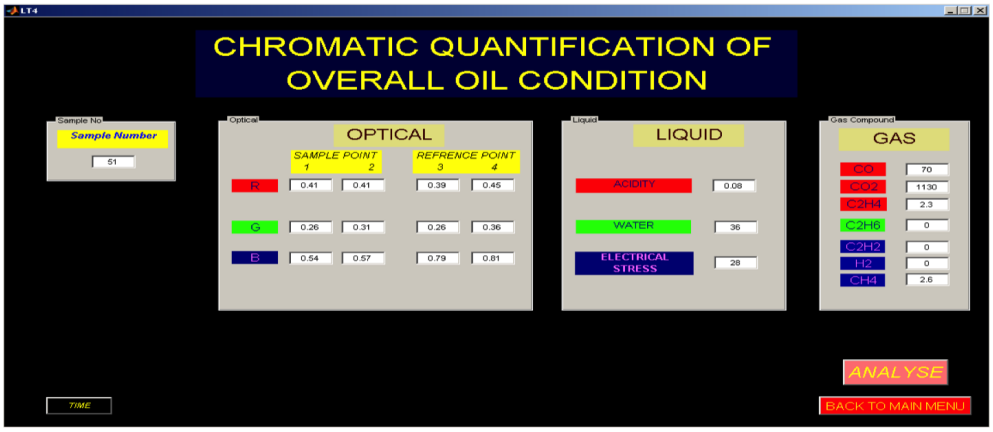

Figure G.3: Optical, liquid and dissolved gas data input window.

G.2.2 General Indication Window

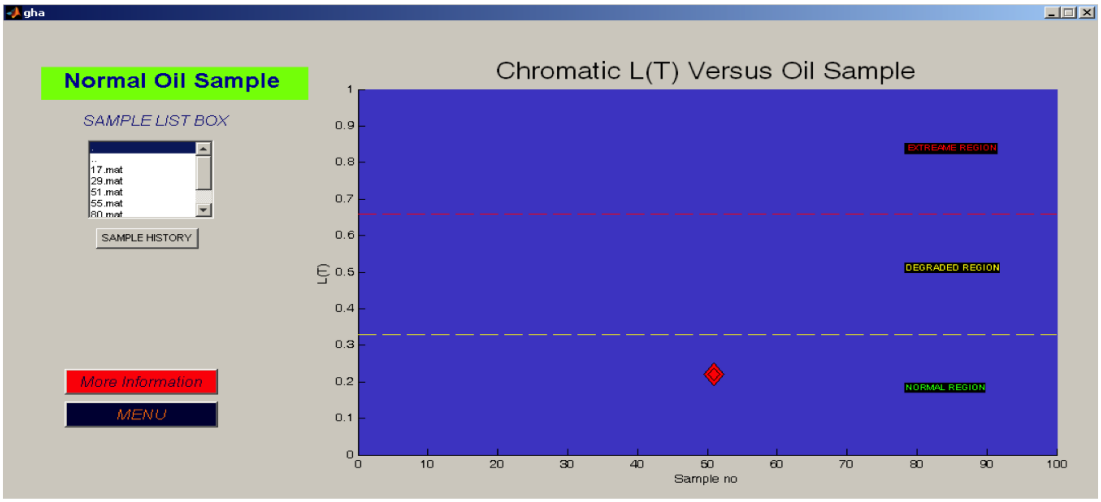

Figure G.4: Chromatic LT indication widow a)Bottom Level is the Normal Region . b)Mid Level is the Moderate Region. c)Top Level is the Extreme Region. .

G.2.3 Dominant Chromatic Parameter Window

G.2.4 Summary Window

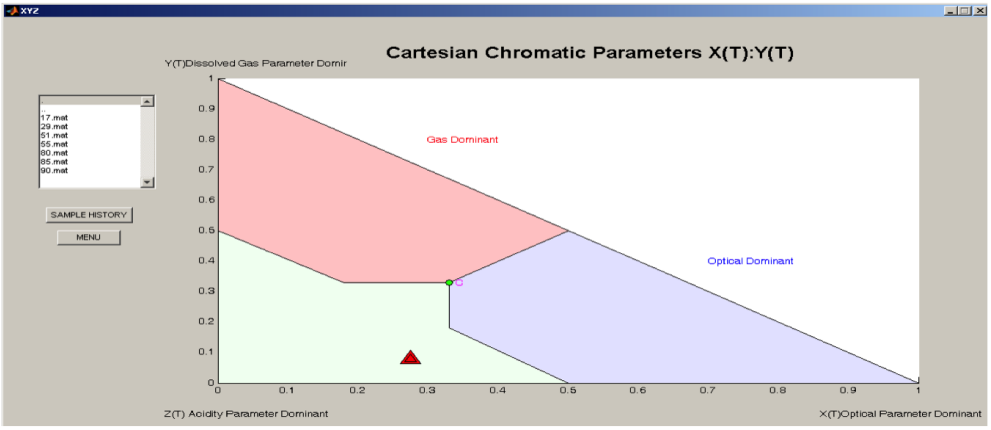

Figure G.5: Chromatic Cartesian detailed widow a)Y(T) Dissolved Gas Parameter Dominant. b)Z(T) Acidity Parameter Dominant. c)X(T) Optical Parameter Dominant.

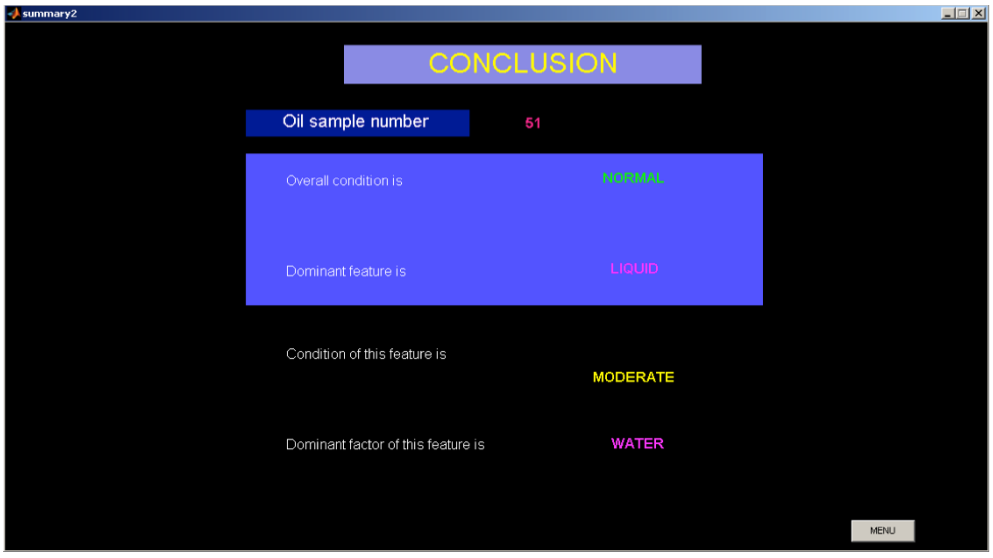

Figure G.6: Summarized widow stating the condition of the oil sample and its reason of its degradation.